



Review

A Review on the Synthesis, Characterization, and Modeling of Polymer Grafting

Miguel Ángel Vega-Hernández ¹, Gema Susana Cano-Díaz ¹, Eduardo Vivaldo-Lima ^{1,2,*} ,
Alberto Rosas-Aburto ¹, Martín G. Hernández-Luna ¹, Alfredo Martínez ³, Joaquín Palacios-Alquisira ⁴,
Yousef Mohammadi ⁵ and Alexander Penlidis ^{2,*} 

- ¹ Departamento de Ingeniería Química, Facultad de Química, Universidad Nacional Autónoma de México, Ciudad de México 04510, Mexico; angeluz_alchemist@hotmail.com (M.Á.V.-H.); suscad@unam.mx (G.S.C.-D.); alberto_rosas_aburto@comunidad.unam.mx (A.R.-A.); martinhl@unam.mx (M.G.H.-L.)
- ² Department of Chemical Engineering, Institute for Polymer Research, University of Waterloo, Waterloo, ON N2L 3G1, Canada
- ³ Instituto de Biotecnología, Universidad Nacional Autónoma de México, Cuernavaca, Morelos 62210, Mexico; alfredo.martinez@mail.ibt.unam.mx
- ⁴ Departamento de Fisicoquímica, Facultad de Química, Universidad Nacional Autónoma de México, Ciudad de México 04510, Mexico; polylab1@unam.mx
- ⁵ Petrochemical Research and Technology Company (NPC-rt), National Petrochemical Company (NPC), Tehran P.O. Box 14358-84711, Iran; mohammadi@npc-rt.ir
- * Correspondence: vivaldo@unam.mx (E.V.-L.); penlidis@uwaterloo.ca (A.P.); Tel.: +519-888-4567 (ext. 36634) (A.P.)



Citation: Vega-Hernández, M.Á.; Cano-Díaz, G.S.; Vivaldo-Lima, E.; Rosas-Aburto, A.; Hernández-Luna, M.G.; Martínez, A.; Palacios-Alquisira, J.; Mohammadi, Y.; Penlidis, A. A Review on the Synthesis, Characterization, and Modeling of Polymer Grafting. *Processes* **2021**, *9*, 375. <https://doi.org/10.3390/pr9020375>

Academic Editor: Selestina Gorgieva
Received: 4 December 2020
Accepted: 26 January 2021
Published: 18 February 2021

Publisher's Note: MDPI stays neutral with regard to jurisdictional claims in published maps and institutional affiliations.



Copyright: © 2021 by the authors. Licensee MDPI, Basel, Switzerland. This article is an open access article distributed under the terms and conditions of the Creative Commons Attribution (CC BY) license (<https://creativecommons.org/licenses/by/4.0/>).

Abstract: A critical review on the synthesis, characterization, and modeling of polymer grafting is presented. Although the motivation stemmed from grafting synthetic polymers onto lignocellulosic biopolymers, a comprehensive overview is also provided on the chemical grafting, characterization, and processing of grafted materials of different types, including synthetic backbones. Although polymer grafting has been studied for many decades—and so has the modeling of polymer branching and crosslinking for that matter, thereby reaching a good level of understanding in order to describe existing branching/crosslinking systems—polymer grafting has remained behind in modeling efforts. Areas of opportunity for further study are suggested within this review.

Keywords: polymer grafting; polymer synthesis; polymer characterization; mathematical modeling; polymer reaction engineering; reversible deactivation radical polymerization

1. Introduction

Graft copolymers consist of branches of polymer segments covalently bonded to primary polymer chains. Graft copolymers containing a single branch are known as *microarm* star copolymers. The backbone and branches can be homo- or copolymers with different chemical structures or compositions [1]. However, if the polymer molecule is a homopolymer, the reaction route to produce the branches is known as polymer branching; polymer grafting is usually considered as a chemical route to produce materials whose branches are chemically different from the backbone or primary polymer chain. The branches typically have the same chain size and are randomly distributed throughout the backbone's length as a consequence of the synthetic route used to synthesize them. However, more efficient methods that allow the synthesis of graft copolymers with equidistant and same-length branches, with which the microstructure and composition can be controlled to a remarkable level, have been developed [1]. From a surface-chemistry perspective, this definition of polymer grafting is extended to composites in which the main chain constitutes a diverse array of materials, ranging from brick and fiberglass to paper and wood [2]. Materials with improved or simply different polymer properties from mechanical, thermal, melt flow or dilute solution perspectives can be synthesized by polymer

grafting [1,3–7]. The structure–properties relationship has been an important issue in the analysis of polymer grafting [1].

Some of the first reports on polymer grafting available in the open literature (e.g., the oldest records available through Web of Science) include the grafting of polystyrene (PSty) [8] and poly(methyl methacrylate) (PMMA) [9] onto “government rubber styrene” (GRS) [8], which is a synthetic copolymer of butadiene and styrene, or onto natural rubber [9]; grafting of PSty, poly(butyl methacrylate) (PBMA), poly(lauryl methacrylate) (PLMA), poly(methyl acrylate) (PMA), and poly(ethyl acrylate) (PEA) onto PMMA with pendant mercaptan groups [10]; grafting of polyacrylamide (PAM) onto polyacrylonitrile (PAN), or the other way around (PAN onto PAM) [11]; grafting of PMMA onto PAN [12]; grafting of PSty onto polyethylene (PE) [13]; and grafting of several polymers, such as PAN, PMMA, PSty, poly(acrylic acid) (PAA), and poly(vinylidene chloride) (PVDC), onto cellulose [14–16], to name a few. A more complete literature review on the chemistry of polymer grafting is summarized in Table 1.

Table 1. Overview of the synthesis and characterization of grafted copolymers with an emphasis on the period 1950 to 1970, plus some additional, more recent ones.

Backbone	Functionalization Method	Graft Chains	Grafting Technique	Grafting Conditions	Measured Properties and Characterization Methods	Ref.
Rubber (GRS or natural)	Generation of internal free radicals by CTP.	PSty or PMMA	Grafting from	95–180 °C; Mass FRP (rubber dissolved in monomer, in presence of initiator); solvent-non-solvent fractionation.	Determination of vinyl unsaturation (peracid and infrared methods); molecular weight by intrinsic viscosity; DMA; mechanical properties: tensile strength, elongation-at-break, hardness, modulus at 100 and 300% elongation, as well as tear at 20, 80, and 120 °C.	[8,9]
PMMA (a copolymer of MMA and small content of GMA)	Incorporation of mercaptan groups by reaction of GMA and hydrogen sulfide in presence of sodium ethoxide catalyst.	PSty, PBMA, PLMA, or PMA	Grafting from	Mass or solution polymerization of monomer in presence of PMMA with pendant mercaptan groups (grafting occurs by chain transfer to mercaptan groups).	Solvent extraction of ungrafted polymer, measured by UV analysis; grafting efficiency calculated with the aid of a kinetic model.	[10]
Either PAN or PAM	Two methods used: (a) CTP; (b) photolysis of a copolymer containing a few per cent of ACN.	PAM, PAN; PMMA (onto PAN) [12]	Grafting from	(a) SP in sodium perchlorate at 55 °C, using persulphate-bisulphite; (b) SP in sodium perchlorate at 25 to 35 °C in a quartz tube under a G.E. Sun Lamp.	Composition by IR; molecular weight by intrinsic viscosity calibrated from light scattering data; phase contrast microscopy; measurement of softening points; analysis of X-ray scattering curves [12].	[11,12]
PE	UV irradiation of surface of sensitized PE.	PSty	Grafting from	(a) Sensitized PE irradiated one minute, stand a week, and then proceed to mass polymerization in Sty at 70 °C; (b) irradiation of plastic in presence of Sty.	Mass difference or ability of the surface to adhere to pressure-sensitive tape under load.	[13]
Cellulose	γ -ray pre-irradiation technique.	PSty	Grafting from	Pre-irradiation by Co ⁶⁰ γ -rays in water or in a H ₂ O ₂ solution; grafting in a 20 vol. Sty solution (methanol/water) at 50 °C.	Degree of grafting by weight gain; estimation of active sites by the ferrous ion method; solubilization of material by acetylation and acetolysis, followed by IR spectroscopy.	[14]
Cellulose	Binding initiators or components of initiation systems by means of ion exchange with such materials.	Various polymers (PAN, PMMA, PSty, PAA, PVDC)	Grafting from	Starting material contacted with a dilute solution of catalyst cation salt; the exchanged cellulose was then placed in the monomer or monomer solution; the mixture was heated or irradiated for the required time.	Swelling by centrifuging; grafting efficiency by solvent extraction; mechanical properties (elongation, moduli; toughness); chemical properties (basic/acid dyeing and hydrolysis, bromination, oxidation, complex formation, etc.); wetting; rotproofing.	[15]

Table 1. Cont.

Backbone	Functionalization Method	Graft Chains	Grafting Technique	Grafting Conditions	Measured Properties and Characterization Methods	Ref.
Cellulose	Formation of free radicals in cellulose by exposure to high energy electrons or to γ -rays from Co^{60} .	PSty	Grafting from	Sty brought into intimate contact with cellulose by the inclusion technique; then, (a) perform irradiation with high energy electrons using a 2-M.e.v. Van de Graaff accelerator; or (b) induce grafting by γ -ray irradiation.	Degree of grating and grafting efficiency from extraction curves (mass determination); drastic hydrolysis of cellulose backbone and molecular weight determination of isolated PSty chains by intrinsic viscosity; calculation of grafted chains per cellulose chain.	[16]
Terpolymer of ethylene–ethyl acrylate–maleic anhydride (EEAMA)	Step-growth polymerization (SGP) between maleic anhydride (MANh) from EEAMA and amine groups from PDMS.	Polydi-methyl-siloxane (PDMS)	Grafting to	Melt reactive mixing proceeded in a Haake Rheocord 3000 batch mixer; $T = 140\text{ }^{\circ}\text{C}$.	Composition and evidence of grafting by ^1H and ^{13}C nuclear magnetic resonance. Molecular weight distributions (MWDs) were determined using a GPC or SEC chromatograph (Alliance GPCV 2000, Waters) with refractive index viscometer detectors. Linear viscoelastic properties were determined using a rheometer (AR 2000, TA Instrument) with a cone-and-plate configuration.	[17]
Cores of different polymers: polystyrene substrates; arborescent poly(γ -benzyl L-glutamate) (PBG)	Typically, successive anionic grafting reactions of pre-formed side chains onto substrates randomly functionalized with coupling sites (e.g., alkyne-azide click chemistry coupling)	poly(2-vinyl pyridine), polyisoprene, poly(tert-butyl methacrylate), and poly(ethylene oxide); poly(γ -benzyl L-glutamate) (PBG); polyglycidol, poly(ethylene oxide) (PEO), or poly(L-glutamic acid) (PGA)		“Dendrigraft polymers” synthesized by different chemical routes.	MWD determined by SEC and static light scattering; morphology of arborescent polystyrene molecules determined by small-angle neutron scattering (SANS); film formation of isoprene copolymers on mica surfaces investigated using atomic force microscopy (AFM) after spin-casting from different solvents; morphologies of core-shell-corona copolymers studied by transmission electron microscopy (TEM).	[18–26]

Abbreviations. ACN: α -chloroacrylonitrile; CTP: chain transfer to polymer; DMA: dynamic mechanical analysis; FRP: conventional free-radical polymerization; GMA: glycidyl methacrylate; IR: infrared spectroscopy; PAA: poly(acrylic acid); PALA: poly(allyl acrylate); PAM: polyacrylamide; PAN: polyacrylonitrile; PBMA: poly(butyl methacrylate); PE: polyethylene; PLMA: poly(lauryl methacrylate); PMA: poly(methyl acrylate); PMMA: poly(methyl methacrylate); PSty: polystyrene; PVDC: poly(vinylidene chloride); REX: reactive extrusion; SP: solution polymerization.

The renewed emphasis on the use of biobased monomers and biopolymers as a viable route to decrease (synthetic) polymer waste and disposal issues has invigorated the research efforts on the development of improved materials with important contents of biopolymers (frequently as backbones); grafting is part of the synthetic procedure of such materials. These trends are in the scope of some recent review papers focused on polymer grafting, which include the grafting of polymers onto cellulose [27,28], chitin/chitosan [29,30], or polysaccharides in general [2,31].

The use of lignocellulosic waste as raw material for biorefining processes aimed at producing value-added chemicals or materials (e.g., bioethanol, cellulose, xylose, or hybrid materials, to name a few) has increased significantly since the start of the present century. Biorefineries from lignocellulosic waste require multistep processes, starting with pretreatment of the biomass. In this way, the constituent biopolymers are available for subsequent reactive processes [32–35]. The synthesis of value-added materials from lignocellulosic waste biomasses by using polymer grafting onto lignocellulose itself [36] or onto its individual components (cellulose [27], hemicellulose [37], or lignin [38]) represents an important route in the concept of biorefineries.

Although a few early studies focused on the mathematical descriptions of polymer grafting under specific circumstances—such as the calculation of grafting efficiency and molecular weight development of the grafted branches onto a pre-formed polymer containing pendant mercaptan groups capable of acting as effective chain transfer agents, based on a comprehensive kinetic model including chain transfer to polymer and bimolecular polymer radical termination [39], or the theoretical calculation of molecular weight distributions of vinyl polymers grafted onto solid polymeric substrates by irradiation, also based on a kinetic description of the growing of the grafted branches [40], and a few comprehensive recent models for other specific situations (e.g., the detailed description of free-radical polymerization (FRP)-induced branching in reactive extrusion of PE [41])—are indeed available, the fact is that the cases addressed by mathematical models are by far less common than the available experimental systems. The purpose of the present review is to first offer a rather detailed summary of what is known from a polymer chemistry angle about polymer grafting, with an emphasis on what backbones and grafts are used, how active sites on backbones are generated, and how polymer branches are grown or grafted, among other process details. The second objective is to review what polymer grafting situations have been modeled, which tools have been used, and what limitations persist. By doing that, we can show areas of opportunity. Do keep in mind that the system that motivated this study was the grafting of synthetic polymers onto lignocellulosic biopolymers.

2. Chemistry of Polymer Grafting

The main chemical routes for polymer grafting are the following: “grafting onto” (also referred as “grafting to”), “grafting from,” and the macromonomer or macromer (or “grafting through”) method [1,2,27,28]. There are general reviews focused on the synthesis of grafted copolymers [1,2]. The ranges of backbones and grafts, backbone activating methods, graft growing (polymerization) routes, characterization techniques, quantification methods of grafting and branching molar mass distributions, and applications are so vast that reviews on specific aspects or subtopics related to these issues have been written. For instance, there are reviews focused on the grafting of polymer branches onto natural polymers [42] and biofibers [43]; grafting onto cellulose [27] or cellulose nanocrystals [28]; grafting onto chitin/chitosan [29,30]; microwave-activated grafting [31,44]; laccase-mediated grafting onto biopolymers and synthetic polymers [2]; radiation-induced RAFT-mediated graft copolymerization [45]; and polymer grafting onto inorganic nanoparticles [46] to name a few.

Herein, brief descriptions of such chemical routes are provided. In Table 1 we provide an overview of the grafted copolymer materials synthesized in the 1950–1970 period, plus some additional more recent cases, considering backbone structure, functionalization or active site generation techniques or procedures, grafted arm structure, polymer grafting

technique, polymer grafting conditions, measured properties and characterization methods, and related references. The literature on polymer grafting onto cellulose, chitin/chitosan, lignocellulosic biopolymers, other polysaccharides and natural biopolymers, inorganic materials, and metallic surfaces is addressed in the subsequent sections of this review.

2.1. Types of Polymer Grafting

As stated earlier, polymer grafting can proceed by the “grafting to” technique, where a polymer molecule with a reactive end group reacts with the functional groups present in the backbone; by “grafting from,” where polymer chains are formed from initiating sites within the backbone; and by “grafting through,” where a macromolecule with a reactive end group copolymerizes with a second monomer of low molecular weight. Simplified representations of these grafting techniques are shown in Figure 1.

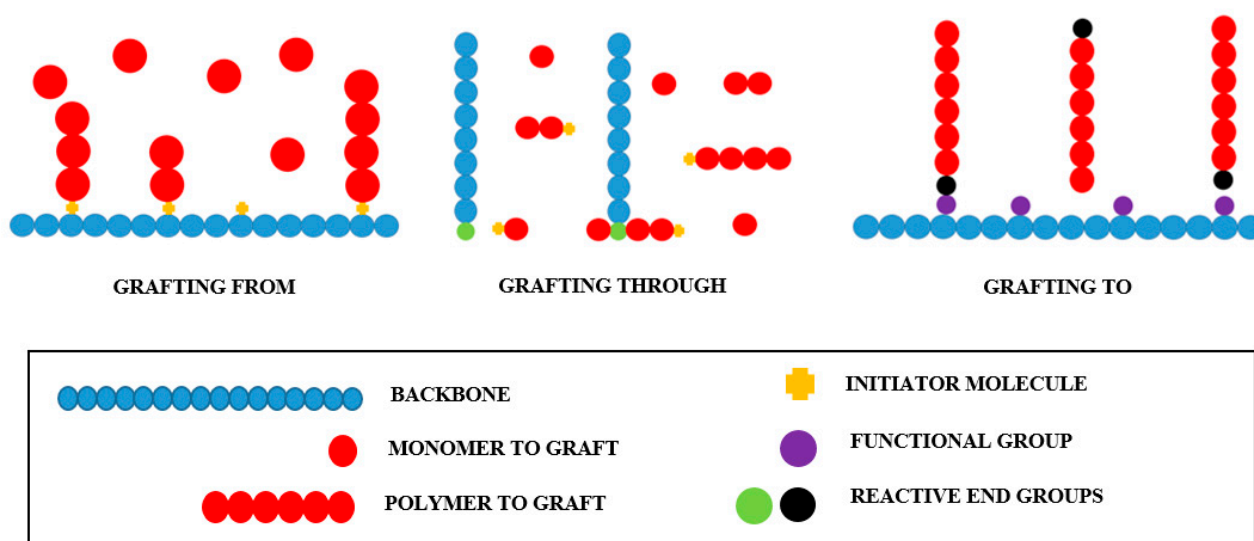


Figure 1. Polymer grafting chemical routes.

“Grafting to” and “grafting from” are the most common polymer grafting chemical routes. Better defined graft segments are obtained by the “grafting to” technique since the polymerization is independent of the union between the backbone and grafts. In contrast, materials of higher grafting densities can be produced by the “grafting from” route due to the lack of steric hindrance restrictions [47].

However, each polymer grafting route has its own advantages and disadvantages in terms of chemical nature, density, dispersity, and length of the grafts obtained, and the ease and efficiency of the chemical reactions involved. Interestingly, different polymer grafting routes can be combined to produce specific grafted materials [48].

2.2. Main Backbones Used in Polymer Grafting

A polymer backbone is a polymer molecule that supports polymeric side chains, called branches or grafts. Side chains can be inserted onto the backbone during the synthesis of the backbone (copolymerization situation) or as a post-production process of the backbone [49]. In the first case, polymers with homogeneous bulk properties are obtained. The second case is very attractive since it allows the modification of many polymeric materials, including natural and synthetic fibers, or inorganic and metal particles. Backbones processed by polymer modification do not usually show significant changes in bulk properties. Surface modification is often carried out following a “grafting from” technique; that is why this method is also known as surface initiated polymerization (SIP) [50]. The backbones used for polymer grafting can be synthetic polymers, biopolymers, or inorganic and metal surfaces.

Synthetic polymers are human-made polymers and include a wide variety of materials, such as polyolefins, vinyl and fluorinated polymers, nylons, etc. The applications of synthetic graft copolymers include the synthesis of antifouling membranes [51], stimuli-response materials [52], and biomedical applications [53].

Biopolymers are produced by the cells of living organisms. Polysaccharides have become important lately because of their characteristics of availability, biocompatibility, low cost, and non-toxicity, making them candidates for substitution of petroleum-based materials [47]. Polysaccharide-based graft copolymers are used as drug delivery carrier, food packaging and wastewater treatment [54]. Some of the most studied polysaccharides are cellulose [27,28], lignin [55], chitin/chitosan [29,56–58], starch [59], and various gums [42].

Surface functionalization of inorganic and metallic particles that allow the incorporation of polymer shells by polymer grafting has also become important, since polymer coatings alter the interfacial properties of the modified particles. Zhou et al. reviewed different applications for inorganic and metallic particles grafted with biopolymers [50]. One important inorganic surface modified by polymer grafting is silica [60].

2.3. Backbone Functionalization Methods

Several chemical modification procedures have been developed due to the wide variety of backbones of interest. Chemical modification reactions depend on the functional groups (or absence thereof) along the backbone. Two main chemical routes used to attach, grow, or graft polymer molecules onto lignin have been proposed [55]: (a) creation of new chemically active sites, and (b) functionalization of hydroxyl groups.

The introduction of functional groups into a polymer backbone increases its reactivity, making it accessible for forward polymerization or coupling reactions. Functionalization reactions are therefore required to generate the end functional pre-formed polymer or the reactive end of the macromolecule species involved in the “grafting to” and “grafting through” polymer grafting techniques, respectively. Functionalization is also required in the formation of the macromolecular species, such as macro-initiators and macro-controllers, involved in the “grafting from” polymer grafting technique [27,61]. The most important functionalization reactions involved in polymer grafting include sulfonation, esterification, etherification, amination, phosphorylation, and thiocarbonation, among others.

2.4. Backbone Activation Methods

Another way to generate grafting sites within the polymer backbone is to use polymer grafting activators, such as free-radical initiators. As shown in Figure 2, polymer grafting activators can be classified into physical, chemical, and biological. The main characteristics of these activators are highlighted in Sections 2.4.1–2.4.4.

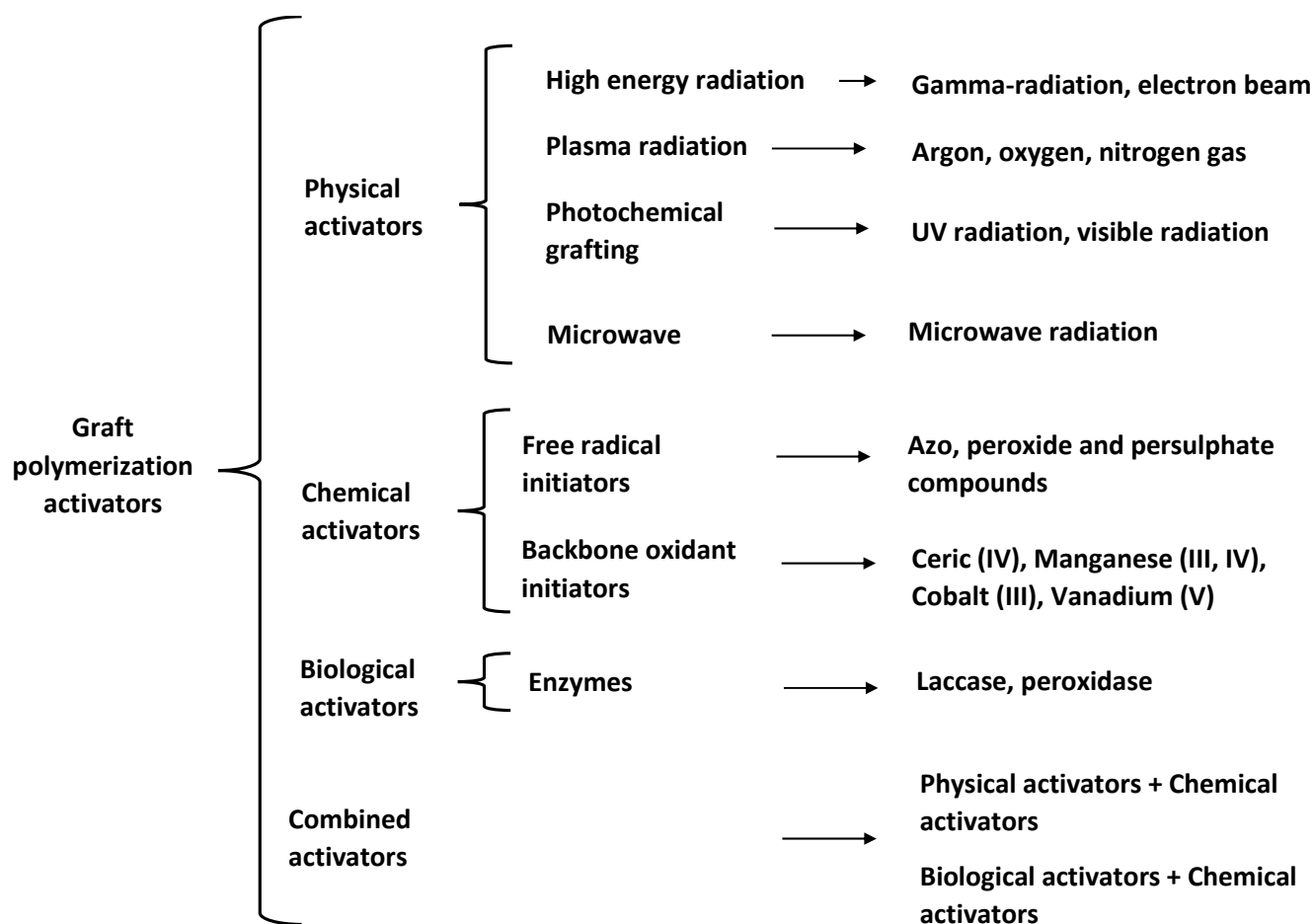


Figure 2. Backbone activators used for polymer grafting.

2.4.1. Physical Activators

High energy radiation, also referred to as ionizing radiation, includes γ -beam and electron-beam radiations. Radiation-promoted grafting may follow one of three possible routes: (a) pre-irradiation of the backbone in the presence of an inert gas to generate free radicals before placing the backbone in contact with monomers; (b) pre-irradiation of the backbone in an environment containing air or oxygen to produce hydroperoxides or diperoxides in its surface, followed by high temperature reaction with monomer; and (c) the mutual irradiation technique, where backbone and monomer are irradiated simultaneously to generate free radicals [62].

Plasma is a partially ionized gas where free electrons, ions, and radicals are mixed. Different functional groups can be introduced, or free radicals can be generated on backbones by this process, depending on the gas used. Polymer grafting reactions carried out in plasma are sometimes classified as high energy radiation reactions [63].

The absorption of UV light on the surface of the material generates free radicals that serve as nucleation sites. The surface is then placed in contact with monomer for subsequent polymerization [64].

Microwave irradiation consists of direct interaction of electromagnetic irradiation with polar molecules and ionic particles, promoting very fast non-contact internal heating, which enhances reaction rates and leads to higher yields. Singh et al. carried out a successful polymerization of acrylamide on guar gum under microwave irradiation [65]. They proposed a mechanism in which free radicals are produced within the polysaccharide backbone by the effect of microwave irradiation on the hydroxyl groups of the biopolymer [65].

2.4.2. Chemical Activators

As shown in Figure 1, chemical activators include free radical and backbone oxidant initiators. Free radical initiators are compounds that present either direct or indirect homolytic fission. The first case involves the initiator itself and the second one requires participation of another molecule from the environment [66].

Oxidant initiators react directly with functional groups from the backbone, generating activation sites. Polymer grafting of polysaccharides using oxidant initiators has been reported in the literature [66].

2.4.3. Biological Activators

Enzymes catalyze polymer modification reactions through functional groups located at chain ends, along the main chain, or at side branches, promoting highly specific non-destructive transformations on backbones, under mild reaction conditions. Successful grafting of lignin by oxidation of its phenolic structures using laccases has been reported recently [2].

2.4.4. Combined Activators

Combinations of physical and chemical activators for polymer grafting have been successfully carried out. For instance, microwave assisted polymerization (MAP) has been combined with the use of chemical activators for the production of hydrogels synthesized by crosslinking graft copolymerization, taking advantage of the short reaction times required to obtain high yields [67,68]. Enzymes are also used in combination with radical initiators for more effective grafting copolymerization processes [69,70].

2.5. Polymer Grafting by Free-Radical Polymerization

As stated earlier, the “grafting through” and “grafting from” techniques require a polymerization reaction to bond the polymer grafts to the backbone. Different polymerization methods have been used for polymer grafting, but the most effective ones use free radical methods (e.g., FRP, RDRP, and REX), due to their versatility to work with different chemical groups, and their tolerance to impurities. A short overview on free-radical polymerization reactions is presented in Table 2. Polymer grafting by FRP, and other reactions, is affected by several factors, including the chemical nature of the components contained in the system—backbone, monomer, initiator, and solvent—and the interactions among them. Other aspects related to polymer grafting, including temperature and the use of additives, need to be considered [67]. The synthetic routes and activators used in graft polymerization provide a variety of interesting and versatile routes for this type of polymer modification.

Table 2. Free-radical polymerization methods.

Polymerization Method	General Description	Type of Reaction
Conventional free-radical polymerization (FRP)	Three steps involved: (1) initiation, with formation of free radicals; (2) propagation, where free radicals react with monomer; and (3) termination of polymer radicals by either combination, disproportionation, or chain transfer to small molecules. The simultaneous participation of these reactions leads to broad molar mass distributions.	Chain transfer reaction: free radicals generated in the system tend to react with backbones by CTP, thereby activating them. Direct generation of free radicals along the backbone: activators generate free radicals from reaction with functional groups placed along the backbone, which correspond to the initiating step of a SIP [27].

Table 2. Cont.

Polymerization Method	General Description	Type of Reaction
Reversible deactivation radical polymerization (RDRP)	A group of polymerization techniques based on free radical technology that controls the growth of polymer molecules during the polymerization. Polymer radicals are reversibly deactivated by effect of controllers that act under some relatively new chemical routes. These techniques allow the development of advanced materials, with various architectures, and well-defined microstructures. Each technique has its own mechanism and conditions that favor them. SIP can proceed by any of the known RDRP techniques.	Atom transfer radical polymerization (ATRP): It is a catalytic process where an alkyl halide macromolecule reacts with the catalyst, allowing the formation of a radical that propagates until it reacts again with the catalyst, in a reversible way [71]. Nitroxide mediated polymerization (NMP): A stable nitroxide free radical acts as controller, reversibly deactivating the propagating and polymer radicals forming dormant polymer molecules with alkoxyamine end functionalities [50]. Reversible addition-fragmentation chain transfer (RAFT) polymerization: Thiocarbonilthio compounds are used as chain transfer agents which control molecular weight development by reversible activation-deactivation reactions [50].
Reactive extrusion (REX)	REX is a set of techniques designed to produce and modify polymers, typically carried out in single or twin extruders. Five main types of reactive polymerizations carried out in extruders have been reported: bulk polymerization, polymer grafting, polymer functionalization, controlled degradation, and reactive blending [72]. Reactions proceed in melt phase. Examples of polymer grafting by REX include polyolefin [73] and starch modifications [74].	Polymer modification by free-radical polymerization: Free radical initiators such as peroxides are used to generate activate sites within the backbone [73,75]. Polymer modification by insertion of active pendant groups: It consists of the copolymerization of monomers who have no functional groups with co-monomers possessing pendant which make polymer grafting easier to accomplish [49].

3. Backbones and Supports Used in Polymer Grafting

As explained earlier, grafted materials consist of side chains or arms attached to primary polymers referred to as backbones. The purpose of polymer grafting is to combine chemical, mechanical, interfacial, electrical, or other polymer properties between the constituent materials. The diversity of backbones and the ways in which side chains are attached to them through polymer grafting will be briefly overviewed in this section.

3.1. Cellulose, Lignin, and Lignocellulosic Biomasses as Backbones

Lignocellulosic biopolymers are abundant in nature. They are made of cellulose, hemicellulose, and lignin. They also contain moisture, extractive organic compounds, and ashes from inorganic compounds in lesser amounts. Each of these components has distinct characteristics. The extractive organic compounds present in lignocellulosic biopolymers are oligomers and oligosaccharides of low molecular weight, sugars, fatty acids, resins, etc. [76].

Cellulose, hemicellulose, and lignin can be modified by polymer grafting leading to new promising materials with interesting properties. However, the extractables are not useful for this purpose since they are not part of a skeleton or stiff structure that may provide support or mechanical stability. Extractables also consume reactants required for the grafting process. They are usually removed prior to the polymer grafting process, although in some studies, they remain in the system during the formation of grafted arms [77].

Polymer grafting of xylan onto lignin has been studied since the early 1960s. Early reports on the topic reported the grafting of organic polymers, such as 4-methyl-2-oxy-3-oxopent-4-ene and methyl methacrylate polymers [78,79], xylan [80], ethylbenzene, and styrene [81–84], onto lignin or lignin derivatives. The topic of polymer grafting of synthetic polymers onto lignocellulosic biopolymers has gained renewed relevance in the last two decades due to environmental and sustainability issues [27,85–94].

Table 3. Overview of grafting of synthetic polymers onto cellulose and natural fibers.

Backbone	Functionalization Method	Grafted Chains	Grafting Technique	Grafting Conditions	Measured Properties and Methods	Refs.
Cotton fabric	FRP by a cellulose thiocarbonate-AIBN redox system.	PMMA, PAA, PAN, PAM	Grafting from	T = 60–80 °C.	Degree of grafting (GP), gravimetric method.	[95]
Cellulose	FRP by a KPS-FAS REDOX system.	PSty, PAN	Grafting from	T = 60 °C; t = 3 h; [STY] = 0.65 M [KPS] = 0.14 M; [FAS] = 0.01 M.	GP, gravimetric method; FTIR and TGA to corroborate GP.	[96]
Cellulose fabrics	FRP by KPS initiation.	PIA	Grafting from	T = 55–80 °C; t = 2.5–5 h; [KPS] = 0.05–0.5 M; [IA] = 0.5–4 M.	GP, gravimetric method; FTIR, XRD, TGA and SEM to corroborate grafting.	[97]
Cellulose	FRP by CAAC initiation.	PMBA, P(N-VP)	Grafting from	T = 30–70 °C; [CAAC] = $2 - 30 \times 10^{-5}$ M.	Grafting yield (GY) and other grafting parameters; gravimetric method.	[98,99]
Cellulose	FRP by CAN-NAC REDOX system.	PEA, PNIPAAm, PAAM-PEA, (AAM-EMA), P(AAM-MA), P(AN-EMA)	Grafting from	T = 10–60 °C; t = 24 h; [CAN] = $1.5 - 32 \times 10^{-3}$ M; [NAC] = $2.5 - 8 \times 10^{-2}$ M.	GY and other grafting parameters, gravimetric method; FTIR and TGA to corroborate grafting. FTIR and EA for composition. MMass by viscometric method and GPC.	[100–105]
Cellulose microfibers	Redox initiation.	PAA	Grafting through	KPS = 0.1–0.4% respect to fiber weight. t = 3 h, T = 75 °C	GP, gravimetric method; FTIR and TGA to corroborate GP.	[106]
Cellulose powder	Co(acac) ₃	N'N'-MBA [98], or N-VP [99]	Grafting from	Cellulose washed with CH ₃ OH, C ₃ H ₆ O, and water; then dried. Reaction under nitrogen atmosphere. Different temperatures, 30–60 °C [98], or 40–50 °C [99]; reaction carried out in water. Kinetic data from 0–150 min [86], or 0–120 min [99].	Percent grafting (% G), true grafting (% GT), grafting efficiency (% GE), homopolymer conversion (% CH), cellulose conversion (% CC), and total conversion (% CT) by gravimetric methods.	[98,99]
Cotton linter Cellulose powder	Ceric ammonium sulfate, 1% sulfuric acid.	AcN EA MMA	Grafting from	Cellulose treated with sodium hydroxide 5–30 % wt./vol at 25 °C. Grafting temperatures: 30, 40 and 60 °C, sodium bisulfite clay as initiator. Polymerization in diluted HCl for 2 h.	Percent grafting (% G), true grafting (% GT), grafting efficiency (% GE), by gravimetric methods.	[107]

Table 3. Cont.

Backbone	Functionalization Method	Grafted Chains	Grafting Technique	Grafting Conditions	Measured Properties and Methods	Refs.
Hydroxypropyl cellulose (HPC)	Steglich esterification of PABTC onto HPC using DCC and DMAP.	EA NIPAAAM	Grafting from	Steglich esterification using DCC and DMAP in chloroform at 40 °C, in presence of HPC and PABTC. 6 days for 50% conversion. Polymerization of EA and NIPAAAM at 60 °C using AIBN; 94% conversion with free polymer in DMAc.	Tg by DSC at 45, 55 and 135 °C for PNIPAAAM, and Tm at 157 °C. TGA from ambient to 600 °C at 10 °C/min, nitrogen atmosphere for HPC, PINIPAAAM and the grafted HPC-g-PNIPAAAM. ¹ HNMR for degree of substitution. SEC for HPC Macro CTA and HPC-g-PNIPAAAM.	[108]
Cellulose chloroacetate (CellClAc)	Macro initiator, Cu(I)Cl/2'2'BIPI catalytic system via ATRP controller.	4NPA MMA	Grafting from	ATRP of 4NPA and MMA carried out in DMF at 130 °C for 24 h, in the presence of CellClAc as macro initiator, Cu(I)Cl/2,2'BIPI catalytic system. Grafting conversion under 15%.	NMR, FTIR, TGA, and elemental analysis.	[109]
Cellulosic <i>Grewia optiva</i> fibers	Redox initiation using FAS-H ₂ O ₂ for grafting of MA, and KPS for polymerization of MA.	MA	Grafting from	1 g of mercerized <i>Grewia optiva</i> fibers was set in distilled aqueous solution with NaOH for 24 h, followed by addition of redox initiator (FAS-H ₂ O ₂). Solution was stirred for 10 min; MA was then added. Solution was polymerized using microwave irradiation at different times.	FTIR, SEM, TGA, swell index.	[110]
Cellulose acetate	Solvents: DMSO, PDX, DMAc, C ₃ H ₆ O. Initiators for grafting and polymerization: CAN, Sn(Oct) ₂ and BPO.	MMA	Grafting from	Focus on solvent effect. 1.25 g of cellulose acetate were dissolved in 125 mL of solvent. CAN or Sn(Oct) ₂ or BPO (0.3–0.5 g) were added with MMA (1.25–2 mL). Nitrogen atmosphere, 2–6 h, 30–80 °C, except acetone, which proceeded at 55 °C.	Grafting yield (GY), total monomer conversion (TC), grafting efficiency (GE) and number of grafting chains per cellulose acetate molecule were obtained by gravimetric methods. TGA, GPC, FTIR, ¹ HNMR.	[111]
Cellulose chloroacetate (CellClAc)	Macro initiator, Cu(I)Cl/2'2'BIPI catalytic system via ATRP controller.	NCA MMA	Grafting from	ATRP of NCA and MMA in DMF at 130 °C, in the presence of CellClAc.	FTIR, TGA, and elemental analysis.	[112]

Table 3. Cont.

Backbone	Functionalization Method	Grafted Chains	Grafting Technique	Grafting Conditions	Measured Properties and Methods	Refs.
Cellulose cotton fibers	Na ₂ CO ₃ and thermal activation.	MTC-b-CD	Grafting to	Grafting of MCT-β-CD onto cotton fabric carried out in alkaline medium; 1 mg of cellulose fiber was impregnated with solutions of 50–150 g/L of MCTβ-CD and 20–80 g/L Na ₂ CO ₃ . Solvent was eliminated at room temperature before heating at 100–160 °C, for 10, 15 and 20 min. Sample were washed to obtain neutral pH. Silver nitrate solutions were added in situ for some samples.	FTIR and microbiological tests [113]. Gravimetric methods and analytical modeling [114]. MODDE software was used to study the relationship between 3 significant independent variables and degree of grafting.	[113,114]
Cotton linter cellulose	CTP using APS as initiator.	MMA	Grafting from in situ polymer formation (embedded)	Cellulose pre-swelling: Cellulose was pre-swollen in DMAc at 160 °C for 0.5 h. Pre-swollen cellulose was filtered. A solution of LiCl in DMAc (8%, w/w) was prepared. The pre-swollen cellulose was added to the DMAc/LiCl solution. The mixture was stirred at 100 °C for 2 h and purged with gaseous N ₂ . MMA polymerization was carried out at 70–90 °C using APS and DMSO.	TGA-DTA, FTIR, SEM, XRD.	[115]
Microcrystalline cellulose	Ring-opening polymerization (ROP) of L-LA with DMAP in an ionic liquid AmimCl.	PLLA	Grafting from	A 4% (w/w) microcrystalline cellulose/AmimCl solution was prepared and stirred at 60 °C, in N ₂ environment for 1 h. L-LA and DMAP were then added. The sample was degassed 3 times in vacuum/N ₂ during 1 h cycles. ROP proceeds at 90 °C in presence of N ₂ atmosphere during 11 h.	Controlled release of vitamin C. Characterization by ¹ HNRM, UV analysis, XRD, TEM, and HPLC.	[116]

Table 3. Cont.

Backbone	Functionalization Method	Grafted Chains	Grafting Technique	Grafting Conditions	Measured Properties and Methods	Refs.
Cellulose (DP=1130)	CTP; APS and MMA embedded.	MMA	Grafting from	Cellulose is pre-swollen in DMAc during 30 min, at 160 °C. 5 g of pre-swollen cellulose are mixed with 95 g of water and proper amounts of APS and MMA. Grafting proceeds at 80 °C. Excess of PMMA was washed with acetone. Macromolecular initiator: Br-iBuBr, CNC, and TEA were dissolved in DMF, and stirred under N ₂ at 70 °C for 24 h. CNC, 2-bromoisobutyrate, styrene and copper(I)bromide were dissolved in anisol; PMDETA was then added. The reaction proceeded at 100 °C for 12 h and N ₂ atmosphere via SI-ATRP. The remanent PS homopolymer was eliminated using methanol, and centrifuging. The modified crystals were dosed into PMMA nanocomposites by solution casting.	Characterization: FTIR, WARD-XRD, SEM, and TGA-DTA.	[117]
Cellulose nanocrystal (CNC)	Macromolecular initiator obtained from the reaction between Br-iBuBr and CNC using TEA as catalyst, via SI-ATRP.	STY. Cast in MMA	Grafting from		Characterization: TEM, SEM, FTIR, UV-Vis., XRD, ¹³ C-NMR, TGA, DSC, and tensile test	[118]
Cellulose nanocrystal(CNC)	L-LA in situ polymerization using MgH ₂ as redox agent. PLLA-g-CNC particles were casted in PLLA.	PLLA	Grafting from	1.50 g of L-LA and 0.05 g of CNCs were pre-mixed. 0.03 g of MgH ₂ were then added and stirred during 30 min. The mixture was heated to 110 °C for 3, 6, 10, 12, 18 and 24 h, under nitrogen atmosphere. Casting method: 1.0 g of PLLA and 0.1 g of CNC or 1.3 g of PLLA-g-CNC were dispersed in 10 mL of chloroform or toluene solution and mixed for 10 h. The mixtures/solutions were poured into Teflon [®] plates and let stand for 18 h at 80 °C. The films were dried under vacuum at 60 °C for 72 h at room temperature.	Characterization: FTIR, ¹ HNMR, ¹³ C-NMR, XRD, XPS, TGA, DSC and DMA.	[119]

Table 3. Cont.

Backbone	Functionalization Method	Grafted Chains	Grafting Technique	Grafting Conditions	Measured Properties and Methods	Refs.
Cellulose cotton fiber pulp	(a) Esterification of maleic anhydride grafted onto PHA (through double bond); (b) PHA-g-MA is grafted onto cellulose cotton fiber pulp (through the anhydride group).	PHA-g-MA	Grafting to	Cotton fibers were defibered into pulp to 25°SR using a PL4-2 speed governing beater; 30 g/m ² paper film was then formed in a RK3-KWTjul Rapid-Koethen sheet former. PHA-g-MA was dissolved in refluxing dichloromethane at 60 °C, and the paper film was dipped into the solution of PHA. The PHA/CF composite film was then washed with dichloromethane and dried.	Characterization: FTIR; XRD; SEM; surface roughness; surface hydrophobicity, with contact angle; tensile test, and TGA.	[120]
Cellulosic filter papers	Radiation-induced graft copolymerization (RIGCP) of AcN.	Acrylonitrile	Grafting from	The reaction took place in a glass tube which contained a Whatman filter paper (W1) and a 45% AcN solution in DMF. The solution was irradiated with cobalt-60 g-rays at a dose rate of 4 kGy/h, in air atmosphere. The grafted material was washed with DMF and water, followed by drying (T = 80 °C, 2 h).	Degree of grafting (G%) was determined. Characterization: FTIR, XRD, XRF, TGA and SEM.	[121]
CellClAc	ATRP grafting of the studied monomers using CuCl, 2'2'BIPI as catalyst.	NCHA, 4VP, DA, DAAM.	Grafting from	Cellulose chloroacetate (ATRP macroinitiator) and any of the monomers (NCHA, 4VP, DAAM or DA) were added to 10 mL of DMF; an inert environment was created using argon. The grafting reaction proceeded at 130 °C for 24 h. The proportion of Cell.ClAc, CuCl, 2'2'BIPI and each monomer was 1:1:3:100. The reacting mass proceeded to filtering and washing using acetonitrile, DMF, chloroform, a mixture of water-ethanol-HCl, pure water, ethanol, acetone, and diethyl ether. The product was dried under vacuum.	Characterization: FTIR, UV-Visible, TGA, elemental analysis, and electrical conductivity.	[122]

Table 3. Cont.

Backbone	Functionalization Method	Grafted Chains	Grafting Technique	Grafting Conditions	Measured Properties and Methods	Refs.
Regenerated cellulose fibers (rayon)	Photo-chemical grafting of PETA without photoinitiator.	PETA	Grafting to	Fibers were washed with a solution of PETA in isopropanol. Monomer content of 1% and 5% was used. The cellulosic material was irradiated with a broadband Hg lamp (emission band of 200 and 300 nm), at 50 W/cm. Layer deposition from homo-polymerization and subsequent grafting-to process onto the fiber took place.	Fiber volume content; tensile and fatigue tests; SEM.	[123]
Cellulose nanofibrils	Nitroxide TEMPO insertion and NMP of HEMA	HEMA	Grafting from	Preparation of TEMPO-oxidized cellulose nanofibrils. A suspension was prepared using HEMA (0.15 g), H ₂ O ₂ (0.0075 g), CaCl ₂ (0.0075 g) and TCNF (0.3 wt.%, 500 g), followed by stirring and heating at 50 °C for 4 h. Either freezer freezing, or gradient freezing in liquid nitrogen were used. The nanofibril suspension was set in a freezer (−25 °C). The frozen material pieces were 3 cm height. Drying in a lyophilizer to form aerogels then took place.	Characterization: XRD; FTIR; XPS; SEM; stress-strain under compression analyses; BET analysis and electrical resistivity.	[124]

Cellulose can be extracted from lignocellulose and used as such or modified for other applications. Table 3 provides an overview of grafting of synthetic polymers onto cellulose and natural fibers. (See the tables of Section 6 for explanation of abbreviations and symbols.)

Lignin follows cellulose in abundance on earth, providing a primary natural source of aromatic compounds [125]. Several industrial applications have been attempted for lignin [55, 125–127] but not all of them have succeeded due to different reasons [125,128–130].

Marton [8] described fifty-four different constituents that can be found in lignin based on interpretation of experimental data from biochemical degradation, oxidation, and other ways of decomposition of different types of lignin materials. The combinations and proportions among these structures lead to different properties of lignin materials. Three decades later, Lewis and Sarkanen [130] organized these fifty-four structures into a map that they called phenylpropanoid pathway. As observed in Figure 3, lignins and lignans are monolignol derived compounds. Sharma and Kumar described lignin as a complex material consisting mostly of three single unit lignol precursors, coniferyl alcohol, p-coumaryl alcohol, and sinapyl alcohol, along with other atypical monolignol constitutive units in trace amounts [55].

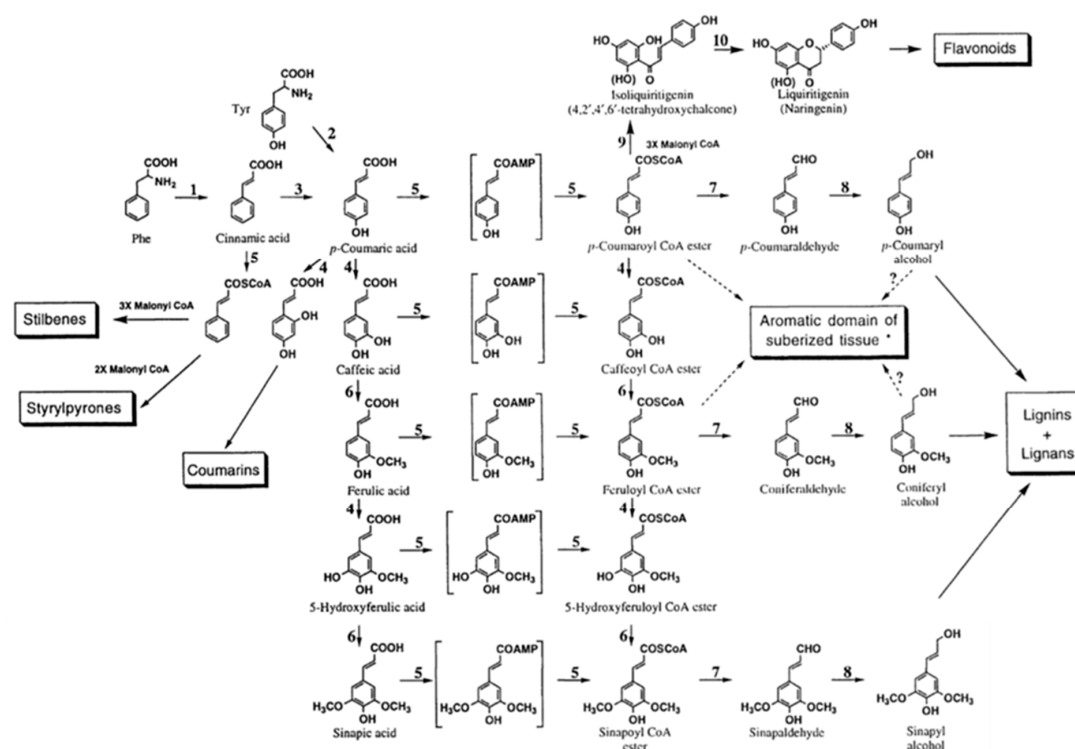


Figure 3. Main steps of the phenylpropanoid pathway: lignins and lignans are monolignol derived. 1, phenylalanine ammonia-lyase; 2, tyrosine ammonia-lyase (mostly in grasses); 3, cinnamate-4-hydroxylase; 4, hydroxylases; 5, CoA ligases involving AMP and CoA ligation, respectively; 6, O-methyltransferases; 7, cinnamoyl-CoA:NADP oxidoreductases; 8, cinnamyl alcohol dehydrogenases; 9, chalcone synthase; 10, chalcone isomerase. (Note: conversions from 7-coumaric acid to sinapic acid and corresponding CoA esters are marked in boxes since dual pathways seem to take place; *: may also involve 7-coumaryl and feruloyl tyramines, and small amounts of single unit lignols). Source: Adapted with permission from Lewis N. G. and Sarkanen S. (1998). Lignin and Lignan Biosynthesis, Washington, D.C.: Oxford University Press pp. 6–7 [130] Copyright © 2021 by American Chemical Society.

The process used for lignin extraction and the final properties of the material depend on the type of biomass employed [55]. Lignin is obtained from woods, which can be hard, soft, bushes, rinds, husks, corncobs, either products or residues. A pulp is obtained from these materials. The yield of lignin extraction depends on temperature, time, dispersion

media, extraction method, and the amount of lignin present in the raw material. Lignin extraction methods can be biological or enzymatic, physical, or chemical. Integrated solutions are employed at the end to remove impurities from lignin so it can be bleached [55]. The complex structure of lignin contains specific surface moieties that provide reactive sites where polymers and other species can be synthesized, bonded, or modified [55]. These moieties were recognized as hydroxyl, carboxyl, carbonyl, and methoxyl groups.

There are two main routes for grafting of polymer chains onto lignin-based biopolymers [55]: (a) synthesis of new reactive sites within lignin's structure; and (b) modification or functionalization of lignin's hydroxyl groups. Route (a) allows lignin to become more reactive, both at the surface, and within the bulk. Polymer modification by route (a) improves both, the properties of lignin and those of the modified materials.

In route (b), a good number of functional groups can be placed in the end groups of lignin (what is sometimes referred to as the surface of lignin). Katahira et al. [131] identified seven side chain structures in the end groups of lignin: p-coumarate, ferulate, hydroxycinnamyl alcohol, hydroxycinnamaldehyde, arylglycerol, dihydrocinnamyl alcohol, and guaiacylpropane-1,3-diol end-units, as shown in Figures 4 and 5 [131]. However, it has been proposed that the phenolic hydroxyl groups shown in Figure 4, and the aliphatic hydroxyl functional groups corresponding to C- α and C- γ positions of the side molecule fragment shown in Figure 5, are the most reactive [55]. Both routes allow one to produce grafted materials, mainly polymers, and most of them come from route (b) above [85,132,133]. Further reports on lignin treatments and grafting can be found elsewhere [55,91,125,128].

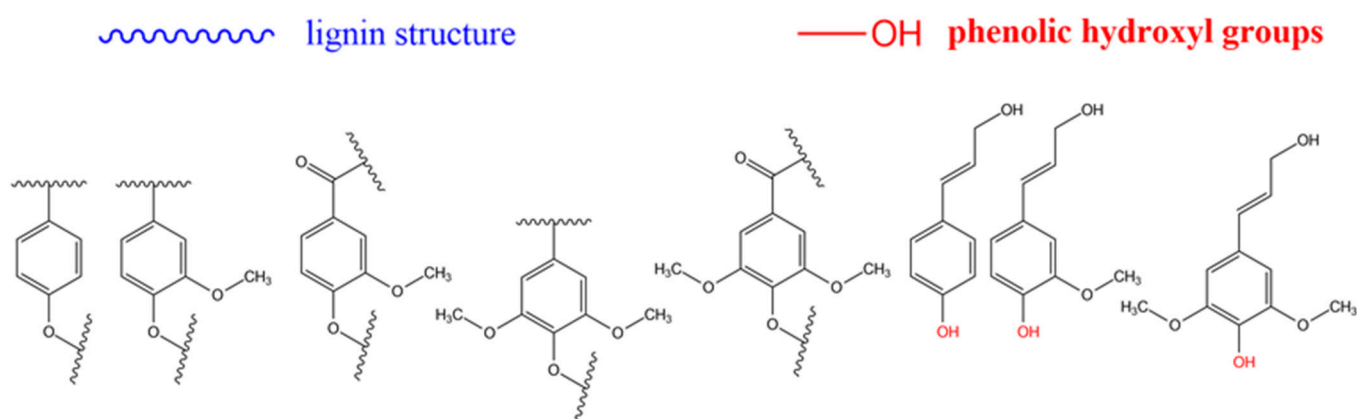


Figure 4. Repeating units in lignin. From left to right: p-hydroxyphenyl, guaiacyl, methoxy guaiacyl, syringyl, methoxy syringyl, p-coumarate, coniferyl alcohol, synapyl alcohol. Source: Adapted with permission from Katahira et al. (2018). Lignin Valorization. Emerging Approaches: Croydon UK pp. 3 [131]. Copyright © 2021 The Royal Society of Chemistry.

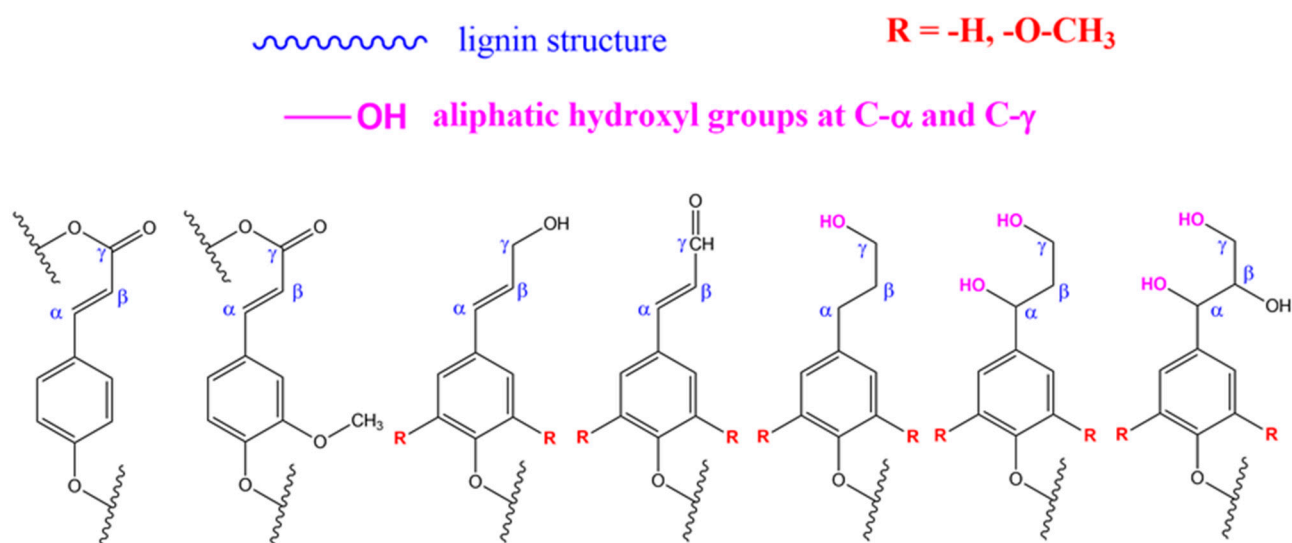


Figure 5. Side chain structure in end-groups in lignin. From left to right: p-coumarate, ferulate, hydroxycinnamyl alcohol, hydroxycinnamaldehyde, dihydrocinnamyl alcohol, arylpropane-1,3-diol, arylglycerol end units. Source: Adapted with permission from Katahira et al. (2018). Lignin Valorization. Emerging Approaches: Croydon UK pp. 5 [131] Copyright © 2021 The Royal Society of Chemistry.

The overview on grafting of synthetic polymers onto cellulose and other lignocellulosic biopolymers presented in Table 3 is further expanded in Table 4 to include other examples of lignocellulosic biomasses, and other natural biopolymers, such as polysaccharides, chitin, and chitosan. Examples of recent research reports (2020–2021) on synthesis of grafted polymers are provided in Table 5. Tables 6–13 contain extensive information related to characterization of polymer grafting. Table 14 summarizes the literature on modeling of polymer grafting. Table 15 shows the polymerization scheme of FRP including CTP and crosslinking. Finally, Tables 16–19 provide information on the many symbols and abbreviations used throughout the review.

Table 4. Overview of grafting of synthetic polymers onto natural polymers: lignin, hemicellulose, polysaccharides, chitosan, and chitin backbones.

Functionalization Method	Grafted Chains	Grafting Technique	Grafting Conditions	Refs.
Steglich esterification of RAFT controller onto organosolv lignin to produce a microcontroller. Subsequent polymerization of soybean oil derived methacrylate monomers.	Poly(soybean oil methacrylate) derivatives. PSBMA, PSBMAH, PSBMAEO	Grafting from	4-cyano-4-(phenylcarbonothioylthio) pentanoic acid was coupled with lignin via Steglich esterification using DCC and DMAP at ambient conditions. [Monomer]/[Lignin-RAFT]/[AIBN] molar ratio = 100:1:0.3; Temperature: 70–80 °C; Time: 24–48 h; Conversion: 74–94%.	[134]
Phosphorylation. S _N 2 reaction mechanism.	Imidazole and POCl ₃ react with (1H-imidazol-1-yl) phosphonic group, which reacts with lignin.	Grafting to	Reacted imidazole-POCl ₃ . DMF, 80 °C, 6h. Lignin-g-(1H-imidazol-1-yl)phosphonic group. 95 °C, 12 h, pH = 3–4 in DMF, yield = 92%. Composites were blended with PP-block-PE, MFI of 1.39 g/10 min (T = 230 °C; standard weight of 2.16 kg), ethylene content 17.8 wt %, from China Petrochemical Co. in a Thermo Haake torque rheometer (180 °C: 10 min; 60 rpm).	[125,135]
	Phosphorus(V) oxide	Grafting to	P ₄ O ₁₀ . Temperature = 20–25 °C, time = 7–8 h. Solvent: THF.	[125,136,137]
Hemicellulose grafting using TBD and ε-caprolactone monomer.	PCL - Hemicellulose (HC-g-PCL)	Grafting from	5 g of dried hemicellulose (5.00 g) were introduced into a reactor containing 10 mL of DMSO at 80 °C. Agitation at 60 rpm took place until a homogeneous viscous solution was obtained. Grafting temperature was 110 °C. ε-caprolactone monomer was added to the hemicellulose solution and agitated during 30 min. TBD, 1% of the total mass, was added. The reaction proceeded during 4 hrs. in a system with flow of nitrogen. Drying at 60 °C under vacuum proceeded for 2 days. FTIR, ¹ HRM, ¹³ CNMR, HSQC, GPC, DSC, TGA-FTIR, Tensile Test, Contact Angle, Biodegradation test.	[37]
Several techniques presented in the review.	Monomers or polymers used in: ATRP: NIPAAM, DMAEMA, STY, MMA, BA, EG; RAFT: AM, AA, others; ROP: PCL, L-LA, EG; Click chemistry: polymer having alkyne or azide groups for the azide-alkyne cycloaddition, EG, PCL, PLLA.	Grafting, from; grafting to; network copolymer grafting	Grafting from: ATRP, RAFT, ROP, and FRP. Grafting onto: Thiol-ene reaction with photo-redox catalysis, click chemistry, epoxide group-mediated reactions, condensation. Network copolymer grafting: Polycondensation, free radical crosslinking.	[9]

Table 4. Cont.

Functionalization Method	Grafted Chains	Grafting Technique	Grafting Conditions	Refs.
Insertion of ACX onto lignin to synthesize a RAFT macrocontroller which polymerized AM and AA.	RAFT polymerization of AM and AA.	Grafting from	0.1 g of RAFT macroinitiator and 0.005 g of AIBN were added to a solution of monomer (0.3 g) in DMF (4 mL). The reactor was degassed with nitrogen for 30 min at ambient conditions. Reaction temperature was 70 °C, target conversion was 98% in 24 h for both monomers. The product was obtained by precipitation, filtration, washing and drying. Grafting was measured using ¹ H NMR. 0.2 g Lignin-g-Pam were dissolved in KOH solution (0.1 g in 1 mL of water), followed by heating (T = 70 °C, t = 12 hrs.), followed by neutralization with HCl. The solution was then precipitated into diethyl ether and dried in air. Ungrafted Pam was withdrawn by extraction with CH ₂ Cl ₂ . The product was vacuum dried, and analyzed by ¹ H NMR and GPC, using adequate solvents.	[138,139]
Several techniques described in the review. Monomers copolymerized with natural extracts.	Several procedures described.	Grafting from Grafting through	Monomers and polymers grafted by: FRP: Guaiacol-AM, Vainillin-LMA. RAFT: Syringyl methacrylate, STY, MMA, 4-propylsyringol, 4-propylguaiacol. ADMET (Acyclic Diene Metathesis Polymerization) and ROP: Ferulic acid, isorbide, butanediol.	[140]
ATRP	NIPAAM → PNIPAAM	Grafting from	Backbone: Kraft lignin (alkali); Catalyst: CuBr/PMDETA; Solvent: water/DMF; T = 50 °C; Thermoresponsive material.	[140,141]
ATRP	DAEA → PDAEA	Grafting from	Backbone: Organosolv lignin; Catalyst: CuBr/Me ₆ TREN; Solvent: THF; T = 65 °C; Hydrophobic polymer composites.	[140,142]
ATRP	PEG-A; NIPAAM	Grafting from	Backbone: Kraft lignin (alkali); Catalyst: CuBr/HMTETA. Solvent: PDX; T = 60–70 °C; Thermogelling material.	[140,143]
ATRP	MMA → PMMA BMA → PBMA	Grafting from	Backbone: Kraft lignin; Catalyst: CuBr/PMDETA; Solvent: water/DMF; T = 80 °C; Thermoplastic elastomers.	[140,144]
SI-ATRP	NIPAAM → PNIPAAM	Grafting from	Backbone: Softwood Kraft lignin; Catalyst: CuCl/HMTETA; Solvent: water; Room temperature; Ionic responsive nanofibrous material.	[140,145]
ATRP	MMA → PMMA STY → PS	Grafting from	PMMA Backbone: Kraft lignin (alkali); Lignin + STY → lignin-g-PS; Catalyst: CuCl/2'2'BIPI; Solvent: DMF; T = 100 °C, 14 days. PS (PSty) Backbone: Kraft lignin (alkali); Lignin + MMA → Lignin-g-PMMA; Catalyst: CuBr/PMDETA; Solvent: DMF; T = 70 °C, 24 h; Thermoplastic lignin composites.	[140,146]

Table 4. Cont.

Functionalization Method	Grafted Chains	Grafting Technique	Grafting Conditions	Refs.
ATRP	MMA → PMMA	Grafting from	Backbone: Kraft lignin (alkali); Lignin + MMA → Lignin-g-PMMA; Catalyst: CuBr/PMDETA; Solvent: DMF; T = 70 °C, 24 h; Thermoplastic lignin composites.	[140,147]
ATRP	PEGMA	Grafting from	Backbone: Kraft lignin (alkali); Lignin-Br + PEGMA → Lignin-g-PEGMA; Catalyst: CuBr/HMTETA; Solvent: Acetone; Room temperature, overnight; Supramolecular hydrogels, self-healing materials.	[140,148]
ATRP	STY → PS	Grafting from	Backbone: Kraft lignin (alkali); Lignin-Br + STY → lignin-g-PS; Catalyst: FeCl ₃ 6H ₂ O/PPh ₃ /ascorbic acid; Solvent: DMF; T = 110 °C, 24 h; Novel polymerization method.	[140,149]
ATRP	MMA → PMMA	Grafting from	Backbone: Kraft lignin (alkali); Lignin + MMA → lignin-g-PMMA; Catalyst: FeCl ₃ 6H ₂ O/PPh ₃ /ascorbic acid; Solvent: DMF; T = 90 °C, 24 h; Novel polymerization approach.	[140,149]
ATRP	DMAEMA → PDMAEMA	Grafting from	Backbone: Kraft lignin (alkali); Lignin-Br + DMAEMA → lignin-g-PDMAEMA; Catalyst: CuBr/HMTETA; Solvent: PDX; T = 65 °C, 48 h; Gene delivery.	[150]
RAFT	AM → PAM	Grafting from	Backbone: Kraft lignin from softwood sources, prepared using KEX, 2-Bromopropionic acid, and thionyl chloride in dry THF in N ₂ atmosphere at 70 °C, overnight. Lignin-KEX + AM → Lignin-KEX-g-PAM; RAFT controller: Lignin Macrocontroller; Initiator: AIBN; Solvent: DMF; T = 70 °C, overnight; Application: Pickering emulsions.	[151]
RAFT	AM → PAM	Grafting from	Backbone: Kraft lignin. Prepared with KEX, 2-Bromopropionic acid, and thionyl chloride in dry THF in N ₂ atmosphere at 70 °C, overnight. Lignin-KEX + AM → Lignin-KEX-g-PAM; RAFT controller: Lignin Macrocontroller; Initiator: AIBN. Solvent: DMF; T = 70 °C; Application: Plasticizer for Portland cement paste.	[152]
Esterification via epoxy group	Lignin + GMA → Lignin-GMA + AM → Lignin-GMA-g-PAM	Grafting from	Backbone: Kraft lignin was first functionalized by reacting with GM through the epoxide ring; Lignin + GMA → Lignin-GMA; Lignin-GMA + AM → Lignin-GMA-g-PAM; RAFT controller: Lignin Macrocontroller; Initiator: AIBN; Solvent: DMF; T = 70 °C; Application: Plasticizer for Portland cement paste.	[153]

Table 4. Cont.

Functionalization Method	Grafted Chains	Grafting Technique	Grafting Conditions	Refs.
RAFT	Lignin + ACX → Lignin-ACX + AM → Lignin-ACX-g-PAM	Grafting from	Backbone: Kraft lignin; Lignin + ACX → Lignin-ACX; Lignin-ACX + AM → Lignin-ACX-g-PAM; RAFT controller: Lignin Macrocontroller; Initiator: AIBN; Solvent: DMF; T = 70 °C; Application: Cationic flocculant.	[153]
RAFT	Lignin + XCA → Lignin-XCA + DMC → Lignin-XCA-g-PDMC	Grafting from	Backbone: Kraft lignin; Lignin + XCA → Lignin-XCA; Lignin-XCA + DMC → Lignin-XCA-g-PDMC; RAFT controller: Lignin; Macrocontroller prepared by Steglich esterification using DCC and DMAP for 48 h; Initiator: AMBN. Solvent: DMF; T = 70 °C, under nitrogen atmosphere; Application: Cationic flocculant.	[154]
ROP	Lignophenol from Japanese cedar + EOX → Lignin-g-PEOX	Grafting from	Backbone: Lignophenol from Japanese cedar; Solvent containing benzyl bromide groups; Monomer: EOX; T = 100 °C, 12 h; Application: Composite materials.	[155]
ROP	Sulfonated Lignin + MOX → Lignin-g-PMOX	Grafting from	Backbone: Lignophenol from Japanese cedar; Initiator: Tosylated lignin; Monomer: MOX; Solvent: DMSO; T = 100 °C, 10 h; Application: Anti-ineffective ointment.	[156]
ROP	Indulin AT lignin + L-LA → Indulin AT lignin-g-PLLA	Grafting from	Backbone: Indulin AT lignin; Initiator: Triazabicyclodecene; Monomer: L-LA; Reaction carried out in bulk; T = 135 °C; Application: composites.	[157]
ROP	Biobutanol lignin + CL → Biobutanol lignin -g-PCL	Grafting from	Backbone: Biobutanol lignin; Initiator: Triazabicyclodecene; Monomer: CL; Reaction carried out in bulk; T = 135 °C; Application: composites.	[158]
ROP	Lignin (organosolv) + CL + L-LA → Lignin-g-PCL/PLLA	Grafting from	Backbone: Lignin orgaosolv; Initiator: Sn(Oct) ₂ (tin(II)2-ethylhexanoate) and alkyl alcohol functional groups on lignin; Monomer: CL and L-LA (ratio 2:1); Solvent: Toluene; T = 120 °C, under Ar atmosphere, during 45 h; Application: composites.	[159]
ROP	Alkali Lignin + B-BL → Lignin-g-PHB	Grafting from	Backbone: Lignin alkali; Initiator: Sn(Oct) ₂ (tin(II)2-ethylhexanoate) and alkyl alcohol functional groups on lignin; Monomer: B-BL; Reaction carried out in bulk; T = 130 °C, under nitrogen atmosphere, during 24 h; Application: Nano-fibers for medical applications.	[160]
ROP	Lignin alkali + CL → Lignin-g-PCL	Grafting from	Backbone: Lignin Alkali; Initiator: Sn(Oct) ₂ (tin(II)2-ethylhexanoate) and alkyl alcohol functional groups on lignin; Monomer: CL; Reaction carried out in bulk; T = 50 °C, under nitrogen atmosphere, during 14–62 h; Application: Nano-fibers for medical applications.	[161]

Table 4. Cont.

Functionalization Method	Grafted Chains	Grafting Technique	Grafting Conditions	Refs.
ROP	Lignin alkali + CL → Lignin-g-PCL	Grafting from	Backbone: Lignin alkali; Initiator: Sn(Oct) ₂ (tin(II)2-ethylhexanoate) and alkyl alcohol functional groups on lignin; Monomer: CL; Reaction carried out in bulk; T = 50 °C, under nitrogen atmosphere, during 14–62 h; Application: Nano-fibers for medical applications.	[162]
ROP	Softwood Kraft lignin from UPM BioPiva + EOX → Lignin-g-PEOX	Grafting from	Backbone: Softwood Kraft lignin from UPM BioPiva; Initiator: P4-t-Bu; Monomer: CL; Solvent: Toluene; T = 180 °C, under Ar atmosphere, during 16 h; Application: Non-ionic surfactants.	[163]
Embedded polymerization and further crosslinking.	Chitosan; N-VP; 4VP; Crosslinking agent: N'N'-MBA	Grafting from	1.5 g of chitosan were dried at 40–50 °C during 24 h and suspended in 150 mL of 2% CH ₃ COOH for 1 to 2 h. 2 mL of monomers in a 1:1 ratio were incorporated and stirred for 30 min. 0.15 mol/L AIBN were then added and stirred for 2 more hours. T = 65 °C, under air environment. Product washed using several solvents, and dried at 50 °C. The yield was 78–86%. A solution of grafted chitosan in acetic acid (0.1 % v/v) was heated at 70 °C; N'N'-MBA was then added and allowed to react during 30 min.	[164]
RAFT; Steglich esterification of phthalic anhydride and 4,4-Azobis(4-cyanovaleric acid).	Chitosan + Phthalic Anhydride → (DCC/DMAP) → Chitosan-Phthaloylated Chitosan-Phthaloylated + 4,4-Azobis(4-cyanovaleric acid) → (DCC/DMAP) → Chitosan-Phthaloylate-RAFT. Chitosan-Phthaloylate-RAFT + NIPAAAM → Chitosan-Phthaloylate-RAFT-g-NIPAAAM.	Grafting from	Phthaloylation of chitosan: A solution of phthalic anhydride (5.5 mmol) in 6 mL of DMF/H ₂ O (95/5 v/v %) was prepared, followed by the addition of chitosan powder in 1.86 mmol. The system was purged by N ₂ for 0.5 h. Heating at 120 °C was maintained during 8 h. The phthaloylated chitosan (1 mmol) was mixed with 1.2 mmol and 4,4-azobis(4-cyanovaleric acid). in 30 mL of dried DMF in the presence of carbonyl activating reagents of DCC (1 mmol) and 4-DMAP (0.12 mmol) as catalysts. Reaction at room temperature for 10 days. Chitosan-Phthaloylate-RAFT (0.0468 g) and dry DMF (5 mL) were mixed by stirring under nitrogen atmosphere. After complete dissolution, initiator 4,4-Azobis(4-cyanovaleric acid) (0.01 mmol) and NIPAAAM monomer (0.50 g; 4.4 mmol) were incorporated. Polymerization conducted at 70 °C for 48 h.	[165]
Cerium (IV) attack	Chitin + acrylic monomers.	Grafting onto	Cerium (IV); Chitin + AM → Chitin-g-PAM; Chitin + AA → Chitin-g-PAA; Chitin + MA → Chitin-g-PMA; Chitin + MMA → Chitin-g-PMMA	[58]
γ-Radiation	Chitin + STY (radiated)	Grafting onto	Chitin + STY → Chitin-g-PS	[58]

Table 4. Cont.

Functionalization Method	Grafted Chains	Grafting Technique	Grafting Conditions	Refs.
ROP	Cyclic and vinyl monomers. Modified Chitin	Grafting from	Surface-initiated ROP graft copolymerization of L-LA and CL with initiation by hydroxy groups on chitin nanofiber, catalyzed by tin(II) 2-ethylhexanoate was performed, obtaining chitin nanofiber-graft-PLA-co-PL, which is a known biodegradable polyester. Chitin was soaked in a solution of LA/CL in toluene; tin(II) 2-ethylhexanoate (ca. 5 mol%) was incorporated. Heating at 80 °C was maintained during 48 h.	[166]
γ -Radiation	Chitosan + AA + TiO ₂ → Chitosan-g-PAA-TiO ₂	Grafting from	A solution of CS-PAAc (1:1 mass/vol) was prepared with different contents of TiO ₂ ; 0.0, 1.0, 2.0 and 3.0 wt.% of the total polymer concentration was incorporated. Each solution was sonicated in a bath for 15 min. The solutions were transferred into small glass vials and were subjected to 60 Co-gamma rays at irradiation dose of 30 kGy.	[167]
ROP	Chitosan + CL → Chitoan-g-PCL	Grafting from	0.5 g chitosan and 15 mL MeSO ₃ H were placed in a round bottom flask under nitrogen atmosphere at 45 °C for 0.5 h. 4.19 g CL monomers were fed to the reactor, followed by stirring and reaction during 4.5 h.	[168]

Polysaccharides are abundant in nature, no matter whether in plants or animals, and are important for *in vivo* functions. As observed in Figure 6, there is a wide variety of polysaccharides, but the most abundant ones are cellulose and chitin. Cellulose provides structure to the cell walls of plants. Chitin, on the other side, is part of the exoskeletons of crustaceans, shellfish, and insects [169].

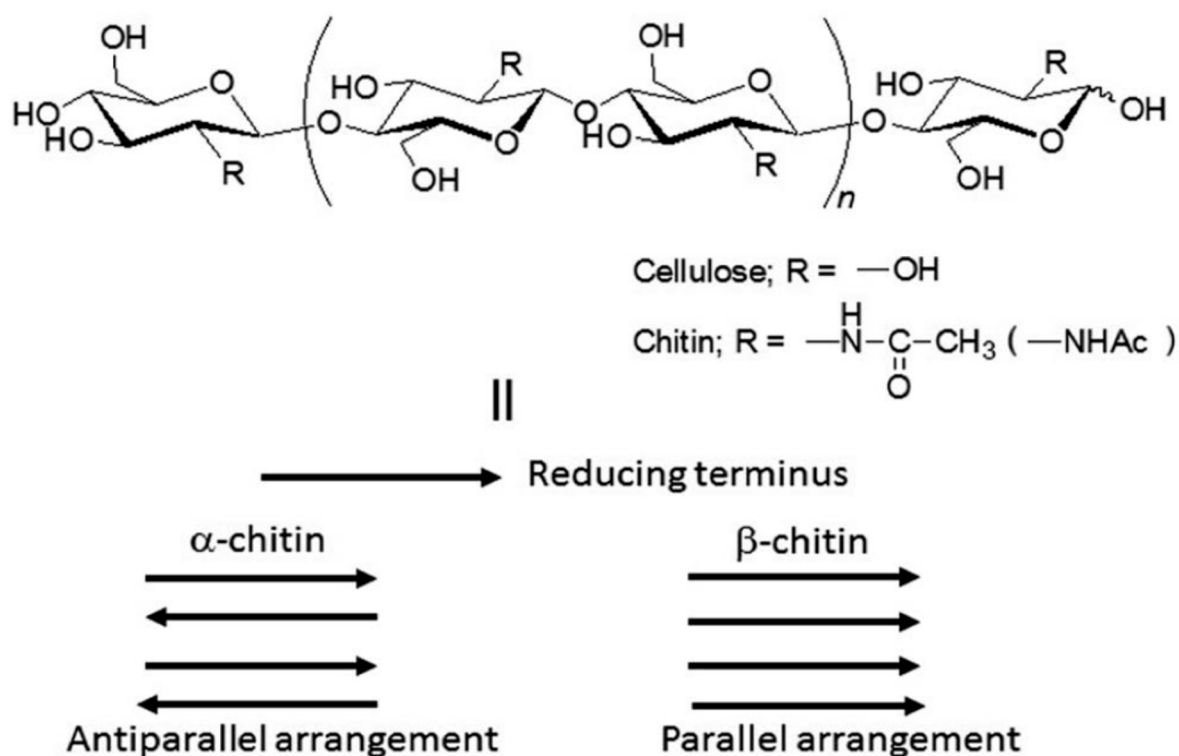


Figure 6. Cellulose and chitin structures (top). II: schematic diagram of crystalline structures for different forms of chitin. Source: Adapted with permission from Jun-ichi Kadokawa (2015). Fabrication of nanostructured and microstructured chitin materials through gelation with suitable dispersion media: RSC Adv. 5 12736 [169]. Copyright © 2021 The Royal Society of Chemistry.

Chitin is an abundant but only marginally used biomass. There are several reasons why not many practical applications for chitin have been developed [169]: (a) bulky structure; (b) insolubility in water and typical organic solvents; (c) it is harmful to recover chitin, since the available procedures require the use of strong acids and bases; (d) native chitin from crustaceans, which have exoskeletons that protect animals from their predators, has fibrous structures rich in proteins and minerals; and (e) there is a need to remove mineral and protein constituents in order to isolate chitin.

Chitosan was developed to overcome the drawbacks of chitin. Chitosan is commercially attractive for production of biocompatible polymers for environmental and biomedical applications [30]. It is basically a copolymer of N-acetyl-D-glucosamine and D-glucosamine. It is obtained from the hydration of chitin. This hydration takes place in alkaline solutions in a temperature range of 80–140 °C during 10 h [170,171].

Chitosan is a cationic polysaccharide, produced by deacetylation of chitin. Deacetylation proceeds to different levels depending on the intended uses. The physical properties of chitosan, particularly solubility, depend on molecular weight and degree of deacetylation of the material [172–174].

Modification of chitosan leads to a diversity of derivatives, with differentiated properties. As shown in Figure 1 of Deng et al. [174], different chitosan moieties are possible. Each one of them is produced from grafting or other chemical or enzymatic modification forms.

They differ in antimicrobial activity. Further studies on chitin-chitosan modification are available in the literature [58,175–178].

3.2. Polymer Backbones

Polymer backbones are the most common substrates for grafting modification. Several techniques can be used to create many possible combinations. Most of these developments are focused on property improvement for industrial applications. They include synthesis of adhesives; reinforcement of mechanical properties; improvement of chemical resistance; synthesis of electro, optical, thermo responsive polymers; health care applications; and self-healing polymers, among others [179].

Polymer grafting techniques have been reported since the late 1950s [8,9,11]. Polymers based on acrylamide and acrylonitrile using polymer grafting techniques are included in the early reports. However, the huge increase in research related to synthesis of materials with controlled microstructures using polymer grafting techniques has been possible due to the advances in reversible deactivation radical polymerization (RDRP) techniques over the last three decades [180–184]. The main RDRP routes are nitroxide mediated polymerization (NMP) [185], reversible addition fragmentation transfer polymerization (RAFT) [180,186,187], and atom transfer radical polymerization (ATRP) [71,188], although there are other polymer synthesis techniques, such as ring-opening polymerization (ROP) [181] and click chemistry, among others, that can be used. Another important aspect in polymer grafting is the solvent used for the reaction, particularly when grafting proceeds as a heterogenous process. As observed in Table 19, solvents such as supercritical fluids, mainly supercritical carbon dioxide, water, DMF, or combinations of solvents are typically used for polymer grafting. These techniques have improved our skills to produce molecularly well-defined, chain-end tethered polymer brush films. The assets of RDRP have substantially impacted the synthesis and properties of surface-grafted polymers. Although vinyl monomers are widely use in graft polymerization for backbones or side-arms, other monomers coming from natural sources are increasingly being used. That is the case, for instance, of ϵ -caprolactone, lactic acid [189], L-lactide, and butyrolactone. It is also observed in Table 19 that other nontraditional monomers such as acrylamide (AM), N-isopropylacrylamide (NIPAA), and acrylates and methyl acrylates, such as methyl methacrylate (MMA) and acrylic acid (AA), are being increasingly used in polymer grafting applications. To get a glimpse of the focus of research papers that involve polymer grafting as the chemical route for polymer modification, Table 5 summarizes journal reports on polymer grafting from the current period (2020–2021). As expected, an increasing trend toward the improvement of natural biopolymers using synthetic polymer arms is observable.

Table 5. Recent reports on the production of materials using polymer grafting (2020–2021).

Title ^a	Reference
Synthesis of diallyl dimethyl ammonium chloride grafted polyvinyl pyrrolidone (PVP-g-DADMAC) and its applications.	[190]
Synthesis and characterization of biocompatible hydrogel based on hydroxyethyl cellulose-g-poly(hydroxyethyl methacrylate).	[191]
Poly(vinylidene fluoride) (PVDF)/PVDF-g-polyvinylpyrrolidone (PVP)/TiO ₂ mixed matrix nanofiltration membranes: preparation and characterization.	[192]
Synthesis and characterization of poly (acrylonitrile-g-lignin) by semi-batch solution polymerization and evaluation of their potential application as carbon materials	[193]
High crosslinked sodium carboxyl methylstarch-g-poly (acrylic acid-co-acrylamide) resin for heavy metal adsorption: its characteristics and mechanisms.	[194]
Preparation and characterization of PLLA/chitosan-graft-poly (ϵ -caprolactone) (CS-g-PCL) composite fibrous mats: The microstructure, performance and proliferation assessment.	[168]
Synthesis of partly debranched starch-g-poly(2-acryloyloxyethyl trimethyl ammonium chloride) catalyzed by horseradish peroxidase and the effect on adhesion to polyester/cotton yarn.	[195]

Table 5. Cont.

Title ^a	Reference
Cellulose Acetate thermoplastics with high modulus, dimensional stability and anti-migration properties by using CA-g-PLA as macromolecular plasticizer.	[196]
Superwetable PVDF/PVDF- g-PEGMA ultrafiltration membranes.	[197]
Removal of malachite green using carboxymethyl cellulose-g-polyacrylamide/montmorillonite nanocomposite hydrogel.	[198]
Ultraviolet illumination responsivity of the Au/n-Si diodes with and without poly (linolenic acid)-g-poly (caprolactone)-g-poly (t-butyl acrylate) interfacial layer.	[199]
Synthesis of CO ₂ -based polycarbonate-: G -polystyrene copolymers via NMRP.	[200]
Compatibilization of iPP/HDPE blends with PE-g-iPP graft copolymers.	[201]
Preparation, characterization of feather protein-g-poly(sodium allyl sulfonate) and its application as a low-temperature adhesive to cotton and viscose fibers for warp sizing.	[202]
Semi-Natural superabsorbents based on starch-g-poly(acrylic acid): Modification, synthesis and application.	[203]
Design and development of polymethylmethacrylate-grafted gellan gum (PMMA-g-GG)-based pH-sensitive novel drug delivery system for antidiabetic therapy.	[204]
Preparation and characterization of bioinert amphiphilic P(VDF-co-CTFE)-g-POEM graft copolymer.	[205]
Preparation, characterization of poly(acrylic acid)-g-feather protein-g-poly(methyl acrylate) and application in improving adhesion of protein to PLA fibers for sizing.	[206]
Antibacterial and pH-responsive quaternized hydroxypropyl cellulose-g-poly(THF-co-epichlorohydrin) graft copolymer: Synthesis, characterization and properties.	[207]
Thermally self-assembled biodegradable poly(casein-g-N-isopropylacrylamide) unimers and their application in drug delivery for cancer therapy.	[208]
Swelling capacity of sugarcane bagasse-g-poly(acrylamide)/attapulgit superabsorbent composites and their application as slow release fertilizer	[209]
Structure formation in pH-sensitive micro porous membrane from well-defined ethyl cellulose-g-PDEAEMA via non-solvent-induced phase separation process	[210]
Micelles with a loose core self-assembled from coil-g-rod graft copolymers displaying high drug loading capacity.	[211]
Synthesis and water absorbing properties of KGM-g-P(AA-AM-(DMAEA-EB)) via grafting polymerization method.	[212]
Preparation of hydrophilic woven fabrics: Surface modification of poly(ethylene terephthalate) by grafting of poly(vinyl alcohol) and poly(vinyl alcohol)-g-(N-vinyl-2-pyrrolidone).	[213]
The preparation, physicochemical and thermal properties of the high moisture, solvent and chemical resistant starch-g-poly(geranyl methacrylate) copolymers.	[214]
Reverse poly(ϵ -caprolactone)-g-dextran graft copolymers. Nano-carriers for intracellular uptake of anticancer drugs.	[215]
High-performance solid-state bendable supercapacitors based on PEGBEM-g-PAEMA graft copolymer electrolyte.	[216]
Design of well-defined polyethylene-g-poly-methyltrifluorosiloxane graft copolymers via direct copolymerization of ethylene with polyfluorosiloxane macromonomers.	[217]
Synthesis and characterization of poly(vinyl chloride-g- ϵ -caprolactone) brush type graft copolymers by ring-opening polymerization and “click” chemistry.	[218]
Adhesion of cornstarch-g-poly (2-hydroxyethyl acrylate) to cotton fibers in sizing.	[219]
Polynorbornene-g-poly(ethylene oxide) through the combination of ROMP and nitroxide radical coupling reactions.	[220]
Potent bioactive bone cements impregnated with polystyrene-g-soybean oil-AgNPs for advanced bone tissue applications.	[221]
Fabrication of cellulose nanocrystal-g-poly(acrylic acid-co-acrylamide) aerogels for efficient Pb(II) removal.	[222]
The compatibilization of PLA-g-TPU graft copolymer on polylactide/thermoplastic polyurethane blends.	[223]
Cellulose-g-poly-(acrylamide-co-acrylic acid) polymeric bioadsorbent for the removal of toxic inorganic pollutants from wastewaters	[224]
Performance improvement for thin-film composite nanofiltration membranes prepared on PSf/PSf-g-PEG blended substrates.	[225]

Table 5. Cont.

Title ^a	Reference
Synthesis and characterization of poly(vinyl chloride-g-methyl methacrylate) graft copolymer by redox polymerization and Cu catalyzed azide-alkyne cycloaddition reaction.	[226]
Encapsulation of NPK fertilizer for slow release using sodium carboxymethyl cellulose-g-poly (AA-C0-AM-C0-AMPS)/ Montmorillonite clay-based nanocomposite hydrogels for sustainable agricultural applications.	[227]
Engineering a “PEG-g-PEI/DNA nanoparticle-in- PLGA microsphere” hybrid-controlled release system to enhance immunogenicity of DNA vaccine.	[228]
Chitosan-g-oligo(L,L-lactide) copolymer hydrogel for nervous tissue regeneration in glutamate excitotoxicity: In vitro feasibility evaluation	[229]

^a Searching criteria used in Scopus: (TITLE (“-g-”) AND TITLE-ABS-KEY (“poly”) AND TITLE-ABS-KEY (“graft”)).

Table 6. Common characterization methods.

Method	Property Measured
Nuclear magnetic resonance (NMR)	NMR identifies the nature of the group and the site where the graft is attached to the polymer backbone. ¹ H NMR and ¹³ C NMR are utilized depending on the chemical nature of the material [73].
Infrared spectroscopy (IR)	Identification of specific functional groups grafted to backbone. It can also be used to quantify grafting functionalities in modified polyolefins by determining the intensity of the characteristic reference bands in the sample, and compare them to a calibration curve of known concentrations of the same functional group [73].
Scanning electron microscopy (SEM)	SEM is useful for the study of surface morphologies of grafted materials; also used as a tool to confirm that grafting has taken place [59].
X-ray diffraction (XRD)	XRD is useful for the study of crystallinity of chemical substances. Polymer grafting is associated with changes in XRD patterns [59].
Size exclusion chromatography (SEC)	It allows determination of molecular weight averages (MW) and molecular weight distributions (MWD) of grafted chains [230], which must be separated from the backbone before carrying out the analyses to focus on the grafts only.
Differential scanning calorimetry (DSC)	This is utilized to evaluate changes in crystallinity through the thermal behavior between backbones and grafted materials.
Thermogravimetric analysis (TGA)	This is used to study changes in thermal decomposition profiles between backbones and grafted materials.

Table 7. Summary of thermal characterization techniques employed in grafted materials.




Backbone	Grafts	Technique	Property Measured	Application	Refs.
Lignin-RAFT macrocontroller	Poly(soybean oil methacrylate) derivatives. PSBMA, PSBMAH, PSBMAEO	DSC	T _g of lignin-g-polymerized soybean oil derived methacrylate. Measured T _g : Lignin-g-PSBMA −5.6 °C, Lignin-g-PSBMAH 27.7 °C, Lignin-g-PSBMAEO −17.4 °C. DSC2000, TA Instruments. 10 mg samples were used with heating from 25 °C to 200 °C at 10 °C/min, and cooling to −70 °C at the same rate. Data was gathered from the second heating scan to 200 °C. Nitrogen flow: 50 mL/min.		[134]
		TGA	Thermal stability of biocomposites. Two MDT values were found for all samples 380 °C and 430 °C. Q5000 TGA system (TA Instruments); 25 to 600 °C, at 10 °C/min, 25 mL/min nitrogen flow.		
Lignin	Imidazole and POCl ₃ react in to (1H-imidazol-1-yl)phosphonic group which reacts with lignin	TGA	MDT values for lignin derivatives and PP blends. Lignin MDT = 398 °C. Lignin-g-IPG MDT > 600 °C. PP = 418 °C, PP/Lignin = 472 °C, PP/20 % Lignin-g-IPG = 479 °C, PP/30 % Lignin-g-IPG = 483 °C. SDTQ600 thermal analyzer; 20 °C/min under nitrogen, from ambient to 600 °C.		[125,135]
		FR	PHRR (kW/m ²) // THR (MJ/m ²) PP = 1350 kW/m ² // 87.3 MJ/m ² , PP/Lignin = 382/333 kW/m ² // 76 MJ/m ² , PP/20%Lignin-g-IPG = 380 kW/m ² // 74.2 MJ/m ² , PP/30%Lignin-g-IPG = 360 kW/m ² // 69.7 MJ/m ² . Heat release rate measured using an FTT UK cone calorimeter following ISO 5660. Incident flux: 35 kW/m ² .		

Table 7. Cont.





Backbone	Grafts	Technique	Property Measured	Application	Refs.
Hydroxypropyl cellulose (HPC)	Steglich esterification of PABTC over HPC using DCC and DMAP and grafting of PABTC and further polymerization of EA NIPAAm.	TGA	TGA 2950 analyzer; nitrogen atmosphere ($60 \text{ cm}^3/\text{min}$). Heating of samples (5–10 mg) from ambient temperature to 600°C , at $10^\circ\text{C}/\text{min}$. Calculations of the onset, the end decomposition temperature, and the residual mass.		[108]
		DSC	Modulated DSC 2920 in nitrogen environment ($60 \text{ cm}^3/\text{min}$). The determination of glass transition temperature (T_g) required 5–10 mg samples. Heating from ambient temperature to 200°C , followed by cooling to -100°C , and reheating to 200°C , using $10^\circ\text{C}/\text{min}$ for both, heating and cooling was used. This sequence occurred three times.		
CellCIAc	ATRP of 4NPA and MMA using $\text{Cu(I)Cl}/2'2'\text{BIP}$ macro initiator.	TGA	Shimadzu TGA-50; heating rate: $10^\circ\text{C}/\text{min}$; nitrogen flow: $10 \text{ mL}/\text{min}$.		[109,112]
Cellulosic <i>Grewia optiva</i> fibers	Redox initiator FAS- H_2O_2 for grafting MA and KPS for polymerization of MA.	TGA	Thermo gravimetric analyses of plain and grafted cellulosic fibers carried out in presence of nitrogen on a Perkin Elmer thermal analyzer. Heating from ambient temperature to $900^\circ\text{C}/\text{min}$, at $10^\circ\text{C}/\text{min}$.		[110]
Cotton linter cellulose	APS with MMA.	TGA-DTA	Samples were analyzed using a Pyris Diamond TG-DTA (STA449C/3/F, Germany). Sample weight: 14.2 mg. Heating rate: $10^\circ\text{C}/\text{min}$. Flow of nitrogen $20 \text{ mL}/\text{min}$.		[115]

Table 7. Cont.





Backbone	Grafts	Technique	Property Measured	Application	Refs.
Cellulose (DP = 1130)	APS and MMA embedded.	TGA-DTA	Samples analyzed in a Pyris Diamond TG/DTA equipment (STA449C/3/F, German). Sample weight: 14.2 mg. Heating/Cooling rate: 10 °C/min. Flow of nitrogen: 20 mL/min.		
Cellulose nanocrystal (CNC)	Macromolecular initiator obtained from the reaction between Br-iBuBr and CNC with TEA as catalyst via SI-ATRP with sTY. Material was casted in PMMA.	TGA	Thermal degradation of studied materials analyzed in a TGA/SDTA 851e in nitrogen atmosphere. Heating from 30 to 550 °C, at 10 °C/min.		[118]
		DSC	Tg determined in a Pyris 1 DSC equipment. Heating from 30 to 200 °C at 10 °C/min.		
Cellulose nanocrystal (CNC)	Macromolecular initiator obtained from the reaction between Br-iBuBr and CNC with TEA as catalyst via SI-ATRP with sTY. Material was casted in PMMA.	TGA	Analyses carried out in a TGA Q50 (TA Instruments), under nitrogen atmosphere (20 mL/min). Heating from 30 to 500 °C at 5, 10, 15, 20, 25 and 30 °C/min for determination of degradation activation energy.		[119]
		DSC	Analyses performed in a Star 1 (Mettler-Toledo). Heating from 25 °C to 200 °C at 5 °C/min, remaining at 200 °C for 5 min. Cooling to −50 °C at 20 °C/min, remaining there for 5 min, followed by heating to 200 °C at 5 °C/min. Tg, Tm, Tc were measured. Crystallinity (v) calculated from melting enthalpy of fully crystalline PLLA.		
Cellulose cotton fiber pulp	Esterification of maleic anhydride grafted over PHA (by double bond). PHA-g-MA grafted over cellulose cotton fiber pulp (by the anhydride group).	TGA	Analyses carried out on a Q500 TGA (TA Instruments), in nitrogen environment. Heating from ambient to 600 °C at 20 °C/min.		[120]

Table 7. Cont.

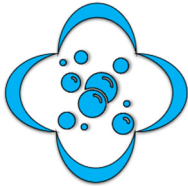


Backbone	Grafts	Technique	Property Measured	Application	Refs.
Cellulosic filter papers	Radiation-induced graft (RIGCP) copolymerization of acrylonitrile.	TGA	Analyses obtained in TGA-50 (Shimadzu). Heating rate: 10 °C/min. N ₂ environment.		[121]
Hemicellulose	Hemicellulose grafting using TBD and ε-caprolactone monomer	TGA	TGA/DSC 1 STARe System (Mettler Toledo). 5–15 mg of a sample. Nitrogen environment (85 mL/min). Heating from 30–500 °C at 10 °C/min. Compositions of produced gases measured in an FTIR (TA, Nicolet, iS); detector coupled to TGA. FTIR analyses from 4000 to 650 cm ^{−1} with a 4 cm ^{−1} resolution.		[37]
		DSC	DSCQ10 (TA Instruments). Hermetic pan (T 090127). Heating from 25 to 165 °C at 10 °C/min. Cooling to 15 °C followed by heating to 165 °C at 10 °C/min. Tg obtained from second heating ramp.		

Table 7. Cont.




Backbone	Grafts	Technique	Property Measured	Application	Refs.
Cellulose	NCHA, 4VP, DA and DAAM grafted by atom transfer radical polymerization (ATRP) using CuCl, 2,2'-BIPY as catalyst.	TGA	Thermal analyses carried out in a Shimadzu TGA-50 at 10 °C/min in nitrogen environment (10 mL/min). Cell-g-DA and Cell-g-4VP exhibited higher decomposition temperatures.	 	[122]
Chitosan	Embedded polymerization N-VP, 4VP. Crosslinking agent: N'-N'-MBA	TGA	TGA analyses carried out using a NETZSCH, STA 409 PG.4.G Luxx. 50 mL/min nitrogen environment. Heating from 20 °C to 400 °C at 10 °C/min.		[164]

Table 8. Summary of spectroscopic characterization techniques employed in grafted materials.




Backbone	Grafts	Technique	Property Measured	Application	Refs.
Lignin-RAFT macrocontroller	Poly(soybean oil methacrylate) derivatives. PSBMA, PSBMAH, PSBMAEO.	¹ H-NMR	Amount of RAFT controller reacted (shifts 7.3, 7.6, 7.9 ppm) and nonattached monomer (shifts 5.3, 5.7 ppm). Varian Mercury 300 spectrometer, 300 MHz; tetramethyl silane as an internal reference.		[134]
		FTIR	Amount of RAFT controller and polymer attached to lignin. Area of peak at 1760 cm ⁻¹ . Perkin Elmer spectrum 100. ATR method, recorded at 4 cm ⁻¹ , 32 scans.		
Lignin	Imidazole and POCl ₃ react in to (1H-imidazol-1-yl) phosphonic group which reacts with lignin.	FTIR	Lignin, lignin-OH, imidazole and lignin-g-IPG were compared at relevant bands (1662, 1260, 1080, 1050, 878, and 791 cm ⁻¹) for determination of C=N, P=O, P-O-C, P-O, -OH, and P-N groups, respectively. A Bruker VECTOR 22 spectrometer was used.		[125,135]
		XPS	Surface elementary composition of samples (wt.%), were compared to determine the amount of functionalized or grafted groups in the surface. Elements analyzed: carbon, oxygen, phosphorous, nitrogen. Lignin, C: 68.2, O: 31.9; Modified lignin-OH, C: 67.5, O: 32.5; Lignin-g-IPG, C: 53.0, O: 31.7, P: 8.1, N: 7.2. A Thermo ESCALAB 250 spectrometer was used. Analyses were carried out from 50 up to 800 eV of binding energy.		

Table 8. Cont.





Backbone	Grafts	Technique	Property Measured	Application	Refs.
Hydroxypropyl cellulose (HPC)	Steglich esterification of PABTC over HPC using DCC and DMAP; grafting of PABTC and further polymerization of EA NIPAAM.	^1H NMR	NMR spectra obtained using a Bruker 300 or 200 MHz in deuterated chloroform or deuterated dimethyl sulfoxide (d_6 -DMSO).		[108]
CellClAc	Macro initiator, $\text{Cu(I)Cl}/2'2'\text{BIPI}$ catalytic system via ATRP of 4NPA and MMA	^1H -NMR	NMR spectra obtained using a Bruker 400 MHz spectrometer at room temperature in DMSO-d_6 .		[109]
		FTIR	FTIR data using solid samples as KBr pellets, from 4000 cm^{-1} to 450 cm^{-1} .		
Cellulosic <i>Grewia optiva</i> fibers	Redox initiator $\text{FAS-H}_2\text{O}_2$ for grafting of MA, and KPS for polymerization of MA.	FTIR	Chemical structures of fibers before and after grafting were studied using FTIR (PERKIN ELMER RXI). Spectrum recorded from 4000 to 400 cm^{-1} .		[110]
Cellulose acetate	Solvents: DMSO, PDX, DMAc, $\text{C}_3\text{H}_6\text{O}$. Initiators for grafting and polymerization: CAN, Sn(Oct)_2 and BPO.	^1H -NMR	Spectra of studied materials obtained using a Bruker WM-400 apparatus, at 300 MHz. Tetramethyl silane (TMS) used as internal standard and DMSO-d_6 as solvent.		[111]
		FTIR	Grafted and ungrafted materials analyzed using a Spectrum RX1 PerkinElmer apparatus. Chloroform used as a solvent. KBr pellet technique used for grafted materials.		

Table 8. Cont.




Backbone	Grafts	Technique	Property Measured	Application	Refs.
CellCIAC	Macro initiator, Cu(I)Cl/2'2'BIPI catalytic system via ATRP controller.	FTIR	FTIR spectrophotometer on solid samples as KBr pellets, from 4000 cm^{-1} to 450 cm^{-1} .		[112]
Cellulose cotton fibers	Na_2CO_3 and thermal activation with MTC-b-CD and silver nitrate.	FTIR	MCT- β -CD grafted and ungrafted cotton fabrics were studied with attenuated total reflection (FTIR-ATR), which permits the study of solid surfaces using a diamond tipped device (SPECAC), connected to a Bruker Vertex 70 spectrophotometer.		[113]
Cotton linter cellulose	APS with MMA.	FTIR	A TENSOR27 FTIR apparatus ($4500\text{--}400\text{ cm}^{-1}$) was used to analyze materials.		[115]
		XRD	X-ray diffractometer (D/max-2500/PC, Rigaku Co) based on a reflection method using a Cu Ka target (40 kV and 60 mA). Diffraction angle: 5° to 60° .		

Table 8. Cont.




Backbone	Grafts	Technique	Property Measured	Application	Refs.
Microcrystalline cellulose	Ring-opening polymerization (ROP) of L-LA with DMAP in an ionic liquid AmimCl to form Cellulose-g-PLLA	¹ H-NMR	Materials analyzed using ¹ H-NMR (Bruker AV400-MHz). Solvent: DMSO-d ₆ with a drop of trifluoroacetic acid-d; internal standard: tetramethyl silane (TMS).		[116]
		XRD WAXD	WAXD carried out using an XRD-6000 X-ray diffractometer (Shimadzu, Japan); Ni-filtered Cu Ka radiation (40 kV, 30 mA); 4°/min at ambient temperature.		
		UV spectroscopy	UV analyses performed in a UV2000 equipment (UNICO, China), to follow the load and controlled release of vitamin C.		
Cellulose (DP = 1130)	APS and MMA embedded.	FTIR	A TENSOR27 FTIR apparatus (4500–400 cm ^{−1}) was used to analyze materials.		[117]
		WAXD-XRD	WAXD carried out in an X-ray diffractometer (D/max-2500/PC, Rigaku Co. Ltd., Tokyo); Cu Ka radiation (40 kV, 60 mA); 2θ = 5°–60°.		
Cellulose nanocrystal (CNC)	Macromolecular initiator obtained from the reaction between Br-iBuBr and CNC with TEA as catalyst via SI-ATRP with STy. Material was casted in PMMA.	FTIR	Spectra obtained at ambient temperature on a NICOLET spectrometer 10 to study surface modification of studied materials. KBr pellet method used for samples. Resolution: 4 cm ^{−1} ; measurement range; 4000–400 cm ^{−1} , and 30 scans.		[118]
		UV-Vis	Transmittance of samples measured using a UV-vis spectrophotometer at wavelengths of 400 to 800 nm.		
		XRD	XRD patterns of studied materials were obtained using a Bruker Siemens D8 X-ray apparatus with operation at 3 kW; CuKa radiation (λ = 0.154 nm); 2θ = 3–60°; 0.02° step.		
		¹³ C-NMR	Chemical structures of studied materials obtained with the help of a Bruker 400 M solid-state ¹³ C-NMR apparatus.		

Table 8. Cont.



Backbone	Grafts	Technique	Property Measured	Application	Refs.
Cellulose nanocrystal (CNC)	Redox agent: MgH_2 . L-LA polymerization in situ. PLLA-g-CNC particles were casted in PLLA.	FTIR	A Perkin Elmer Spectrum 100 apparatus in ATR mode, equipped with a Zn-Se crystal, was used. Modified and unmodified CNC samples. Range: 4000 to 650 cm^{-1} . Accuracy: 4 cm^{-1} for 64 scans.		[119]
		^1H -NMR ^{13}C -NMR	A Bruker-300 apparatus with DMSO-d6 as solvent was used. Small amounts of CDCl_3 were used to improve solubility of grafted product in DMSO-d6.		
		XRD	XRD analyses carried out in a PAN analytical apparatus; Cu Ka radiation ($\lambda = 1.541\text{ \AA}$); incidence angle: 10 to 40° , 0.07° steps.		
		XPS	XPS analyses performed in an ESCALAB 250 equipment (Thermo Scientific). Analyzed surface: 400 mm^2 . Atomic concentrations estimated from areas of photoelectron peaks considering atomic sensitivity factors. All binding energies were charge-corrected to 284.8 eV.		
Cellulose cotton fiber pulp	Esterification of maleic anhydride grafted onto PHA (through double bond). PHA-g-MA grafted onto cellulose cotton fiber pulp (through the anhydride group).	FTIR	ATR-FTIR analyses of ungrafted and grafted materials acquired using KBr discs on a Vector 33 Bruker apparatus.		[120]
		XRD	XRD analyses carried out in a Bruker D8 ADVANCE X-ray apparatus with operation at 40 mA and 40 kV. Cu K α filtered radiation ($\lambda = 0.15418\text{ nm}$). Scattering angle (2θ): 5° to 50° , 0.02° step.		

Table 8. Cont.

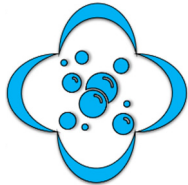


Backbone	Grafts	Technique	Property Measured	Application	Refs.
Cellulosic filter papers	Radiation-induced graft (RIGCP) copolymerization of acrylonitrile.	FTIR	FTIR analyses of studied materials (using KBr disks) were obtained using a Perkin Elmer-1650 FTIR apparatus.		[121]
		XRD	XRD analyses of studied materials in an angle range $2\theta = 5\text{--}50^\circ$ were obtained in a Shimadzu XRD-610 equipment, with Cu K α radiation (1.5418°A). Operating conditions: $8^\circ/\text{min}$ and 1.0 s; 30 kV and 20 mA. Peak height methods were used to estimate crystallinity index (CI).		
		XRF	XRF analyses performed using a Philips wavelength dispersive equipment X' Unique II, including flow and scintillation (fs) detectors. Qualitative analyses of chelating filter paper-metal complexes were obtained by X-ray fluorescence.		
Hemicellulose	Hemicellulose grafting using TBD and ϵ -caprolactone monomers	FTIR	A Nicolet Nexus spectrophotometer with single reflection ATR was used. Range: 4000 to 700 cm^{-1} . Resolution: 4 cm^{-1} ; 60 scans.		[37]
		^1H -NMR ^{13}C -NMR HSQC	Apparatus: Bruker Advance III 400 MHz, containing a 5 mm multinuclear broad band probe (BBFO+) and z-gradient coil. 30 mg of sample dissolved in 1 mL of d ₆ -DMSO. T = 60°C . 128 scans for $^1\text{D}^1\text{H}$; 32 scans and 128 increments for 2D ^1H – ^1H COSY. 16 scans and 256 increments for 2D ^1H – ^{13}C HSQC.		

Table 8. Cont.






Backbone	Grafts	Technique	Property Measured	Application	Refs.
CellClAc	NCHA, 4VP, DA and DAAM grafted by ATRP using CuCl, 2'2'BIP1 as catalyst.	FTIR	Apparatus: Perkin Elmer Spectrum One. Solid samples as KBr pellets.		[122]
		UV-Visible	Apparatus: Shimadzu 3600 UV-VIR-NIR.		
Chitosan	Embedded polymerizations of N-VP and 4VP. Crosslinking agent: N'N'-MBA	FTIR	Apparatus: AVATAR 370 Thermo Nicolet. Range: 4000 to 500 cm^{-1} , using the KBr pellet method. Spectral resolution: 4 cm^{-1} .		[164]
		XRD	Apparatus: Bruker Advance D8 equipment (Germany). Diffractograms comprised (2 θ) 0.020 imaging; scattering rates: 3 to 800; scanning speeds: 2.0 min^{-1} ; accelerated tension of 40 kV; intensity of 35 mA.		
Cellulose nanofibrils	Nitroxide TEMPO insertion and nitroxide mediated polymerization of HEMA	XRD	XRD using a Bruker D8 Advance spectrometer. Analyses carried out from 5° to 40° at 4°/min, with a current of 40 mA. Measured property: CI.		[124]
		FTIR	Apparatus: Bruker spectrometer, accumulation of 128 scans. Resolution: 4 cm^{-1} . Range: 4000–400 cm^{-1} ; absorbance mode.		
		XPS	XPS analyses using Thermo Electron Scientific Instruments were performed using a 1486.6 eV Al K α X-ray source.		

Table 8. Cont.


Backbone	Grafts	Technique	Property Measured	Application	Refs.
Lignin	Insertion of ACX onto lignin to get a RAFT macrocontroller able to polymerize AM and AA.	Dynamic light scattering (Particle size distribution)	Particle size distributions (PSD) measured in an aqueous solution (1 mg/mL) using a DLS Zeta-sizer (Malvern Instruments).		[139]
		^1H -NMR	Apparatus: Bruker 300 Advance; PFB used as internal standard to transform proton intensities into initiator concentration ($\mu\text{mol}/(\text{g lignin})$).		

Table 9. Summary of digital imaging and microscopy characterization techniques employed in grafted materials.





Backbone	Grafts	Technique	Property Measured	Application	Refs.
Lignin	Imidazole and POCl ₃ react to produce (1H-imidazol-1-yl) phosphonic, which reacts with lignin.	SEM with EDAX	S4800 FEI SEM; 5 kV accelerating voltage. Comparison of morphologies of char residues after cone calorimeter analyses. PP/Lignin displayed loosely spheroidal structures with C: 86.5 wt.%, O: 13.5 wt.%. PP/30 °% Lignin-g-IPG formed a continuous and compact spheroidal structure.		[125,135]
		Digital photo	Digital photos comparing PP composite sample test probes after cone calorimeter measurements were obtained.		
Cellulosic <i>Grewia optiva</i> fibers	FAS-H ₂ O ₂ redox initiation for grafting of MA and KPS, for polymerization of MA.	SEM.	The morphologies of ungrafted and grafted fibers were studied using a SEM apparatus (LEO 435 VP).		[110]
Cotton linter cellulose	APS with MMA.	SEM	Apparatus: JSM-6700F scanning microscope. Samples coated with gold prior to study. Morphologies and differences between ungrafted and grafted cellulose materials were analyzed.		[115]
Microcrystalline cellulose	Ring-opening polymerization (ROP) of L-LA using DMAP in an ionic liquid (AmimCl) to produce Cellulose-g-PLLA	TEM	Apparatus: JEM-100CXa TEM at an acceleration voltage of 100 kV..Sample preparation involved dissolving them in DMSO 0.01% (<i>w/v</i>) and placement on a copper grid with formvar film.		[116]

Table 9. Cont.




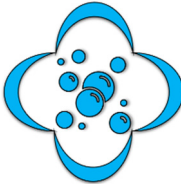

Backbone	Grafts	Technique	Property Measured	Application	Refs.
Cellulose (DP = 1130)	Embedded APS and MMA.	SEM	Apparatus: JSM-6700F scanning microscope. Coating with a thin layer of gold required for samples.		[117]
Cellulose nanocrystal (CNC)	Macromolecular initiator obtained from Br-iBuBr and CNC with TEA as catalyst via SI-ATRP with Sty. Material was casted in PMMA.	SEM	Apparatus: su1510 (Hitachi Zosen Corporation) operating at 30 kV. Focus: measurement of homogeneity of PMMA composites.		[118]
		TEM	Apparatus: JEM-2100 electron microscope. Operation involves acceleration voltage of 200 kV. Focus: Analysis of morphological features and distribution of cellulose nanocrystals.		
Cellulose cotton fiber pulp	Esterification of maleic anhydride grafted onto PHA (through double bond). PHA-g-MA grafted onto cellulose cotton fiber pulp (through the anhydride group).	SEM	Apparatus: Nova Nano SEM 430 (FEI Company); high-resolution field emission with operation at an acceleration voltage of 15 kV. Focus: Morphological analysis of PHA/CF composite films.		[108]
Cellulosic filter papers	Radiation-induced graft (RIGCP) copolymerization of acrylonitrile.	SEM	SEM micrographs of samples were obtained on a JEOL-SEM 5400 microscope.		[109]
Chitosan	Embedded polymerization of N-VP and 4VP; Crosslinking agent: N'N'-MBA	SEM	Morphological surface images of ungrafted and grafted chitosan with or without doxocycline were obtained using a JSM-6390 SEM microscope.		[153]

Table 9. Cont.






Backbone	Grafts	Technique	Property Measured	Application	Refs.
Regenerated cellulose fibres (rayon)	Photo-chemical grafting of PETA without photoinitiator.	SEM	Apparatus: JSM-6510 instrument (Joel GmbH, Freising, DE). Samples prepared following standard procedures. Micrographs obtained in SE mode; acceleration voltage: 5 and 10 kV. Purpose: Analyses of qualitative fracture.		[111]
					
					
Cellulose nanofibrils	Nitroxide TEMPO insertion and NMP of HEMA	SEM	Apparatus: Hitachi S-4800 SEM microscope. Purpose: Analysis of morphologies of materials at working distances of 15 mm. Operating voltage: of 2 kV.		[112]
					

Table 10. Summary of rheological characterization techniques used for grafted materials.




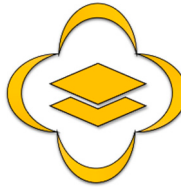
Backbone	Grafts	Technique	Property Measured	Application	Refs.
Cellulose nanocrystal (CNC)	Redox agent: MgH_2 ; in situ L-LA polymerization. PLLA-g-CNC particles were casted in PLLA.	DMA. Casted PLLA-g-CNC particles in PLLA matrix.	Apparatus: DMA 50, Metravib, tensile mode. Dimensions of sample specimens: $6.5 \times 10.0 \times 0.2$ mm. Storage E' and loss E'' moduli were registered. Heating rate: $5^\circ\text{C}/\text{min}$; -100 – 200°C ; 1 Hz.		[119]
		Molten Rheometry; Casted PLLA-g-CNC particles in PLLA matrix.	Dynamic Anton Paar MCR 102 rheometer. Materials analyzed in molten state; $T = 180^\circ\text{C}$; Parallel plates geometry, 25-mm diameter; G' and G'' moduli were registered; 100 to 10^{-3} rad/s.		
Cellulose nanofibrils	Nitroxide TEMPO insertion and NMP of HEMA	Stress-strain compression	Apparatus: Instron 5848; 50 N load cell. Test: cyclic compressive stress and strain; 5 mm/min for 70% strain, followed by the same releasing rate until zero loading, for 2 min.	  ELECTRONICS	[124]
Lignin	Insertion of ACX onto lignin to produce a RAFT macrocontroller to polymerize AM or AA.	Viscosity determination of an aqueous solution of grafted material.	Apparatus: Brookfield cone-and-plate viscometer. Steady shear measurements using 100 rpm.		[139]

Table 11. Summary of chromatographic characterization techniques used for grafted materials.






Backbone	Grafts	Technique	Property Measured	Application	Refs.
Lignin-RAFT macrocontroller	Poly(soybean oil methacrylate) derivatives. PSBMA, PSBMAH, PSBMAEO.	GPC	Mn and MWD of different lignin-g-poly(soybean) synthesized materials: Lignin-g-PSBMA (31.9 M g/mol/2.7); Lignin-g-PSBMAH (57.1 M g/mol/4.4); Lignin-g-PSBMAEO (64.3 M g/mol/4.0). T = 35 °C; refractive index detector. Columns: HR1, HR3 and HR5E. Solvent: THF at 1 mL/min. Calibration with polystyrene standards. Samples prepared in THF (4 mg/mL) and filtered using a 0.2 mm mesh.	 	[134]
Hydroxypropyl cellulose (HPC)	Steglich esterification of PABTC over HPC using DCC and DMAP, and grafting of PABTC, with further polymerization of EA and NIPAAM	SEC	MWD by SEC; two PL polar gel M and one PL polar gel 5 mm guard columns; refractive index detector; Eluent: N,N-dimethylformamide/ 0.3 M LiBr, 0.5 mL/min.		[108]
Cellulose acetate	Solvents: DMSO, PDX, DMAc, C ₃ H ₆ O; initiators for grafting and polymerization: CAN, Sn(Oct) ₂ and BPO.	GPC	Number average molecular weights (M _n) and dispersity values (Đ) of grafted PMMA extracted from samples of graft copolymer. Apparatus: Agilent 1100 with 3 PSS GPC 8 300 mm, 5 mm, 10 ⁶ , 10 ⁵ , 10 ³ Å columns; eluent: THF, 0.8 mL/min, at 20°C. Calibration using polystyrene standards with molecular weights ranging 200–10 ⁶ g/mol.		[111]
Microcrystalline cellulose	ROP of L-LA with DMAP in an ionic liquid (AmimCl) to produce Cellulose-g-PLLA.	HPLC	Apparatus: Agilent 1200 with an XDB-C18 phase column. Eluent: H ₂ O—methanol (20:80 by vol.), 0.8 mL/min.		[116]

Table 11. Cont.



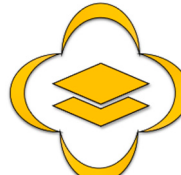
Backbone	Grafts	Technique	Property Measured	Application	Refs.
Hemicellulose	Hemicellulose grafting using TBD and ϵ -caprolactone monomers.	GPC	Apparatus: Malvern Viscotek HT GPC 350; refractive index (RI) and viscometer detectors. PSS-GRAM columns covering a range of 100–1,000,000 g/mol. Eluent: DMSO at 80 °C. Universal calibration using pullulan polysaccharide standards.	 	[37]
Lignin	Insertion of ACX onto lignin to produce a RAFT macro-controller which polymerizes AM and AA.	GPC	Apparatus: Waters Alliance 2695; eluent: aqueous solution of 0.1 M sodium phosphate buffer and 0.01% NaN_3 , at ambient temperature, 1 mL/min.		[139]

Table 12. Summary of characterization techniques based on mechanical properties used for grafted materials.





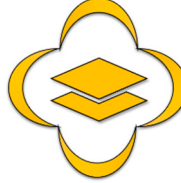
Backbone	Grafts	Technique	Property Measured	Application	Refs.
Lignin-RAFT macro-controller	Poly(soybean oil methacrylate) derivatives. PSBMA, PSBMAH, PSBMAEO.	Tensile strength	TT s/e values for Lignin-g-PSBMAH (1.5 MPa/220 %), PSBMAH (3.0 MPa/120 %) and epoxy resin prepared from grafted materials (17 MPa/22.5 %). Tensile tests were carried out using a crosshead speed of 20 mm/min at ambient temperature. Samples were casted to obtain films. THF polymer solution samples were dried for 12 h under vacuum at ambient temperature and for 6 h, at 60 °C. Films were cut into dog-bone tensile samples of 20 mm length and 5 mm width.	 	[134]
Cellulosic <i>Grewia optiva</i> fibers	FAS-H ₂ O ₂ redox initiation for grafting of MA and KPS, followed by polymerization of MA.	Swell index	Swelling of raw and grafted fibers in different solvents (DMF, water, methanol, and isobutyl alcohol) was measured.		[110]
Cellulose nanocrystal (CNC)	Macromolecular initiator obtained from the reaction between Br-iBuBr and CNC using TEA as catalyst, via SI-ATRP with Sty. Material was casted in PMMA.	Tensile strength	The mechanical properties of nanocomposites were investigated through breaking strength and elongation at break tests.		[118]
Cellulose cotton fiber pulp	Esterification of maleic anhydride grafted over PHA (through double bonds). PHA-g-MA grafted onto cellulose cotton fiber pulp (through the anhydride group).	Tensile strength	Apparatus: Lloyd Instruments, Model LR5 K; 100 mm/min (ASTM D638); pieces sized 150 × 15 mm (length × width). Mean values were determined from measurements from four specimens.		[120]

Table 12. Cont.



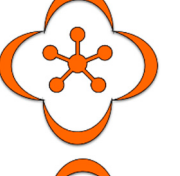
Backbone	Grafts	Technique	Property Measured	Application	Refs.
Hemicellulose	Hemicellulose grafting using TBD and ϵ -caprolactone monomer	Tensile strength	Apparatus: Shimadzu Autograph AG-500A. Method: ISO 527-2. Specimen size: $35 \times 4 \times 0.3$ mm. Tests carried out at ambient conditions; 10 mm/min, 12 mm distance between grips. Properties measured: ultimate strength, Young's modulus, and elongation at break (5 repeats).	 	[37]
Regenerated cellulose fibers (rayon)	Photo-chemical grafting of PETA without photoinitiator.	Tensile strength	Apparatus: Z020 universal testing device with 20 kN load cell. Clamping length: 25 mm, 1 mm/min, pre-load stress of 5 N, and a clamping pressure of 2.5 bar. Specimen: $100 \text{ mm} \times 10 \text{ mm} \times 2 \text{ mm}$.	  	[123]
		Fatigue	Apparatus: 858 Mini Bionix II, MTS testing machine, Systems Corporation. Cyclic tests under tensile stresses ($R = 0.1$) were performed. Experiments reaching total cycle numbers of 1 million were considered as runouts. Fatigue tests performed uniformly at 10 Hz. Experiments proceeded until breakage or reaching runout conditions.		

Table 13. Summary of biological, functional, and compositional characterization techniques employed in grafted materials.





Backbone	Grafts	Technique	Property Measured	Application	Refs.
CellClAc	Macro initiator, Cu(I)Cl/2'2'BIPI catalytic system via ATRP of 4NPA and MMA	Elemental analysis	Apparatus: Leco CHNS-932. Elements determined: C, N and H elements.		[109]
CellClAc	Macro initiator, Cu(I)Cl/2'2'BIPI catalytic system via ATRP controller.	Elemental analysis	Apparatus: Leco CHNS-932. Elements determined: C, N and H elements.		[112]
Cellulose cotton fibers	Na ₂ CO ₃ and thermal activation using MTC-b-CD and silver nitrate	Microbiological investigations	Materials treated with Ag ⁰ and Ag ⁺ were evaluated for antibacterial activity. Gram-positive coccus (<i>Staphylococcus aureus</i> ATCC 25923) and Gram-negative bacillus (<i>Escherichia coli</i> ATCC 25922) microorganisms were used. The Kirby-Bauer diffusimetrical method was used to achieve this purpose. Bacterial cultures were standardized according to McFarland scale for 18 h, yielding 10 ⁷ –10 ⁸ CFU/mL. After inoculation, sample discs were placed on the surface of the medium. Antibacterial activity was assessed after 24 h of incubation, at 37 °C.		[113]
Microcrystalline cellulose	ROP of L-LA with DMAP in an ionic liquid (AmimCl) to produce Cellulose-g-PLLA	Load and controlled release	A solution of grafted material (60.0 mg) and vitamin C (60.0 mg) in 2 mL of PBS was prepared and then transferred to a dialysis bag. Dialysis against 1 L distilled water for 24 h (water refreshment after 12 h) followed. Afterwards, the dialysis bag was immersed into a 400 mL phosphate buffer solution, at conditions similar to those of intestinal fluid (pH 7.40) at 37 °C. 2 mL samples were taken at predetermined times, and analyzed at I _{max} = 245 nm for vitamin C.		[116]

Table 13. Cont.


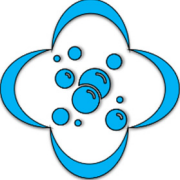


Backbone	Grafts	Technique	Property Measured	Application	Refs.
Cellulose cotton fiber pulp	Esterification of maleic anhydride grafted onto PHA (through double bonds). PHA-g-MA grafted onto cellulose cotton fiber pulp (through the anhydride group).	Surface roughness	Measurement of surface roughness accomplished using an L&M CE165 PPS tester.		[120]
		Contact angle (hydrophobicity)	Surface hydrophilicity was analyzed by contact angle measurements. Tests carried out at ambient conditions using a Dataphysics OCA40 Micro instrument. Surface free energy parameters were estimated from these data.		
Cellulosic filter papers	Radiation-induced graft (RIGCP) copolymerization of acrylonitrile.	Chelating rare elements	Chelation of uranium, thorium, and lanthanides by the batch procedure took place.		[121]
Hemicellulose	Hemicellulose grafting using TBD and ϵ -caprolactone monomers.	Contact angle	Measurements carried out using an NRL Contact Angle Goniometer by Rame-Hart, model 100–00.		[37]
		Biodegradation test	Method: ISO 14851. Biochemical Oxygen Demand (BOD) measurements were obtained under aerobic conditions.		

Table 13. Cont.




Backbone	Grafts	Technique	Property Measured	Application	Refs.
CellClAc	NCHA, 4VP, DA and DAAM grafted by atom transfer radical polymerization (ATRP) using CuCl, 2,2'-BIP as catalyst.	Elemental analysis	Elemental analyses carried out in a Leco CHNS-932 apparatus.		[122]
		Electrical conductivity	Electrical conductivity determined with a Keithley 6517A electrometer. Cell-g-4VP was the only material that behaved as semiconductor.		
Chitosan	Embedded polymerization of N-VP and 4VP. Crosslinking agent: N'-N'-MBA	Swell index	Swelling measurements were carried out in distilled water, in simulated intestinal buffer of pH 6.8 and in simulated gastric buffer of pH 1.4 (7 mL of HCl, 2 g of NaCl and 0.1 L of distilled water) at ambient conditions. A known weight of dry sample was placed into a teabag and immersed into aqueous medium. After a while, the bag was taken out and hung for 5–10 min to eliminate excess unabsorbed water, and then weighed.		[164]
		Load and controlled release	The loading capacity (milligrams of doxocycline entrapped per 100 milligrams of dried drug-loaded gels, %) of CS graft gels (CS-g) was determined as follows: the drug loaded CS-g gel was ground to fine power followed by immersion of a known amount of it into 0.1 L of HCl aqueous solution for 24 h under magnetic stirring. Then, the solution was filtered and used to determine the absorbance (A) of the drug contained in it using a Perkin Elmer Lambda 35 apparatus at 280 nm. Release profiles of the model drug (doxocycline) from the drug-loaded polymers were determined in distilled water (pH = 1.5) and in buffer solutions (pH = 6.8). All the studies were carried out in triplicate.		

Table 13. Cont.






Backbone	Grafts	Technique	Property Measured	Application	Refs.
Regenerated cellulose fibres (rayon)	Photo-chemical grafting of PETA without photoinitiator.	Fiber volume content	Volume of materials was determined by measuring the dimensions of samples (calliper gauge 500-171-20, Mitutoyo), and from grammage and density of fibers, referred to the total mass determined using a type 440 35N fine-scale.		[123]
					
					
Cellulose nanofibrils	Nitroxide TEMPO insertion and NMP of HEMA	BET	Apparatus: NOVA 1200e Quantachrome. Method: Brunauer–Emmett–Teller (BET) method for analysis of N ₂ gas adsorption isotherms. Estimated properties: specific surface area (SBET) and average pore volumes. BET surface area improved from 9.87 m ² /g for TEMPO-Cellulose to 19.7283 m ² /g for HEMA–TEMPO-Cellulose. The microporous volume (V _{total}) increased from 0.0484 cm ³ /g to 0.0705 cm ³ /g, for HEMA–TEMPO-Cellulose.		[124]
		Electrical conductivity	Electrical resistivity determined using a four-point probe system (ST 2253, Suzhou Jingge Electronic Co.). The direct freezing method was compared against the unidirectional gradient freezing method. Samples produced using the direct freezing method exhibited higher resistivity values.		

Table 13. Cont.


Backbone	Grafts	Technique	Property Measured	Application	Refs.
Lignin	Insertion of ACX onto lignin to produce a RAFT macro-controller that polymerizes AM and AA	Surface tension	Apparatus: De Nouy ring-type tensiometer (Krüss), at 25 °C.		[139]
		Emulsification test	Absorbance of solutions of dissolved grafted material in deionized water and mixtures of hexanes (ultrasonication required for dissolution) was measured using a Cary 300 spectrophotometer. Comparison of this value with that of the starting aqueous solution allowed calculation of lignin content in the emulsion phase.		

Table 14. Overview of studies focused on the modeling of polymer grafting.

Backbone	Functionalization Method	Graft Chains	Modeling Approach	Highlights/Comments	Ref.
Pre-polymer containing highly active chain transfer sites (pendant mercaptan groups).	CTP between polymer radicals and pendant mercaptan groups.	Vinyl polymer	Kinetic model for FRP including CTP; model equations solved numerically and approximate closed form equations were also used.	Calculated properties/variables: grafting efficiency (Equation (1)) and number average molecular weights of the different polymer molecules (Equations (2)–(6)).	[39]
Solid polymeric substrates.	Irradiation of polymer/monomer mixture.	Vinyl polymer	Calculation of r_n , r_w and number full chain length distributions (n_x) from kinetic equations.	Two limiting cases were considered in the calculation of n_x : (a) radicals terminating by disproportion, no significant chain transfer and complete conversion; and (b) no chain transfer and incomplete conversion (see Equation (7)).	[40]
Polyolefins	High temperature CTP.	Vinyl polymer	Kinetic modeling from a given polymerization scheme.	Review paper considering chemical modification of polyolefins by FRP in extruders.	[231]
Silica substrate	Formation of a growing grafted polymer chain from reaction between an initiator derived primary free radical and a “surface site.”	Poly(vinylpyrrolidone)	Use of a “conservational polymerization and molecular-weight distribution” (CPMWD) numerical method to solve the kinetic equations.	The proposed numerical approach provides monomer conversion, grafting yield, and full MWDs of active and inactive homopolymer and graft polymer species.	[232]
Porous silica beads	Chain transfer reaction to fixed mercapto groups present in the pre-functionalized silica beads.	Polystyrene	Kinetic model that allows calculation of full MWD and \bar{D} ; no details on numerical approach or software used were provided.	MWDs were approximated assuming them, as a first approach, to follow a normal distribution function.	[233]
PE	CTP by FRP in melt, in a twin-screw extruder (TSE).	Poly(glycidyl methacrylate) (PGMA)	Coupling of flow characteristics from a TSE simulation program and a reactor model consisting of plug flow and “axial dispersion” reactor cells.	Overall GMA conversion was predicted, showing general good agreement with experimental data.	[234]
PE	CTP by FRP in melt, in a twin-screw extruder (TSE).	Poly(maleic anhydride) (PMAH)	Coupling of reaction kinetics to flow equations in a twin-screw extruder.	Satisfactory agreement between calculated and experimental data.	[235]

Table 14. Cont.

Backbone	Functionalization Method	Graft Chains	Modeling Approach	Highlights/Comments	Ref.
Polypropylene (PP)	CTP by FRP in melt	PMAH	A kinetic model which captures the effect of MAH and initiator concentrations on grafting yield and MWDs during the grafting process was derived.	Model performance assessed by comparing calculated and experimental data from different sources, for batch (internal mixer, static film) and continuous systems (twin-screw extruder), under a wide window of operating conditions.	[236]
Cellulose or cellulose containing fibers	Not specified (empirical approach)	Monochlorotriazinyl- β -cyclodextrin	Neural network modeling (semi-empirical approach).	A good approximation of the studied grafting process was obtained.	[237–239]
PP	CTP by FRP in solid state, in presence and absence of supercritical CO ₂ (scCO ₂).	PMAH	A kinetic model focused on polymerization and grafting rates was used.	The effect of presence or absence of scCO ₂ on grafting rate was analyzed.	[240]
PP	CTP by FRP in solid state, with and without scCO ₂ .	Not specified	The kinetic model and grafting mechanism of the scCO ₂ assisted grafting of PP in the solid state were reviewed.	Grafting rate controlled by diffusion in absence of scCO ₂ and by the chemical grafting step in presence of scCO ₂ .	[241]
Polybutadiene (PB)	CTP by FRP in production of high-impact PSty (HIPS).	PSty	An existent heterogeneous model is generalized to consider bivariate distributions of graft copolymer topologies; each topology is determined by the number of trifunctional branching points per molecule.	Polymerization in two phases is assumed. Adjustment of a single kinetic parameter is required. Grafting efficiencies obtained from solvent extraction/gravimetry are contrasted against estimates obtained by the deconvolution of size exclusion chromatograms for total polymer.	[242]
Poly[ethylene-co-(1-octene)]	CTP by FRP in molten state	PMMA	A model compound approach was used.	The focus was on assessing the effect of temperature, polymerization time and initiator content on MMA polymerization rate and number average chain length, in the presence of alkoxyl radicals and alkanes.	[243]

Table 14. Cont.

Backbone	Functionalization Method	Graft Chains	Modeling Approach	Highlights/Comments	Ref.
PSty	Use of a Friedel-Crafts reaction, which gives rise to a mixture of unmodified PE, modified PS and a PE-g-PS copolymer.	PE	A model for predicting the complete MWD of the homopolymers, and the chemical composition distribution (CCD) of the graft copolymer was presented. Probability generating functions were used to carry out the calculations.	The model takes into account the opposing effects of rival reactions that occur in the studied grafting reaction.	[244,245]
PE	CTP by FRP	PSty	A kinetic mechanism for the whole process and application of the method of moments to solve the mass balance equations are proposed.	The model is able to calculate average molecular weights and the amount of grafted PS.	[246]
PP	CTP by FRP	PMAH	A kinetic model for the free-radical grafting of maleic anhydride MAH onto PP, considering that the reaction medium is heterogeneous due to the incomplete solubility of MAH in the polymer melt was developed.	Two different approaches are considered that derive from the limiting cases of very fast mass transfer (equilibrium) and no mass transfer between the two phases. The physical parameters considered in the model include the solubility of MAH in PP and the partition coefficient of the initiator between the two phases.	[247]
Carboxyl functionalized hydrophilic Sephadex (a cross-linked dextran gel used for gel filtration) derivatives.	Covalent amine conjugation method analyzed using XPS.	Poly(ethylene glycol) (PEG)	Langmuir and Langmuir-Freundlich isotherm models are used to study PEG-grafting kinetics. Fractional C-O intensities obtained from high-resolution C 1s scans are correlated with grafting.	The models are assessed by comparing calculated profiles and experimental data.	[248]

Table 14. Cont.

Backbone	Functionalization Method	Graft Chains	Modeling Approach	Highlights/Comments	Ref.
Various surfaces	Surface-initiated controlled radical polymerization.	Polymers from 2-methacryloyloxyethyl phosphorylcholine (MPC), methyl acrylate, acrylamide, and N-isopropylacrylamide.	A kinetic model for surface-initiated atom transfer radical polymerization (SI-ATRP) with addition of excess deactivator in solution was presented.	Polymer layer thickness, and concentrations of radical, dormant and dead polymer molecules can be calculated. A simple but reliable analytical solution is proposed for estimation of the evolution of polymer layer thickness.	[249]
Partially fluorinated polymers such as poly(vinylidene fluoride) and poly(ethylene-co-tetrafluoro ethene).	Radiation induced grafting	Poly(4-vinylpyridine)	Box-Behnken factorial designs and response surface method (RSM) were used.	A quadratic model was used to obtain the optimal set of conditions (absorbed dose, monomer concentration, grafting time and reaction temperature) to maximize the degree of grafting (G%), using a statistical software. Adequate agreement between model predictions and experimental data supported the approach proposed.	[250,251]
Poly(propylene glycol) (PPG)	CTP by FRP	Poly(styrene-co-acrylonitrile) (SAN)	A batch kinetic model for grafting copolymerization of Sty and acrylonitrile (AN) in the presence of PPG is modified to include semi-continuous and continuous processes.	The semi-continuous model is validated using experimental data, although molecular weight agreement is poor. The continuous process is simulated but not contrasted against experimental data. According to the model, graft efficiency increases drastically, and Mw decreases with decreasing St/AN weight ratio.	[252]
Starch	(Mechanically activated) CTP by FRP	Polyacrylamide	A kinetic model for an inverse emulsion copolymerization system was used. The effects of initiator, monomer, starch, and emulsifier content on reaction rate of graft co-polymerization (Rg) were determined. The kinetic model was modified to provide acceptable agreement with experimental data.	It was observed that the relationship between Rg and the concentration of components in the polymerization system can be expressed for all of the four components by the following equation: $Rg \propto [mSt]^{1.24} [I]^{0.76} [M]^{1.54} [E]^{0.33}$, which is consistent with the kinetic equation from theoretical studies: $Rp \propto [mSt]^{0.5 \sim 1} [I]^{0.5 \sim 1} [M]^{1 \sim 1.5} [E]^{0.6}$.	[253]

Table 14. Cont.

Backbone	Functionalization Method	Graft Chains	Modeling Approach	Highlights/Comments	Ref.
PB seed latex particles	CTP by emulsion FRP	SAN	Emulsion grafting copolymerization is model using a two-phase kinetic model. Monomer concentrations in the different phases is calculated.	Partition of components between phases calculated as in previous models. The model is extended to account for calculation of grafting efficiency and copolymer composition of free and grafted molecules.	[254]
PE	CTP by FRP in REX	PAA	Monomer conversion to homo- and grafted-polymers are calculated separately using an incremental theory. The approach allows calculation of degree of grafting, mass of homopolymer and grafting efficiency.	The focus was on analyzing the effect of temperature and initial concentrations of monomer and initiator on degree of grafting. Both grafting and amount of homopolymer increase with temperature and monomer concentration.	[255]
Natural rubber latex (core-shell particles)	CTP by emulsion FRP	PMMA	The model consists on rate expressions of polymer chain formation. A decrease of CHPO by TEPA and a population event of radicals between core/shell phases are considered in the model.	Grafting efficiency and polymer composition for free and grafted polymer populations can be calculated in terms of initial conditions (monomer and initiator content, and rubber weight ratio and temperature).	[256]
Vinyl/divinyl copolymer synthesized by RAFT chemistry.	CTP by FRP	Non-specified RAFT synthesized graft	A RAFT crosslinking model was used to address the molecular imprinting step. The size of grafted brushes was estimated from MWD calculations for a RAFT homo-polymerization.	The model includes the two steps involved in the production of MIP responsive particles. Limitations and ways to improve the model are discussed.	[257]
High-density PE (HDPE)	Melt free-radical grafting (semi-empirical approach)	GMA	Response surface, desirability function, and artificial intelligence approaches were combined to account for polymer grafting. Input variables: monomer content, initiator concentration, and melt-processing time.	An in-house code that learns and mimics processing torque and grafting of GMA onto HDPE was developed. Optimization of the process and quantification of the competition between grafting and crosslinking was carried out.	[258]

Table 14. Cont.

Backbone	Functionalization Method	Graft Chains	Modeling Approach	Highlights/Comments	Ref.
PE	CTP by FRP in post-polymerization modification	Vinyl polymers	A kinetic Monte-Carlo (kMC) modeling approach for free radical induced grafting of vinyl monomers onto polyethylene (PE), assuming isothermicity, perfect macromixing and diffusion-controlled effects was developed.	Calculated variables: monomer conversion, grafting selectivity and yield, MWDs of all macromolecular species involved, average grafting (from/to) and crosslink densities, number of grafts and crosslinks per individual polymer molecule, and chain length of every graft.	[259]
PE	CTP by FRP (batch operation)	Vinyl polymers	A kMC model was used. Reactions included: initiator dissociation, hydrogen abstraction, graft chain initiation, graft (de)propagation, crosslinking, and homo (de) polymerization.	Assumptions: isothermicity and single-phase polymerization. It is found that the grafting kinetics is affected by hydrogen abstraction and depropagation kinetic rate constants, equilibrium coefficient K_{eq} , and initial content of monomer, initiator, and polyolefin.	[260]
PE	CTP by FRP (tubular reactor)	Vinyl polymers	kMC, as in [260]	They found that functionalization, selectivity and grafting density are able to reach remarkably better values (e.g., 100%) if multiple injection points are considered for monomer, initiator and/or a temperature profile.	[261]
PE	CTP by FRP (two-phase system)	Vinyl polymers	kMC; the model of [260,261] is further extended to include two phases.	The partition of monomer and initiator between the two phases is addressed by introducing overall mass transfer coefficients. The model is tested with a monomer with low to negligible homo-propagation. Positive agreement with industrial experimental data was obtained.	[41]

Table 15. Polymerization scheme for free-radical polymerization including CTP and crosslinking.

Reaction Step	Kinetic Expression	Remarks
Initiator decomposition	$I \xrightarrow{k_d} 2R$	
First propagation	$R + M \xrightarrow{k_i} P_1$	
Propagation	$P_n + M \xrightarrow{k_p} P_{n+1}$	$n = 1, \dots \infty$
Termination by disproportionation	$P_n + P_m \xrightarrow{k_{td}} D_n + D_m$	$n, m = 1, \dots \infty$
Propagation through intermediate free radicals	$P_{n,b} + M \xrightarrow{k_p} P_{n+1,b}$	$n = 1, \dots \infty$ $b = 0, \dots \infty$
Chain transfer to polymer	$P_{n,b} + D_{m,c} \xrightarrow{k_{trp}} D_{n,b} + P_{m,c+1}$	$n, m = 1, \dots \infty$ $b, c = 0, \dots \infty$
Propagation through pendant double bonds (crosslinking), assuming a pseudo-kinetic rate constants method (pseudo-homopolymer) approach	$P_r + D_s \xrightarrow{k_p^{*0}} P_{r+s}$	$r, s = 1, \dots \infty$

Table 16. Symbols of application fields.




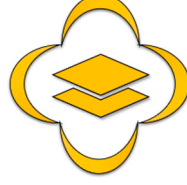
Symbol of Corresponding Application	Meaning
	Biocomposites and biomaterials.
	Green chemistry and innovative processes.
	Electronic materials, electrical properties, and conjugated polymers.
	Surface modification, hydrophilic or hydrophobic surfaces.

Table 16. Cont.





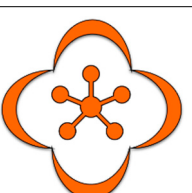
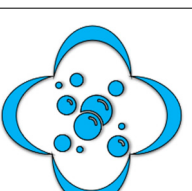
Symbol of Corresponding Application	Meaning
	Flame retardancy, additives for flame retardancy in polymer blends, thermal resistance materials.
	Antimicrobial applications.
	Adhesives, polymer networks, crosslinked polymers, gels.
	Controlled release of drugs and chemicals.
	Polymer composites and blends, by extrusion, casting or co-precipitation.
	Chelating properties, membranes, effluent remediation.

Table 16. Cont.




Symbol of Corresponding Application	Meaning
	Mechanical properties improvement, micro and nano reinforcement.
	Application in polyolefins, polyethylene, polypropylene.
	Aerogels, light, or porous materials.

Table 17. Abbreviations used for characterization techniques.

Abbreviation	Meaning
FTIR	Fourier transformed mid-infrared spectroscopy.
ATR	Attenuated total reflection.
^1H -NMR	Proton nuclear magnetic resonance.
^{13}C -NMR	Carbon nuclear magnetic resonance.
TT	Tensile test.
DMA	Dynamical mechanical analysis.
GPC	Gel permeation chromatography.
TGA	Thermogravimetric analysis.
DSC	Differential scanning calorimetry.
FR	Flame retardancy.
XPS	X-ray photoelectron spectroscopy.
EDAX	Energy-dispersive X-ray analysis/spectroscopy.
WAXD	Wide Angle X-ray Scattering.
XRF	X-ray fluorescence.

Table 18. Abbreviations of properties and variables measured by characterization techniques.

Technique	Abbreviation	Explanation	Units
Chromatography	MWD	Molecular weight distribution of polymers.	-
	M_n	Number average molecular weight.	g/gmol
Thermal	Tg	Glass transition temperature.	°C
	MDT	Maximum degradation temperature.	°C
	MFI	Melt flow index.	g/10 min
	THR	Total heat release.	MJ/m ²
	PHRR	Peak heat release rate.	kW/m ²
Mechanical	σ	Maximum stress measured in tensile test.	MPa
	ϵ	Maximum elongation observed in tensile test.	%

Table 19. Abbreviations and formulae of some chemical compounds and materials used.


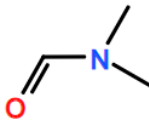
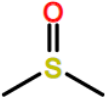
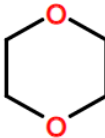
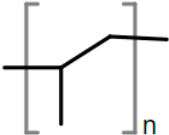
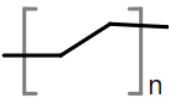
Abbreviation	Compound	Chemical Structure	Ref.
"P"	Before the name or abbreviation of a monomer means polymer of that monomer.		
"B-g-C"	Means "C" chains grafted to "B" backbone.		
THF	Tetrahydrofuran.		[17,18]
DMF	Dimethylformamide.		[121,125,139,141,144,146,147,151,152,165]
DMSO	Dimethyl Sulfoxide.		[37,111]
PDX	1,4-dioxane.		[111,140,142,150]
PP	Polypropylene.		[135]
PE	Polyethylene.		[135]

Table 19. Cont.

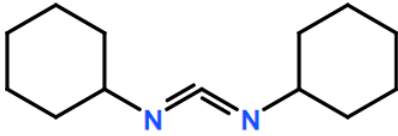
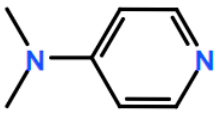
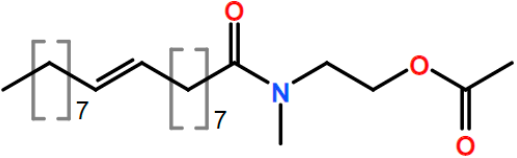
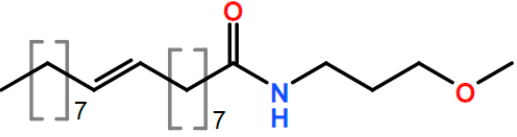
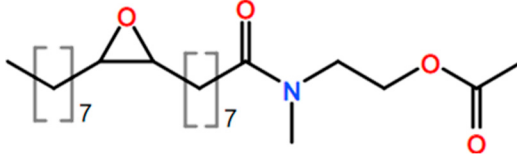
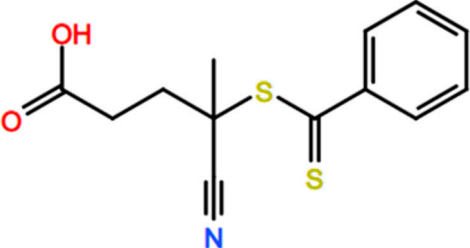
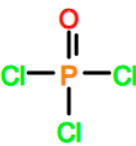
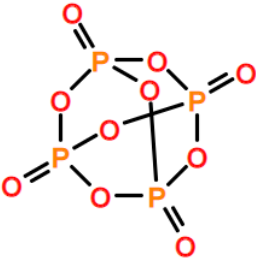
Abbreviation	Compound	Chemical Structure	Ref.
DCC	Dicyclohexylcarbodiimide.		[108,165]
DMAP	4-Dimethylaminopyridine.		[108,116,165]
SBMA	(E)-2-(N-methyloctadec-9-enamido)ethyl methacrylate.		[134]
SBMAH	(E)-3-(octadec-9-enamido)propyl methacrylate.		[134]
SBMAEO	2-(N-methyl-8-(3-octyloxiran-2-yl)octanamido)ethyl methacrylate.		[134]
	4-cyano-4-(phenylcarbonothioylthio) pentanoic acid.		[134]
POCl ₃	Phosphoryl trichloride.		[125,135]
P ₄ O ₁₀	Phosphorus(V) oxide.		[125,136,137]

Table 19. Cont.

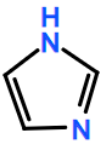
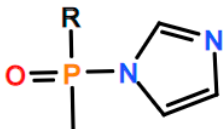
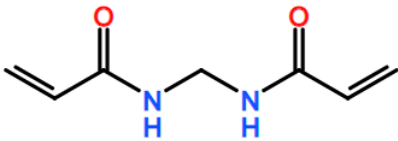
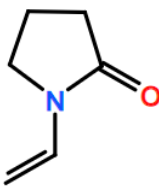
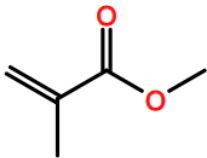
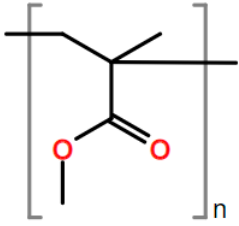

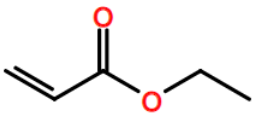
Abbreviation	Compound	Chemical Structure	Ref.
	Imidazole.		[125,135]
IPG	(1H-imidazol-1-yl) phosphonic group.		[125,135]
N'N'-MBA	N'N'-methylenebisacrylamide.		[98,164]
N-VP	N-vinyl pyrrolidone.		[99,164]
Co(acac) ₃	Cobaltacetylacetonate complex.		[99,103]
MMA	Methyl methacrylate.		[58,107,111,117,140,144,146,149]
PMMA	Poly(methyl methacrylate).		[58,107,111,117,140,144,146,149]
AcN	Acrylonitrile.		[107,121]
EA	Ethyl acrylate.		[107,108]

Table 19. Cont.

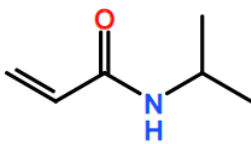
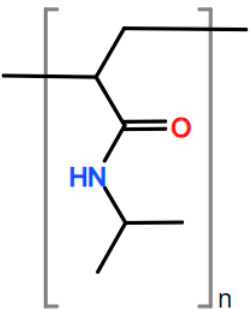
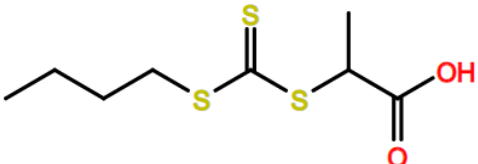
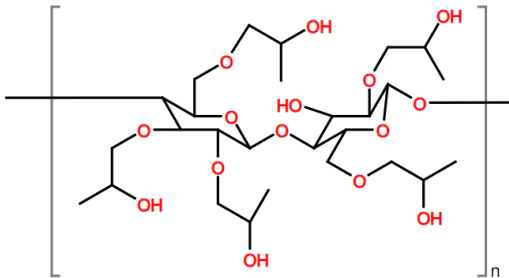
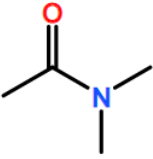
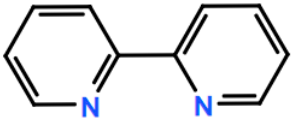
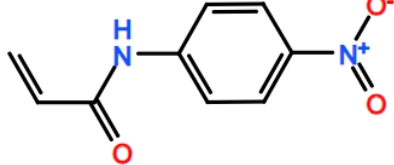
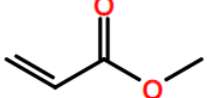
Abbreviation	Compound	Chemical Structure	Ref.
NIPAAM	N-isopropylacrylamide.		[108,138,140,141,143,145,165]
PNIPAAM	Poly(N-isopropylacrylamide).		[108,138,140,141,143,145,165]
PABTC	Propionic acidyl butyl trithiocarbonate.		[108]
HPC	Hydroxypropyl cellulose.		[108]
DMAc	Dimethylacetamide.		[108]
CellClAc	Cellulose chloroacetate.		[109,122]
2'2'BIPI	2,2'-bipyridine.		[109,122,140,146,147]
4NPA	N-(4-nitrophenyl) acrylamide.		[109]
MA	Methyl acrylate.		[110]

Table 19. Cont.

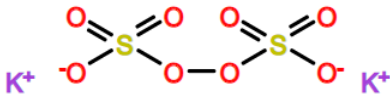
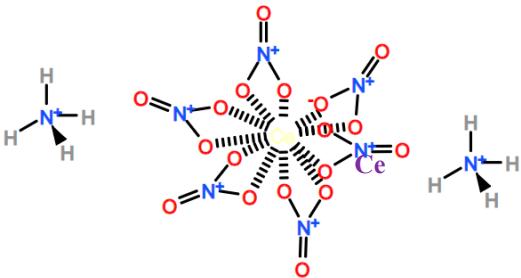
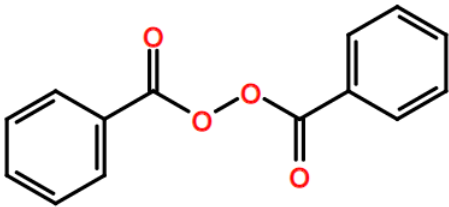
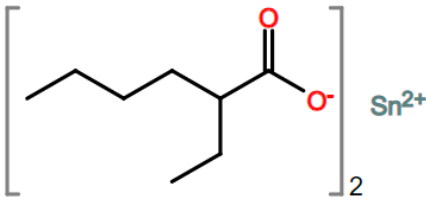
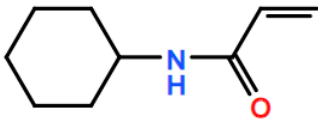
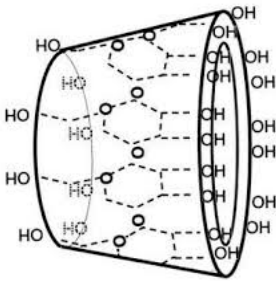
Abbreviation	Compound	Chemical Structure	Ref.
FAS	Ferrous ammonium sulphate.	$(\text{NH}_4)_2\text{Fe}(\text{SO}_4)_2 \cdot 6\text{H}_2\text{O}$	[110]
KPS	Potassium persulphate.		[110]
CAN	Ceric ammonium nitrate.		[111]
BPO	Benzoyl peroxide.		[111]
Sn(Oct) ₂	Tin(II) 2-ethyl hexanoate.		[111]
NCA	N-cyclohexylacrylamide.		[112]
AgNPs	Silver nanoparticles.	Ag	[113]
b-CD	β-cyclodextrin.		[113,114]

Table 19. Cont.

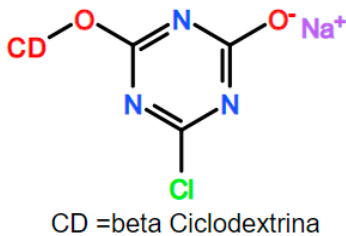
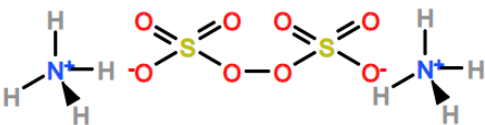
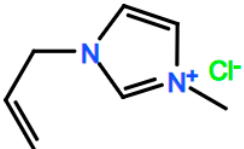
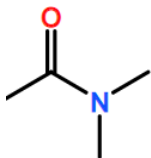
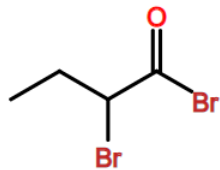
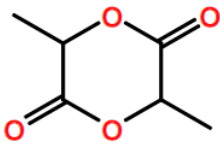
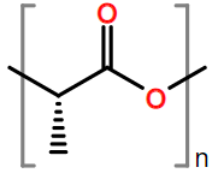
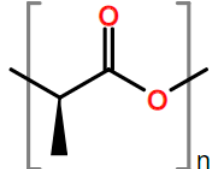
Abbreviation	Compound	Chemical Structure	Ref.
MTC-b-CD	Monochlorotriazinyl- β -cyclodextrin.	 <p>CD =beta Ciclodextrina</p>	[113,114]
APS	Ammonium persulfate.		[115,117]
AmimCl	1-allyl-3-methylimidazolium chloride.		[116]
PBS	Phosphate-buffered saline solutions.		[116]
DMAc	N,N-dimethyl acetamide.		[111,117]
Br-iBuBr	2-Bromoisobutyryl bromide.		[118]
L-LA D-LA	L-lactide. D-lactide.		[116,119,157,159]
PLLA	Poly(L-lactide).		[116,119,157,159]
PDLA	Poly(D-lactide).		

Table 19. Cont.

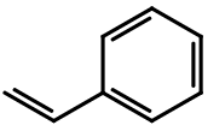
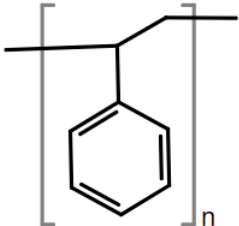
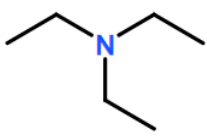
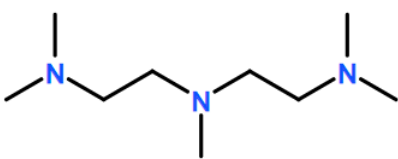
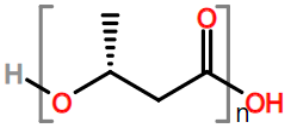
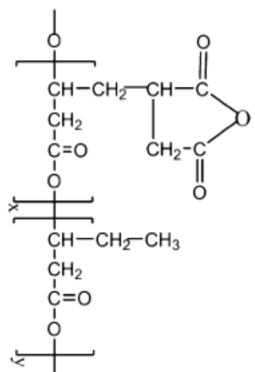
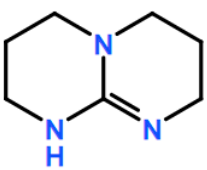
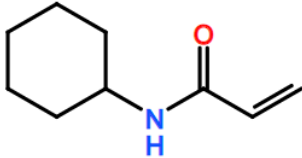
Abbreviation	Compound	Chemical Structure	Ref.
STY or Sty	Styrene.		[58,118,140,146,147,149]
PS or PSty	Polystyrene.		[58,118,140,146,147,149]
TEA	Triethylamine.		[118]
PMDETA	N, N, N', N', N''-Pentamethyldiethylenetriamine.		[118,140,146]
PHA	Polyhydroxyalkanoate.		[120]
PHA-g-MA	Poly(hydroxyalkanoate-grafted-maleic anhydride).		[120]
TBD	1,5,7- triazabicyclodecene [4.4.0].		[37]
NCHA	N-cyclohexylacrylamide.		[122]

Table 19. Cont.

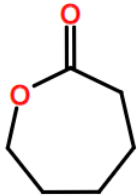
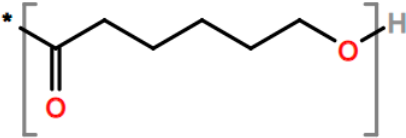
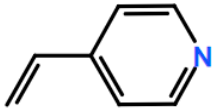
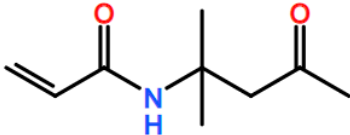
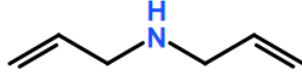
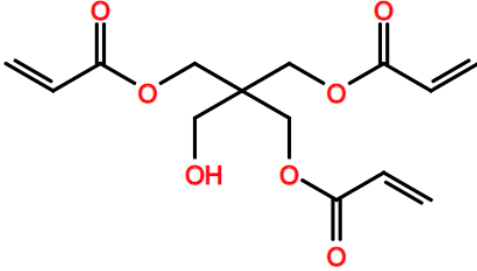
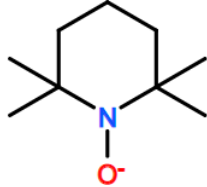
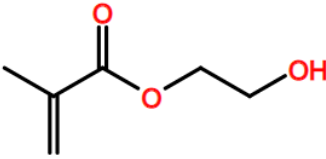
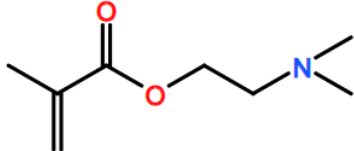
Abbreviation	Compound	Chemical Structure	Ref.
CL	ϵ -Caprolactone..		[37,158,159,161,162]
PCL	Poly-(ϵ -caprolactone).		[37,158,159,161,162]
4VP	4-vinylpyridine.		[122,164]
DAAM	Diacetone acrylamide.		[122]
DA	Diallylamine.		[122]
PETA	Pentaerythritol triacrylate.		[123]
TEMPO	TEMPO nitroxide.		[124]
HEMA	2-hydroxyethyl methacrylate.		[124]
DMAEMA	2-dimethylaminoethyl methacrylate.		[138,150]

Table 19. Cont.

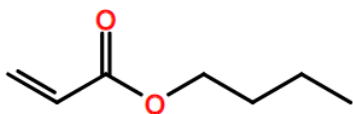
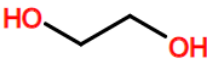
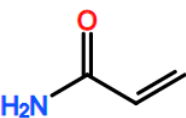
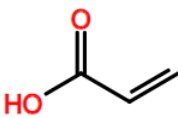
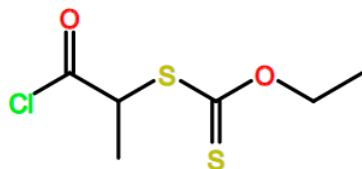
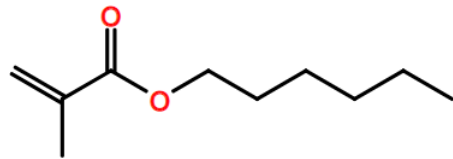
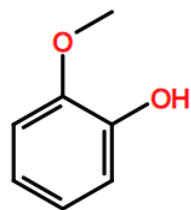
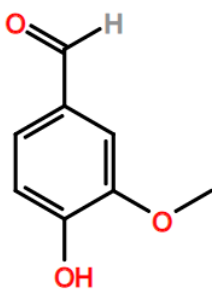
Abbreviation	Compound	Chemical Structure	Ref.
BA	Butyl acrylate.		[138]
EG	Ethylene glycol.		[138]
AM	Acrylamide.		[58,138,139,151,153]
AA	Acrylic Acid.		[58,138,139]
ACX	Acyl chloride xanthate.		[139,153]
LMA	Lauryl methacrylate.		[140]
	Guaiacol.		[140]
	Vainillin.		[140]

Table 19. Cont.

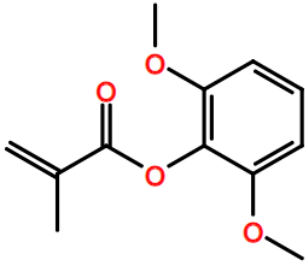
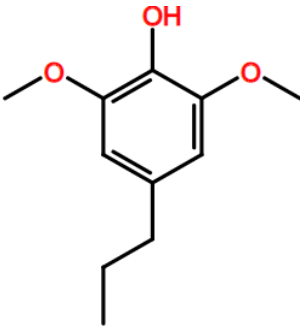
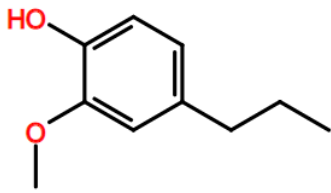
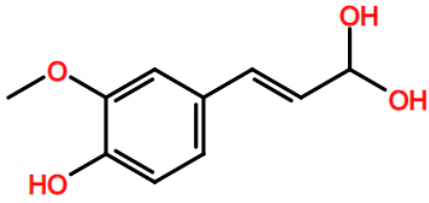
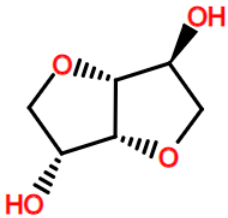
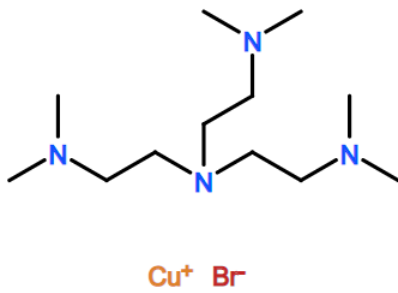
Abbreviation	Compound	Chemical Structure	Ref.
	Syringyl methacrylate.		[140]
	4-propylsyringol.		[140]
	4-propylguaiaicol.		[140]
	Ferulic acid.		[140]
	Isorbide.		[140]
CuBr/HMTETA	1,1,4,7,10,10-Hexamethyltriethylenetetramine Cu(I)Br complex.		[140,143,150]

Table 19. Cont.

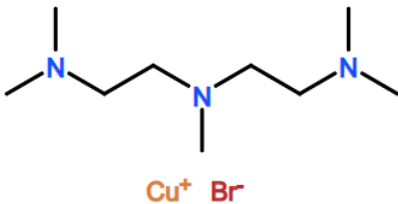
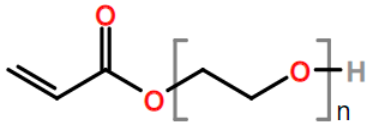
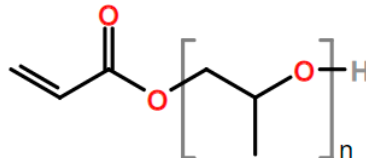
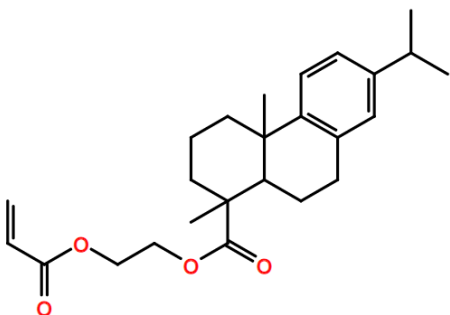
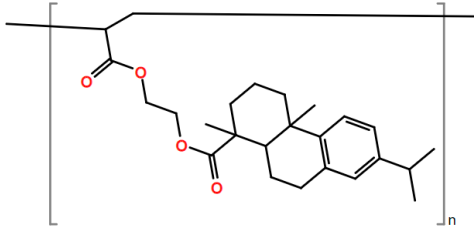
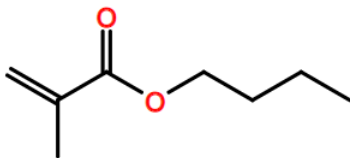
Abbreviation	Compound	Chemical Structure	Ref.
CuBr/PMDETA	N,N,N',N'',N'''-Pentamethyldiethylenetriamine Cu(I)Br complex.		[140,141,146,147]
PEG-A	Poly(ethylene glycol) acrylate. n = 9		[140,143]
PPG-A	Poly(propylene glycol) acrylate. n = 5		[140,143]
DAEA	Dehydroabietic ethyl acrylate.		[140,142]
PDAEA	Poly(dehydroabietic ethyl acrylate).		[140,142]
BMA	Butyl methacrylate.		[140,144]

Table 19. Cont.

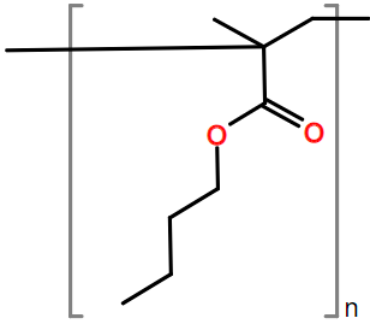
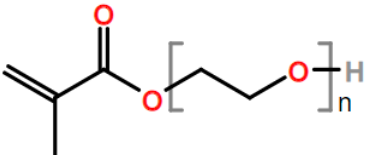
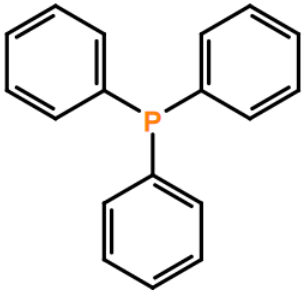
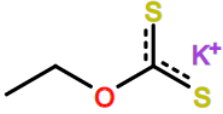
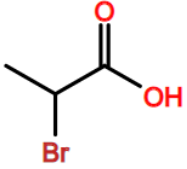
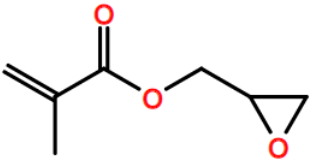
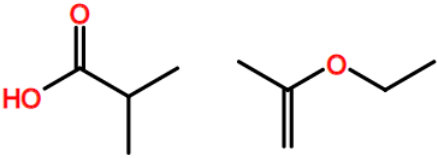
Abbreviation	Compound	Chemical Structure	Ref.
PBMA	Poly(butyl methacrylate).		[140,144]
PEGMA	Poly(ethylene glycol) methacrylate.		[140,148]
PPh ₃	Triphenyl phosphine.		[149]
KEX	Potassium ethyl xanthate.		[151,152]
	2-Bromopropionic acid.		[151,152]
GMA	Glycidyl methacrylate.		[153]
XCA	Xanthate carboxylic acid.		[154]

Table 19. Cont.

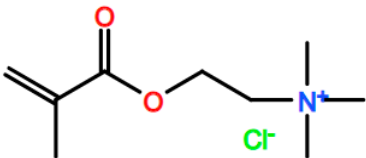
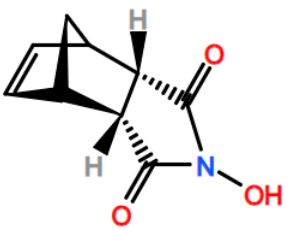
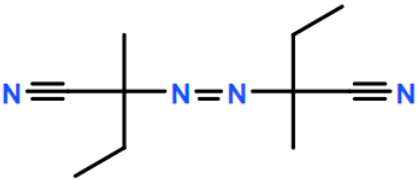
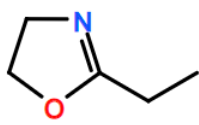
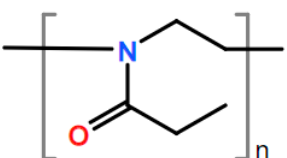
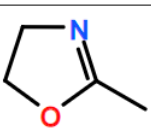
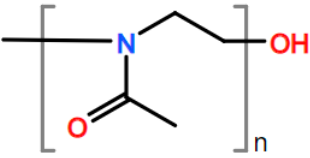
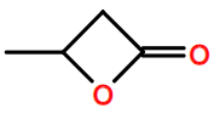
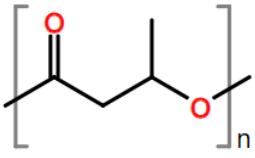

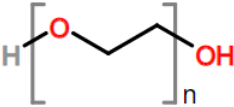
Abbreviation	Compound	Chemical Structure	Ref.
DMC	[2-(Methacryloyloxy)ethyl] trimethyl-ammonium chloride.		[154]
HONB	N-Hydroxy-5-norbornene-2,3-dicarboxylic.		[154]
AMBN	2,2'-azobis (2-methylbutyronitrile).		[154]
EOX	2-ethyl-2-oxazoline.		[155]
PEOX	Poly(2-ethyl-2-oxazoline).		[155]
MOX	2-methyl-2-oxazoline.		[156]
PMOX	Poly(2-methyl-2-oxazoline).		[156]
B-BL	β-Butyrolactone.		[160]
PHB	Poly(3-hydroxybutyrate).		[160]

Table 19. Cont.

Abbreviation	Compound	Chemical Structure	Ref.
EOX	Ethylene oxide.		[163]
PEO	Poly(ethylene oxide).		[161]
P4-t-Bu	1-tert-butyl-4,4,4-tris(dimethylamino)-2,2-bis[tris(dimethylamino)-phosphoranylideneamino]-215,415-catenadi (phosphazene) solution in hexane.		[163]

4. Characterization Techniques Used for Polymer Grafted Materials

The characterization of polymer grafted materials requires the use of a variety of methods due to the many possible combinations of backbones and polymer grafts [59]. The characterization methods can be classified as direct or indirect.

Direct methods are those used to identify changes in the chemical structure of grafted materials, such as the bonds between backbone and grafts. These methods include proton and carbon magnetic nuclear resonance, ^1H -NMR, and ^{13}C -NMR, respectively.

Indirect methods are based on differences in properties between the starting and grafted materials, relating these changes to the modified structures. Microscopy and thermal analysis are examples of indirect methods. A summary of the main characterization methods used for grafted materials is presented in Table 6.

The relevant information contained in selected articles is also gathered in this review to show how the characterization techniques were used to provide evidence of polymer grafting onto the corresponding backbones. Tables 7–12 summarize the use of thermal, spectroscopic, imaging and microscopy, rheological, chromatographical, and mechanical characterization techniques, respectively, in the analysis of polymer grafted materials. Finally, a summary of biological, functional, and composition characterization techniques used for grafted materials is provided in Table 13.

5. Modeling of Polymer Grafting

5.1. Literature review on Modeling of Polymer Grafting

An overview of the literature on the modeling of polymer grafting is summarized in Table 14. The backbones considered, the functionalization methods, the polymer chains grafted, and summary comments on the modeling approaches used to carry out the simulations are included in the table.

5.2. Modeling of Polymer Branching and Crosslinking

As observed in Table 14, most reports on the modeling of polymer grafting are related to cases where grafting involves free-radical growth of the grafts, and the generation of active sites proceeds through chain transfer to polymer reactions. In that sense, the growth of polymer grafts resembles the formation and growth of branches in polymer branching. The difference would be that the branches and primary polymer chains contain the same monomers, whereas grafts and backbones contain different monomers in polymer grafting. There are several papers focused on the modeling of polymer branching [262–268]. In some cases, as in the grafting of monochlorotriazinyl- β -cyclodextrin onto cellulose, the activation mechanism is not specified, and the modeling approach is fully empirical (neural network modeling) [237–239].

In general terms, the polymerization scheme of FRP including chain transfer to polymer (CTP) is given by the reactions shown in Table 15. The specific mathematical expressions containing CTP terms are given by Equations (1)–(7). I, R, and M in Table 15 are initiator, primary free radical, and monomer molecules, respectively; P_n and D_m denote live and dead polymer molecules, respectively, of sizes n and m . k_i , k_p , k_{td} , and k_{trp} (also denoted as k_{fp} in Equations (8) and (9)) denote initiation, propagation, termination by disproportionation, and chain transfer to polymer kinetic rate constants, respectively.

Polymer branching can be modeled using a bivariate distribution of chain length and number of branches resulting from polymerizations involving branched polymers [269]. $P_{n,b}$ in Table 15 accounts for a bivariate distribution of live polymer of length n and number of branches b . The moment equations shown below consider only the kinetic steps of propagation and chain transfer to polymer, for illustrative purposes. For a batch reactor, the application of the mass action law considering only these two kinetic steps results in Equation (1) [269]. It should be noticed that in the transfer to polymer reaction there are as many possible sites of reaction as monomeric units in the dead polymer chain participating in the reaction.

$$\frac{dP_{n,b}}{dt} = \dots - k_p(P_{n,b}M + P_{n-1,b}M) - k_{trp}P_{n,b} \left(\sum_{m=1}^{\infty} \sum_{c=0}^{\infty} mD_{m,c} \right) + k_{trp}nD_{n,b-1} \sum_{h=1}^{\infty} \sum_{e=0}^{\infty} P_{h,c} + \dots \quad (1)$$

$$n = 1, \dots, \infty; b = 0, \dots, \infty$$

The bivariate moments for active and inactive polymer are defined respectively as shown in Equations (2) and (3). Number and weight-averaged molecular weights, and the average number of branches, are given by Equations (4)–(6) [269].

$$\mu_{G,H} = \sum_{n=1}^{\infty} \sum_{b=0}^{\infty} n^G b^H P_{n,b} \quad (2)$$

$$\lambda_{G,H} = \sum_{n=1}^{\infty} \sum_{b=0}^{\infty} n^G b^H D_{n,b} \quad (3)$$

$$M_n = \frac{\mu_{1,0} + \lambda_{1,0}}{\mu_{0,0} + \lambda_{0,0}} W_m \quad (4)$$

$$M_w = \frac{\mu_{2,0} + \lambda_{2,0}}{\mu_{1,0} + \lambda_{1,0}} W_m \quad (5)$$

$$B_n = \frac{\mu_{0,1} + \lambda_{0,1}}{\mu_{0,0} + \lambda_{0,0}} \quad (6)$$

The moment equations for live polymer are given by Equation (7) [269].

$$\frac{d\mu_{G,H}}{dt} = -k_p M \mu_{G,H} + k_p M \sum_{R=0}^G \binom{G}{R} \mu_{G-R,H} - k_{trp} \mu_{G,H} \lambda_{1,0} + k_{trp} \mu_{0,0} \sum_{K=0}^H \binom{H}{K} \lambda_{G+1,H} + \dots \quad (7)$$

Another approach with which to address the modeling of polymer branching in FRP is to use the concept of branching density, denoted as ρ , which is given by the ratio of the number of branching points to that of monomeric units, and it can be estimated using Equation (8), which when solved leads to Equation (9) [270]. k_{fp} and k_p in Equations (8) and (9) are chain transfer to polymer and propagation kinetic rate constants, respectively, and x is monomer conversion.

$$\frac{d(x\rho)}{dx} = \frac{k_{fp}x}{k_p(1-x)} \quad (8)$$

$$\beta = -\frac{k_{fp}}{k_p} \left[1 + \frac{\ln(1-x)}{x} \right] \quad (9)$$

CTP and terminal double bond (TDB) polymerization produce tri-functional (long) branches, in addition to increasing the weight-averaged molecular weight and broadening the MWD. A reaction “similar” to TDB polymerization is the polymerization with internal

(pendant) double bonds (double bonds “internal” in dead polymer chains, appearing therein due to (co)polymerization of di-functional (divinyl) monomers (e.g., butadiene). Internal double bond (IDB) polymerization produces tetra-functional (long) branches and leads eventually to the formation of crosslinked polymer (gel). Both molecular weight averages increase due to IDB polymerization and the MWD broadens considerably [43]. Crosslinking can be considered as interconnected branching, and in that sense, its growth by CTP and its modeling in terms of a crosslink density, denoted as ρ_a , can also be taken as a useful basis for the modeling of polymer grafting by CTP and propagation through the intermediate free radicals. Balance equations for polymer radicals of size r (R_r^*) and ρ_a for a case of copolymerization with crosslinking of vinyl/divinyl monomers, using the pseudo-kinetic rate constants method, are given by Equations (10) and (11), respectively, where P_s is a dead polymer of size r ; Q_1 is first-order moment for the dead polymer; and k_{cp} and k_{cs} are primary and secondary cyclization rate constants, respectively [271].

$$\frac{1}{V} \frac{d(V[R_r^*])}{dt} = k_p [M] [R_{r-1}^*] + k_{fp} r [P_r] [R^*] + k_p^* \sum_{s=1}^{r-1} s [R_{r-s}^*] [P_s] - (k_p^*) [M] [R_r^*] - (k_{td} + k_{tc}) [R^*] [R_r^*] - (k_p^* + k_{fp}) Q_1 [R_r^*] \quad (10)$$

$$\frac{d[x\rho_a]}{dt} = \frac{k_p^* [\bar{F}_2(1 - k_{cp}) - \bar{\rho}_a(1 + k_{cs})]}{k_p(1 - x)} \times \frac{dx}{dt} \quad (11)$$

5.3. Main Modeling Equations for Polymer Grafting

Grafting efficiency (ε) and number average molecular weights for the different polymer populations (W_{IH} , W_{SH} , W_{II} , W_{IS} , and W_{SS}) for the grafting of vinyl polymers onto pre-formed polymer with highly active chain transfer sites of (pendant mercaptan groups) are given by Equations (12)–(17) [39]. Subscripts IH and SH in the molecular weights shown in Equations (12)–(17) account for primary chains formed by chain transfer or by disproportionation termination (without distinguishing between terminally saturated and unsaturated chains) of polymer radicals starting with I and S fragments, respectively. Subscripts II, IS, and SS, on the other hand, account for primary chains produced by combination of the appropriate pair of polymer radicals starting with I and S fragments, respectively. r in Equations (12)–(18) is the ratio of propagation to termination kinetic rate constants, namely, $r = k_p/2k_t$.

$$\varepsilon = \frac{W_{SH} + W_{SS} + W_{IS}}{W_{SH} + W_{SS} + W_{IS} + W_{IH} + W_{II}} \quad (12)$$

$$W_{IH} = m[M]_0 \int_0^\infty \left\{ \frac{y_0}{y_0 + (1 - \alpha)^{C_s}} - \frac{(1 - r)y_0^2}{[y_0 + (1 - \alpha)^{C_s}]^2} \right\} d\alpha \quad (13)$$

$$W_{SH} = m[M]_0 \int_0^\infty \left\{ \frac{(1 - \alpha)^{C_s}}{y_0 + (1 - \alpha)^{C_s}} - \frac{(1 - r)y_0(1 - \alpha)^{C_s}}{[y_0 + (1 - \alpha)^{C_s}]^2} \right\} d\alpha \quad (14)$$

$$W_{II} = m[M]_0 \int_0^\infty \left\{ \frac{(1 - r)y_0^3}{[y_0 + (1 - \alpha)^{C_s}]^3} \right\} d\alpha \quad (15)$$

$$W_{IS} = 2m[M]_0 \int_0^\infty \left\{ \frac{(1 - r)y_0^2(1 - \alpha)^{C_s}}{[y_0 + (1 - \alpha)^{C_s}]^3} \right\} d\alpha \quad (16)$$

$$W_{SS} = m[M]_0 \int_0^\infty \left\{ \frac{(1-r)y_0(1-\alpha)^{2C_S}}{[y_0 + (1-\alpha)^{C_S}]^3} \right\} d\alpha \quad (17)$$

An example of calculation of the mole fraction chain length distribution (number distribution) (n_x) for the case of polymer grafting of vinyl polymers onto solid polymeric substrates, considering no chain transfer and incomplete conversion, is shown in Equation (18) [40].

$$n_{x,1} = \frac{[R_0]}{r[M]_0 \left\{ 1 - \left(\frac{[M]}{[M]_0} \right)^{1/r} \right\}} \left\{ 1 + \frac{[R_0](1-r)x}{r[M]_0} \right\}^{\frac{r-2}{1-r}} \quad (18)$$

When addressing the modeling of polymer grafting of vinyl polymer onto polyolefins in extruders by CTP, Hamielec et al. [231] proposed a polymerization scheme and the corresponding kinetic equations where the prepolymer molecule bears abstractable hydrogens on its backbone and a second compound, denoted as additive (A), is bound to the prepolymer backbone via reaction with a free radical. The backbone radical then transfers its radical center to the active molecules. The radical is finally terminated with other radicals. Proper kinetic equations were written down for the participating species, and a degree of grafting, g , which is the average of number of grafted molecules per monomer unit on the prepolymer backbone, was defined as shown in Equation (19), where Q_1 is the concentration of monomer units on prepolymer backbones which remains constant during branching, $K_{a,3}$ is the kinetic coefficient for the grafting (additive addition) reaction, and $R_{0,3}$ designates a primary radical with radical center on backbone R_0 . Further mathematical treatment by the authors leads to Equation (20) for calculation of the full chain length distribution of the polymer population, $w(r,s)$, where $w_0(r)$ is the initial chain length distribution of the prepolymer [231].

$$\frac{dg}{dt} = \frac{K_{a,3}R_{0,3}A}{Q_1} \quad (19)$$

$$w(r,s) = \left(1 + \frac{s}{r} \right) \frac{w_0(r)}{(1+g)s!} (gr)^s e^{-gr} \quad (20)$$

As stated above in Table 14, Gianoglio Pantano et al. [245] developed a very detailed model for grafting of PSty onto PE. Among the concentrations of species calculated by the model, the concentration of poly(ethylene-g-styrene) is calculated using Equation (21), and the concentration of grafted PS, denoted as Gr , is obtained from Equation (22). $G(t)$ is a matrix array of “infinite” size whose elements contain the molar concentrations of the individual species with degree of polymerization indicated by its subscripts. VG is a vector that contains the corresponding reaction rate terms, $I_{1,0}$ is a bivariate moment of order 1 for PS and order 0 for PE, which represents the mass of PS grafted onto PE, and M^{PS}_1 is the molar mass of PS.

$$\frac{dG(t)}{dt} = VG; G(0) = 0 \quad (21)$$

$$Gr = 100 \frac{I_{1,0}}{M^{PS}_1(t=0)} \quad (22)$$

Very detailed simulation studies for the grafting of vinyl polymers onto PE using kMC were presented by Hernández-Ortiz et al. [41,259–261]. Some of the key reactions considered in this study are shown in Figure 7 and the modeling strategy is summarized in Figure 8 [259].

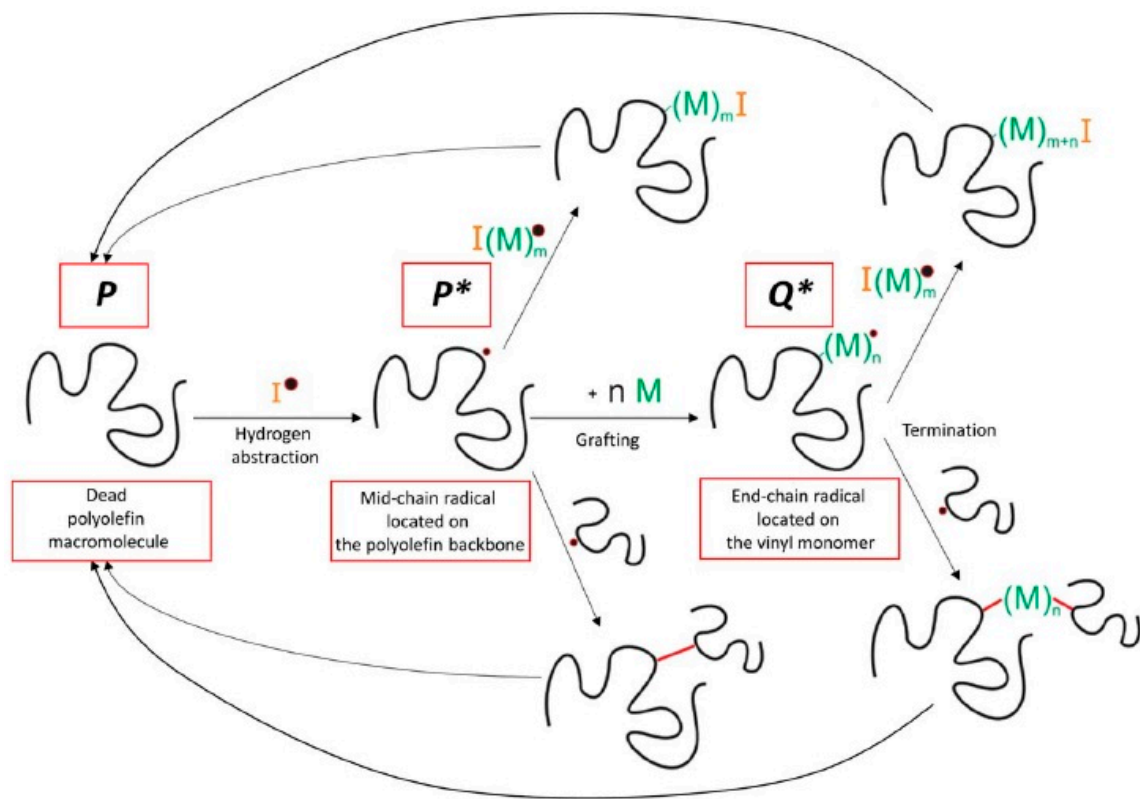


Figure 7. Some of the key reactions present in the grafting of polyolefins with vinyl monomer M . Reprinted with permission from Hernández-Ortiz et al., *AIChE J.*, 63(11), 4944–4961 [259]. Copyright 2017 John Wiley and Sons, New York.

of RDRP techniques is that they require longer reaction times. For instance, polymer grafting by RAFT polymerization lasts from 8 to 48 h, plus the time required to prepare the related microcontrollers, which in many cases includes an esterification step through Steglich or anhydride procedures. Polymer grafting by ATRP takes from 24 h to several days.

Polymer grafting by ROP procedures using L-lactide (L-LA) and ϵ -caprolactone (CL) for the synthesis of poly(l-lactic acid) and poly(ϵ -caprolactone) polymer grafts is gaining importance [181,182,189]. Other monomers used are 2-ethyl-2-oxazoline, to produce PEOX, and ethylene glycol, to produce PEG. These reactions are commonly conducted at temperatures higher than 80 °C, which complicates solvent selection, when using metal catalysts such as Sn (Oct)₂. Solvents should dissolve monomer and polymer, perform adequately at the selected temperatures, and show “green” characteristics. DMF, DMSO, p-dioxane, and toluene are some of the solvents most commonly used for polymer grafting by ROP. However, the recent advent of metal-free and organocatalyzed ROP has facilitated the polymerization at room temperature. For example, poly(lactide) materials can be made by ROP of L-LA at ambient conditions in the presence of 1,5,7-triazabicyclo[4.4.0]dec-5-ene (TBD) and 1,8-diazabicyclo[5.4.0]undec-7-ene (DBU) [272].

Polymer grafting is also important in the synthesis of “dendrigraft copolymers.” A large variety of heterogeneous dendrigraft copolymer architectures with core-shell and core-shell-corona morphologies can be produced, at significantly lower costs than for conventional dendrimer syntheses [18].

As observed in Table 14, the modeling of polymer grafting has focused on CTP or site formation by irradiation with FRP chemistry, in conventional flasks, stirred-tank reactors, or extruders. Other chemical routes have been addressed using semi-empirical approaches only. Therefore, there is still much to do in and contribute to this area.

Author Contributions: E.V.-L. and A.P. conceived the original idea (with discussions with A.R.-A., J.P.-A., M.G.H.-L., and A.M.). E.V.-L., M.G.H.-L., and A.M. assured funding acquisition through a project where experimental and theoretical work on polymer grafting of biopolymers from lignocellulosic biomasses has been carried out and provided background and motivation for this contribution. M.Á.V.-H., G.S.C.-D., A.R.-A., and E.V.-L. carried out critical literature reviews on different topics of the review. M.Á.V.-H., A.R.-A., and E.V.-L. wrote the original draft of the paper; E.V.-L., A.M., A.P., and Y.M. read and corrected different versions of the manuscript and provided extra references and discussion points. All authors have read and agreed to the published version of the manuscript.

Funding: This research was funded by: (a) Consejo Nacional de Ciencia y Tecnología (CONACYT, México), PhD scholarships granted to M.A.V.-H. and G.S.C.-D.; (b) DGAPA-UNAM, Projects PAPIIT IG100718, IV100119, TA100818, and TA102120, granted to E.V.-L.—the first two—and to A.R.-A.—the last two; and PASPA sabbatical support to E.V.-L. while at the University of Waterloo, in Ontario, Canada; (c) Facultad de Química, UNAM, research funds granted to E.V.-L. (PAIP 5000-9078) and A.R.-A. (PAIP 5000-9167); (d) NSERC funding to A.P.; and (e) the Department of Chemical Engineering, University of Waterloo, Canada, partial sabbatical support to E.V.-L. with research funds from A.P. No funding was received for APC.

Institutional Review Board Statement: Not applicable.

Informed Consent Statement: Not applicable.

Data Availability Statement: Data sharing is not applicable to this article.

Conflicts of Interest: The authors declare no conflict of interest. The funders had no role in the design of the study; in the collection, analyses, or interpretation of data; in the writing of the manuscript, or in the decision to publish the results.

References

1. Hadjichristidis, N.; Pitsikalis, M.; Iatrou, H.; Driva, P.; Chatzichris, M.; Sakellariou, G.; Lohse, D. Graft copolymers. In *Encyclopedia of Polymer Science and Technology*, 2nd ed.; Matyjaszewski, K., Ed.; John Wiley & Sons: Hoboken, NJ, USA, 2010; pp. 1–38, ISBN 978-047-144-026-0.

2. Slagman, S.; Zuilhof, H.; Franssen, M.C.R. Laccase-Mediated Grafting on Biopolymers and Synthetic Polymers: A Critical Review. *ChemBioChem* **2017**, *19*, 288–311. [\[CrossRef\]](#)
3. Stannett, V.T. Block and graft copolymerization. In *Journal of Polymer Science: Polymer Letters*, 1st ed.; Ceresa, R.J., Ed.; John Wiley & Sons: Hoboken, NJ, USA, 1973; Volume 1, pp. 669–670. [\[CrossRef\]](#)
4. Meier, D.J. Theory of block copolymers. I. Domain formation in A-B block copolymers. *J. Polym. Sci. C Polym. Symp.* **1969**, *26*, 81–98. [\[CrossRef\]](#)
5. Helfand, E.; Block Copolymer Theory. III. Statistical Mechanics of the Microdomain Structure. *Macromolecules* **1975**, *8*, 552–556. [\[CrossRef\]](#)
6. Helfand, E.; Wasserman, Z.R. Block Copolymer Theory. 4. Narrow Interphase Approximation. *Macromolecules* **1976**, *9*, 879–888. [\[CrossRef\]](#)
7. Helfand, E. Block copolymers, polymer-polymer interfaces, and the theory of inhomogeneous polymers. *Acc. Chem. Res.* **1975**, *8*, 295–299. [\[CrossRef\]](#)
8. Blanchette, J.A.; Nielsen, L.E. Characterization of graft polymers. *J. Polym. Sci.* **1956**, *20*, 317–326. [\[CrossRef\]](#)
9. Merret, F.M. Graft polymers with preset molecular configurations. *J. Polym. Sci.* **1957**, *24*, 467–477. [\[CrossRef\]](#)
10. Gluckman, M.S.; Kampf, M.J.; O'Brien, L.J.; Fox, T.G.; Graham, R.K. Graft copolymers from polymers having pendant mercaptan groups. II. Synthesis and characterization. *J. Polym. Sci.* **1959**, *37*, 411–423. [\[CrossRef\]](#)
11. Miller, M.L. Block and graft polymers I. Graft polymers from acrylamide and acrylonitrile. *Can. J. Chem.* **1957**, *36*, 303–308. [\[CrossRef\]](#)
12. Beevers, R.B.; White, E.F.T.; Brown, L. Physical properties of vinyl polymers. Part 3.—X-ray scattering in block, random and graft methyl methacrylate + acrylonitrile copolymers. *Trans. Faraday Soc.* **1960**, *56*, 1535–1541. [\[CrossRef\]](#)
13. Oster, G.; Oster, G.K.; Moroson, H. Ultraviolet induced crosslinking and grafting of solid high polymers. *J. Polym. Sci.* **1959**, *XXXIV*, 671–684. [\[CrossRef\]](#)
14. Kobayashi, Y. Gamma-ray-induced graft copolymerization of styrene onto cellulose and some chemical properties of the grafted polymer. *J. Polym. Sci.* **1961**, *51*, 359–372. [\[CrossRef\]](#)
15. Bridgeford, D.J. Catalytic Deposition and Grafting of Olefin Polymers into Cellulosic Materials. *Ind. Eng. Chem. Prod. Res. Dev.* **1962**, *1*, 45–52. [\[CrossRef\]](#)
16. Huang, R.Y.-M.; Immergut, B.; Immergut, E.H.; Rapson, W.H. Grafting vinyl polymers onto cellulose by high energy radiation. I. High energy radiation-induced graft copolymerization of styrene onto cellulose. *J. Polym. Sci. A Gen. Pap.* **1963**, *1*, 1257–1270. [\[CrossRef\]](#)
17. McManus, N.; Zhu, S.-H.; Tzoganakis, C.; Penlidis, A. Grafting of ethylene-ethyl acrylate-maleic anhydride terpolymer with amino-terminated polydimethylsiloxane during reactive processing. *J. Appl. Polym. Sci.* **2006**, *101*, 4230–4237. [\[CrossRef\]](#)
18. Cadena, L.-E.; Gauthier, M. Phase-segregated dendrigraft copolymer architectures. *Polymers* **2010**, *2*, 596–622. [\[CrossRef\]](#)
19. Aridi, T.; Gauthier, M. Chapter 6. Arborescent polymers with a mesoscopic scale. In *Complex Macromolecular Architectures: Synthesis, Characterization, and Self-Assembly*, 1st ed.; Hadjichristidis, N., Hirao, A., Tezuka, Y., Du Prez, F., Eds.; John Wiley & Sons: Hoboken, NJ, USA, 2011; pp. 169–194. ISBN 978-047-082-514-3.
20. Moingeon, F.; Wu, Y.; Cadena-Sánchez, L.; Gauthier, M. Synthesis of arborescent styrene homopolymers and copolymers from epoxidized substrates. *J. Polym. Sci. A Polym. Chem.* **2012**, *50*, 1819–1826. [\[CrossRef\]](#)
21. Whitton, G.; Gauthier, M. Arborescent polypeptides from γ -benzyl L-glutamic acid. *J. Polym. Sci. A Polym. Chem.* **2013**, *51*, 5270–5279. [\[CrossRef\]](#)
22. Aridi, T.; Gauthier, M. Synthesis of arborescent polymers by click grafting. *Mater. Res. Soc. Symp. Proc.* **2014**, *1613*, 23–31. [\[CrossRef\]](#)
23. Dockendorff, J.; Gauthier, M. Synthesis of arborescent polystyrene-g-[poly(2-vinylpyridine)-b- polystyrene] core-shell-corona copolymers. *J. Polym. Sci. A Polym. Chem.* **2014**, *52*, 1075–1085. [\[CrossRef\]](#)
24. Whitton, G.; Gauthier, M. Arborescent micelles: Dendritic poly(γ -benzyl L-glutamate) cores grafted with hydrophilic chain segments. *J. Polym. Sci. A Polym. Chem.* **2016**, *54*, 1197–1209. [\[CrossRef\]](#)
25. Gauthier, M.; Whitton, G. Arborescent unimolecular micelles: Poly(γ -benzyl L-glutamate) core grafted with a hydrophilic shell by copper(I)-catalyzed azide-alkyne cycloaddition coupling. *Polymers* **2017**, *9*, 540. [\[CrossRef\]](#)
26. Gauthier, M.; Aridi, T. Synthesis of arborescent polystyrene by “click” grafting. *J. Polym. Sci. A Polym. Chem.* **2019**, *57*, 1730–1740. [\[CrossRef\]](#)
27. Roy, D.; Semsarilar, M.; Guthrie, J.T.; Perrier, S. Cellulose modification by polymer grafting: A review. *Chem. Soc. Rev.* **2009**, *38*, 2046–2064. [\[CrossRef\]](#) [\[PubMed\]](#)
28. Wohlhauser, S.; Delepierre, G.; Labet, M.; Morandi, G.; Thielemans, W.; Weder, C.; Zoppe, J.O. Grafting Polymers from Cellulose Nanocrystals: Synthesis, Properties, and Applications. *Macromolecules* **2018**, *51*, 6157–6189. [\[CrossRef\]](#)
29. Jenkins, D.W.; Hudson, S.M. Review of vinyl graft copolymerization featuring recent advances toward controlled radical-based reactions and illustrated with chitin/chitosan trunk polymers. *Chem. Rev.* **2001**, *101*, 3245–3274. [\[CrossRef\]](#) [\[PubMed\]](#)
30. Thakur, V.K.; Thakur, M.K. Recent Advances in Graft Copolymerization and Applications of Chitosan: A Review. *ACS Sustain. Chem. Eng.* **2014**, *2*, 2637–2652. [\[CrossRef\]](#)
31. Kaur, L.; Gupta, G.D. A review on microwave assisted grafting of polymers. *Int. J. Pharm. Sci. Res.* **2017**, *8*, 422–426. [\[CrossRef\]](#)

32. Brodin, M.; Vallejos, M.; Opedal, M.T.; Area, M.C.; Chinga-Carrasco, G. Lignocellulosics as sustainable resources for production of bioplastics—A review. *J. Clean. Prod.* **2017**, *162*, 646–664. [\[CrossRef\]](#)
33. Niphadkar, S.; Bagade, P.; Ahmed, S. Bioethanol production: Insight into past, present and future perspectives. *Biofuels* **2018**, *9*, 229–238. [\[CrossRef\]](#)
34. Banerjee, J.; Singh, R.; Vijayaraghavan, R.; MacFarlane, D.; Patti, A.F.; Arora, A. Bioactives from fruit processing wastes: Green approaches to valuable chemicals. *Food Chem.* **2017**, *225*, 10–22. [\[CrossRef\]](#)
35. Neuling, U.; Kaltschmitt, M. Review of Biofuel Production—Feedstock, Processes and Markets. *J. Oil Palm Res.* **2019**, *29*, 137–167. [\[CrossRef\]](#)
36. Vega-Hernández, M.Á.; Rosas-Aburto, A.; Vivaldo-Lima, E.; Vázquez-Torres, H.; Cano-Díaz, G.S.; Pérez-Salinas, P.; Hernández-Luna, M.G.; Alcaraz-Cienfuegos, J.; Zolotukhin, M.G. Development of polystyrene composites based on blue agave bagasse by in situ RAFT polymerization. *J. Appl. Polym. Sci.* **2019**, *136*, 47089. [\[CrossRef\]](#)
37. Farhat, W.; Venditti, R.; Ayoub, A.; Prochazka, F.; Fernández-de-Alba, C.; Mignard, N.; Taha, M.; Becquart, F. Towards thermoplastic hemicellulose: Chemistry and characteristics of poly-(ϵ -caprolactone) grafting onto hemicellulose backbones. *Mater. Des.* **2018**, *153*, 298–307. [\[CrossRef\]](#)
38. Sun, Y.; Ma, Z.; Xu, X.; Liu, X.; Liu, L.; Huang, G.; Liu, L.; Wang, H.; Song, P. Grafting Lignin with Bioderived Polyacrylates for Low-Cost, Ductile, and Fully Biobased Poly(lactic acid) Composites. *ACS Sustain. Chem. Eng.* **2020**, *8*, 2267–2276. [\[CrossRef\]](#)
39. Fox, T.G.; Gluckman, M.S.; Gornick, F.; Graham, R.K.; Gratch, S. Graft copolymers from polymers having pendant mercaptan groups. I. Kinetic considerations. *J. Polym. Sci.* **1959**, *XXXVII*, 397–409. [\[CrossRef\]](#)
40. Zimmerman, J. Molecular weight distributions of vinyl polymers grafted to a solid polymeric substrate by irradiation (theoretical). *J. Polym. Sci.* **1960**, *XLIV*, 107–116. [\[CrossRef\]](#)
41. Hernández-Ortiz, J.C.; Van Steenberge, P.H.M.; Duchateau, J.N.E.; Toloza, C.; Schreurs, F.; Reyniers, M.-F.; Marin, G.B.; D’hooge, D.R. A two-phase stochastic model to describe mass transport and kinetics during reactive processing of polyolefins. *Chem. Eng. J.* **2019**, *377*, 119980. [\[CrossRef\]](#)
42. Gandhi, A.; Verma, S.; Imam, S.S.; Vyas, M. A review on techniques for grafting of natural polymers and their applications. *Plant Arch* **2019**, *19*, 972–978.
43. Wei, L.; McDonald, A.G. A Review on Grafting of Biofibers for Biocomposites. *Materials* **2016**, *9*, 303. [\[CrossRef\]](#)
44. De Jesús Muñoz Prieto, E.; Rivas, B.; Sánchez, J. Natural polymer grafted with syntethic monomer by microwave for water treatment—A review. *Cienc. Desarro.* **2012**, *4*, 219–240. [\[CrossRef\]](#)
45. Barsbay, M.; Güven, O. A short review of radiation-induced raft-mediated graft copolymerization: A powerful combination for modifying the surface properties of polymers in a controlled manner. *Radiat. Phys. Chem.* **2009**, *78*, 1054–1059. [\[CrossRef\]](#)
46. Francis, R.; Joy, N.; Aparna, E.P.; Vijayan, R. Polymer Grafted Inorganic Nanoparticles, Preparation, Properties, and Applications: A Review. *Polym. Rev.* **2014**, *54*, 268–347. [\[CrossRef\]](#)
47. Garcia-Valdez, O.; Champagne, P.; Cunningham, M.F. Graft modification of natural polysaccharides via reversible deactivation radical polymerization. *Prog. Polym. Sci.* **2018**, *76*, 151–173. [\[CrossRef\]](#)
48. Sun, H.; Yang, L.; Thompson, M.P.; Schara, S.; Cao, W.; Choi, W.C.; Hu, Z.; Zang, N.; Tan, W.; Gianneschi, N.C. Recent Advances in Amphiphilic Polymer–Oligonucleotide Nanomaterials via Living/Controlled Polymerization Technologies. *Bioconjugate Chem.* **2019**, *30*, 1889–1904. [\[CrossRef\]](#) [\[PubMed\]](#)
49. Chung, T.C. Synthesis of functional polyolefin copolymers with graft and block structures. *Prog. Polym. Sci.* **2002**, *27*, 39–85. [\[CrossRef\]](#)
50. Zhou, T.; Zhu, Y.; Li, X.; Liu, X.; Yeung, K.W.K.; Wu, S.; Wang, X.; Cui, Z.; Yang, X.; Chu, P.K. Surface functionalization of biomaterials by radical polymerization. *Prog. Mater. Sci.* **2016**, *83*, 191–235. [\[CrossRef\]](#)
51. Ayyavoo, J.; Nguyen, T.P.N.; Jun, B.-M.; Kim, I.-C.; Kwon, Y.N. Protection of polymeric membranes with antifouling surfacing via surface modifications. *Colloids Surf. A Physicochem. Eng. Asp.* **2016**, *506*, 190–201. [\[CrossRef\]](#)
52. Weber, C.; Hoogenboom, R.; Schubert, U.S. Temperature responsive bio-compatible polymers based on poly(ethylene oxide) and poly(2-oxazoline)s. *Prog. Polym. Sci.* **2012**, *37*, 686–714. [\[CrossRef\]](#)
53. Sun, H.; Choi, W.; Zang, N.; Battistella, C.; Thompson, M.P.; Cao, W.; Zhou, X.; Forman, C.; Gianneschi, N.C. Bioactive Peptide Brush Polymers via Photoinduced Reversible-Deactivation Radical Polymerization. *Angew. Chem. Int. Ed.* **2019**, *58*, 17359–17364. [\[CrossRef\]](#)
54. Kumar, R.; Sharma, R.K.; Singh, A.P. Grafted cellulose: A bio-based polymer for durable applications. *Polym. Bull.* **2018**, *75*, 2213–2242. [\[CrossRef\]](#)
55. Sharma, S.; Kumar, A. *Lignin. Biosynthesis and Transformation for Industrial Applications*; Springer Series on Polymer and Composite Materials; Springer Nature: Cham, Switzerland, 2020; pp. 1–252. ISBN 978-303-040-663-9.
56. Mourya, V.K.; Inamdar, N.N. Chitosan-modifications and applications. *React. Funct. Polym.* **2008**, *68*, 1013–1051. [\[CrossRef\]](#)
57. Argüelles-Monal, W.M.; Lizardi-Mendoza, J.; Fernández-Quiroz, D.; Recillas-Mota, M.T.; Montiel-Herrera, M. Chitosan Derivatives: Inducing new functionalities with a controlled molecular architecture for innovative materials. *Polymers* **2018**, *10*, 342. [\[CrossRef\]](#)
58. Kurita, K. Controlled functionalization of the polysaccharide chitin. *Prog. Polym. Sci.* **2001**, *26*, 1921–1971. [\[CrossRef\]](#)
59. Lele, V.V.; Kumari, S.; Niju, H. Syntheses, characterization and applications of graft copolymers of sago starch. *Starch* **2018**, *70*, 1700133. [\[CrossRef\]](#)

60. Radhakrishnan, B.; Ranjan, R.; Brittain, W.J. Surface initiated polymerization from silica nanoparticles. *Soft Matter* **2006**, *2*, 386–396. [CrossRef] [PubMed]
61. Foster, J.C.; Radzinsky, S.C.; Matson, J.B. Graft polymer synthesis by RAFT transfer-to. *J. Polym. Sci. A Polym. Chem.* **2017**, *55*, 2865–2876. [CrossRef]
62. Bhattacharya, A. Radiation and industrial polymers. *Prog. Polym. Sci.* **2000**, *25*, 371–401. [CrossRef]
63. Desmet, T.; Morent, R.; De Geyter, N.; Leys, C.; Schacht, E.; Dubruel, P. Nonthermal plasma technology as a versatile strategy for polymeric biomaterials surface modification: A review. *Biomacromolecules* **2009**, *10*, 2351–2378. [CrossRef]
64. Ngo, T.H.A.; Tran, D.T.; Dinh, C.H. Surface photochemical graft polymerization of acrylic acid onto polyamide thin film composite membranes. *J. Appl. Polym. Sci.* **2017**, *134*, 44418. [CrossRef]
65. Singh, V.; Tiwari, A.; Tripathi, D.N.; Sanghi, R. Microwave assisted synthesis of guar-g-polyacrylamide. *Carbohydr. Polym.* **2004**, *58*, 1–6. [CrossRef]
66. Bhattacharya, A.; Misra, B.N. Grafting: A versatile means to modify polymers technics, factors and applications. *Prog. Polym. Sci.* **2004**, *29*, 767–814. [CrossRef]
67. Sosnik, A.; Gotelli, G.; Abraham, G.A. Microwave-assisted polymer synthesis (MAPS) as a tool in biomaterials science: How new and how powerful. *Prog. Polym. Sci.* **2011**, *36*, 1050–1078. [CrossRef]
68. Kumar, D.; Pandey, J.; Raj, V.; Kumar, P. A review on the modification of polysaccharide through graft copolymerization for various potential applications. *Open Med. Chem. J.* **2017**, *11*, 109–126. [CrossRef]
69. Fan, G.; Zhao, J.; Zhang, Y.; Guo, Z. Grafting modification of kevlar fiber using horseradish peroxidase. *Polym. Bull.* **2006**, *56*, 507–515. [CrossRef]
70. Cannatelli, M.D.; Ragauskas, A.J. Conversion of lignin into value-added materials and chemicals via laccase-assisted copolymerization. *Appl. Microbiol. Biotechnol.* **2016**, *100*, 8685–8691. [CrossRef] [PubMed]
71. Ran, J.; Wu, L.; Zhang, Z.; Xu, T. Atom transfer radical polymerization (ATRP): A versatile and forceful tool for functional membranes. *Prog. Polym. Sci.* **2014**, *39*, 124–144. [CrossRef]
72. Crawford, D.E. Extrusion-back to the future: Using an established technique to reform automated chemical synthesis. *Beilstein J. Org. Chem.* **2017**, *13*, 65–75. [CrossRef]
73. Moad, G. The synthesis of polyolefin graft copolymers by reactive extrusion. *Prog. Polym. Sci.* **1999**, *24*, 81–142. [CrossRef]
74. Moad, G. Chemical modification of starch by reactive extrusion. *Prog. Polym. Sci.* **2011**, *36*, 218–237. [CrossRef]
75. Russell, K.E. Free radical graft polymerization and copolymerization at higher temperatures. *Prog. Polym. Sci.* **2002**, *27*, 1007–1038. [CrossRef]
76. Monties, B. *Les Polymères Végétaux: Polymères Pariétaux et Alimentaires non Azotés*, 1st ed.; Gauthier-Villars: Paris, France, 1980; ISBN 978-204-010-480-1.
77. Casarrubias-Cervantes, R.A. *Análisis Fisicoquímico de Procesos de Pretratamiento de Materiales Lignocelulósicos para su Uso en Polímeros Conductores*. Bachelor Degree, Facultad de Química—Universidad Nacional Autónoma de México, Ciudad Universitaria, CDMX, 2019, Biblioteca Digital UNAM. Available online: <http://132.248.9.195/ptd2019/abril/0788572/Index.html> (accessed on 25 May 2020).
78. Koshijima, T.; Muraki, E. Radiation Grafting of Methyl Methacrylate onto Lignin. *J. Jpn. Wood Res. Soc.* **1964**, *10*, 110–115.
79. Koshijima, T.; Muraki, E. Degradation of Lignin-Methyl Metacrylate Graft Copolymer by γ -Ray Irradiation. *J. Jpn. Wood Res. Soc.* **1964**, *10*, 116–119.
80. Koshijima, T.; Timell, T.E. Factors Affecting Number Average Molecular Weights Determination of Hardwood Xylan. *J. Jpn. Wood Res. Soc.* **1966**, *12*, 166–172.
81. Koshijima, T.; Muraki, E. Solvent Effects upon Radiation-Induced Graft-copolymerization of Styrene onto Lignin. *J. Jpn. Wood Res. Soc.* **1966**, *12*, 139.
82. Koshijima, T. Oxidation of Lignin-Styrene Graft polymer. *J. Jpn. Wood Res. Soc.* **1966**, *12*, 114.
83. Koshijima, T.; Muraki, E. Radial Grafting on Lignin (II). Grafting of styrene into Lignin by Initiators. *J. Jpn. Wood Res. Soc.* **1967**, *13*, 355–358.
84. Koshijima, T.; Muraki, E.; Naito, K.; Adachi, K. Radical Grafting on Lignin. IV. Semi-Conductive Properties of Lignin-Styrene Graftpolymer. *J. Jpn. Wood Res. Soc.* **1968**, *14*, 52–54.
85. Meister, J.J. Modification of Lignin. *J. Macromol. Sci. Polymer Rev.* **2002**, *42*, 235–289. [CrossRef]
86. Hon, D.N.S. *Chemical Modification of Lignocellulosic Materials*, 1st ed.; Marcel Dekker, Inc.: New York, NY, USA, 1996; ISBN 978-082-479-472-9.
87. McDowall, D.J.; Gupta, B.S.; Stannett, V.T. Grafting of vinyl monomers to cellulose by ceric ion initiation. *Prog. Polym. Sci.* **1984**, *10*, 1–50. [CrossRef]
88. Bhattacharyya, S.N.; Maldas, D. Graft copolymerization onto cellulose. *Prog. Polym. Sci.* **1984**, *10*, 171–270. [CrossRef]
89. Hon, D.N.S. *Graft Copolymerization of Lignocellulosic Fibers*; ACS Symposium Series 187; American Chemical Society: Washington, DC, USA, 1982; ISBN 978-084-120-721-9.
90. Mansour, O.Y.; Nagaty, A. Grafting of synthetic polymers to natural polymers by chemical processes. *Prog. Polym. Sci.* **1985**, *11*, 91–165. [CrossRef]
91. Feldman, D.; Lacasse, M.; Bernaczuk, L.M. Lignin-polymer systems and some applications. *Prog. Polym. Sci.* **1986**, *12*, 271–299. [CrossRef]

92. Matyjaszewski, K.; Möller, M. Celluloses and polyoses/hemicelluloses. In *Polymer Science: A Comprehensive Reference*; Elsevier: Amsterdam, The Netherlands, 2012; ISBN 978-008-087-862-1.
93. Pantelakis, S.; Tserpes, K. *Revolutionizing Aircraft Materials and Processes*; Springer Nature AG: Cham, Switzerland, 2020; ISBN 978-303-035-346-9.
94. Rol, F.; Belgacem, M.N.; Gandinia, A.; Bras, J. Recent advances in surface-modified cellulose nanofibrils. *Prog. Polym. Sci.* **2019**, *88*, 241–264. [[CrossRef](#)]
95. Zahran, M.K.; Morsy, M.; Mahmoud, R. Grafting of acrylic monomers onto cotton fabric using an activated cellulose thiocarbonate–azobisisobutyronitrile redox system. *J. Appl. Polym. Sci.* **2003**, *91*, 1261–1274. [[CrossRef](#)]
96. Chauhan, G.S.; Lal, H.; Sharma, R.; Sarwade, B.D. Grafting of a styrene–acrylonitrile binary monomer mixture onto cellulose extracted from pine needles. *J. Appl. Polym. Sci.* **2001**, *83*, 2000–2007. [[CrossRef](#)]
97. Sabaa, M.W.; Mokhtar, S.M. Chemically induced graft copolymerization of itaconic acid onto cellulose fibers. *Polym. Test.* **2002**, *21*, 337–343. [[CrossRef](#)]
98. Gupta, K.C.; Sahoo, S. Grafting of N,N'-methylenebisacrylamide onto cellulose using Co(III)-acetylacetonate complex in aqueous medium. *J. Appl. Polym. Sci.* **2000**, *76*, 906–912. [[CrossRef](#)]
99. Gupta, K.C.; Sahoo, S. Co(III) acetylacetonate-complex-initiated grafting of N-vinyl pyrrolidone on cellulose in aqueous media. *J. Appl. Polym. Sci.* **2001**, *81*, 2286–2296. [[CrossRef](#)]
100. Gupta, K.C.; Khandekar, K. Temperature-Responsive Cellulose by Ceric(IV) Ion-Initiated Graft Copolymerization of N-Isopropylacrylamide. *Biomacromolecules* **2003**, *4*, 758–765. [[CrossRef](#)]
101. Gupta, K.C.; Khandekar, K. Graft copolymerization of acrylamide–methylacrylate comonomers onto cellulose using ceric ammonium nitrate. *J. Appl. Polym. Sci.* **2002**, *86*, 2631–2642. [[CrossRef](#)]
102. Gupta, K.C.; Khandekar, K. Graft copolymerization of acrylamide onto cellulose in presence of comonomer using ceric ammonium nitrate as initiator. *J. Appl. Polym. Sci.* **2006**, *101*, 2546–2558. [[CrossRef](#)]
103. Gupta, K.C.; Sahoo, S. Graft Copolymerization of Acrylonitrile and Ethyl Methacrylate Comonomers on Cellulose Using Ceric Ions. *Biomacromolecules* **2001**, *2*, 239–247. [[CrossRef](#)]
104. Gupta, K.C.; Sahoo, S.; Khandekar, K. Graft Copolymerization of Ethyl Acrylate onto Cellulose Using Ceric Ammonium Nitrate as Initiator in Aqueous Medium. *Biomacromolecules* **2002**, *3*, 1087–1094. [[CrossRef](#)] [[PubMed](#)]
105. Gupta, K.C.; Khandekar, K. Ceric(IV) ion-induced graft copolymerization of acrylamide and ethyl acrylate onto cellulose. *Polym. Int.* **2005**, *55*, 139–150. [[CrossRef](#)]
106. Toledano-Thompson, T.; Loria-Bastarrachea, M.I.; Aguilar-Vega, M.J. Characterization of henequen cellulose microfibers treated with an epoxide and grafted with poly(acrylic acid). *Carbohydr. Polym.* **2005**, *62*, 67–73. [[CrossRef](#)]
107. Mansour, O.Y.; Nagieb, Z.A.; Basta, A.H. Graft polymerization of some vinyl monomers onto alkali-treated cellulose. *J. Appl. Polym. Sci.* **1991**, *43*, 1147–1158. [[CrossRef](#)]
108. Semsarilar, M.; Ladmiral, V.; Perrier, S. Synthesis of a cellulose supported chain transfer agent and its application to RAFT polymerization. *J. Polym. Sci. A Polym. Chem.* **2010**, *48*, 4361–4365. [[CrossRef](#)]
109. Cankaya, N.; Temüz, M. Characterization and monomer reactivity ratios of grafted cellulose with n-(4-nitrophenyl)acrylamide and methyl methacrylate by atom transfer radical polymerization. *Cell. Chem. Technol.* **2012**, *46*, 551–558.
110. Thakur, V.K.; Thakur, M.K.; Gupta, R.K. Rapid synthesis of graft copolymers from natural cellulose fibers. *Carbohydr. Polym.* **2013**, *98*, 820–828. [[CrossRef](#)]
111. Routray, C.; Tosh, B. Graft copolymerization of methyl methacrylate (mma) onto cellulose acetate in homogeneous medium: Effect of solvent, initiator and homopolymer inhibitor. *Cell. Chem. Technol.* **2013**, *47*, 171–190.
112. Cankaya, N.; Temüz, M.M. Monomer reactivity ratios of cellulose grafted with N-cyclohexylacrylamide and methyl methacrylate by atom transfer radical polymerization. *Cell. Chem. Technol.* **2014**, *48*, 209–215.
113. Popescu, O.; Dunca, S.; Grigoriu, A. Antibacterial action of silver applied on cellulose fibers grafted with monochlorotriazinyl- β -cyclodextrin. *Cell. Chem. Technol.* **2013**, *47*, 247–255.
114. Popescu, O.; Grigoriu, A.; Diaconescu, R.M.; Vasluiuanu, E. Optimization of the cellulosic materials functionalization with monochlorotriazinyl- β -cyclodextrin in basic medium. *Ind. Textilă* **2012**, *63*, 68–75.
115. Sun, Z.; Chen, F. Homogeneous grafting copolymerization of methylmethacrylate onto cellulose using ammonium persulfate. *Cell. Chem. Technol.* **2014**, *48*, 217–223.
116. Dai, L.; Shen, Y.; Li, D.; Xiao, S.; He, J. Cellulose-graft-poly(l-lactide) as a degradable drugdelivery system: Synthesis, degradation and drug release. *Cell. Chem. Technol.* **2014**, *48*, 237–245.
117. Xiaoming, S.; Songlin, W.; Shanshan, G.; Fushan, C.; Fusheng, L. Study on grafting copolymerization of methyl methacrylate onto cellulose under heterogeneous conditions. *Cell. Chem. Technol.* **2016**, *50*, 65–70.
118. Yin, Y.; Jiang, T.X.; Wang, H.; Gao, W. Modification of cellulose nanocrystal via SI-ATRP of styrene and themechanism of its reinforcement of polymethylmethacrylate. *Carbohydr. Polym.* **2016**, *142*, 206–212. [[CrossRef](#)] [[PubMed](#)]
119. Paula, E.L.; Roig, F.; Mas, A.; Habas, J.P.; Mano, V.; Vargas Pereira, F.; Robin, J.J. Effect of surface-grafted cellulose nanocrystals on the thermal and mechanical properties of PLLA based nanocomposites. *Eur. Polym. J.* **2016**, *84*, 173–187. [[CrossRef](#)]
120. Zhao, C.; Li, J.; He, B.; Zhao, L. Fabrication of hydrophobic biocomposite by combining cellulosic fibers with polyhydroxyalkanoate. *Cellulose* **2017**, *24*, 2265–2274. [[CrossRef](#)]

121. Badawy, S.M. Functional cellulosic filter papers prepared by radiation-induced graft copolymerization for chelation of rare earth elements. *Cell. Chem. Technol.* **2017**, *51*, 551–558.
122. Çankaya, N.; Temüz, M.M.; Yakuphanoglu, F. Grafting of some monomers onto cellulose by atom transfer radical polymerization. Electrical conductivity and thermal properties of resulting copolymers. *Cell. Chem. Technol.* **2018**, *52*, 19–26.
123. Müssig, J.; Kelch, M.; Gebert, B.; Hohe, J.; Luke, M.; Bahners, T. Improvement of the fatigue behaviour of cellulose/polyolefin composites using photo-chemical fibre surface modification bio-inspired by natural role models. *Cellulose* **2020**, *27*, 5815–5827. [\[CrossRef\]](#)
124. Chen, Y.; Yu, Z.; Han, Y.; Yang, S.; Fan, D.; Li, G.; Wang, S. Combination of water soluble chemical grafting and gradient freezing to fabricate elasticity enhanced and anisotropic nanocellulose aerogels. *Appl. Nanosci.* **2020**, *10*, 411–419. [\[CrossRef\]](#)
125. Eraghi Kazzaz, A.; Hosseinpour Feizi, Z.; Fatehi, P. Grafting strategies for hydroxy groups of lignin for producing materials. *Green Chem.* **2019**, *21*, 5714–5752. [\[CrossRef\]](#)
126. Abe, A.; Dusek, K.; Kobayashi, S. *Biopolymers. Lignin, Proteins, Bioactive Nanocomposites*, 1st ed.; Springer: Heidelberg/Berlin, Germany, 2010; Volume 232, ISBN 978-364-213-630-6.
127. Huang, J.; Fu, S.; Gan, L. *Lignin Chemistry and Applications*, 1st ed.; Elsevier: Amsterdam, The Netherlands, 2019; ISBN 978-012-813-963-9.
128. Marton, J. *Lignin. Structure and Reactions*, 1st ed.; Advances in Chemistry Series 59; American Chemical Society: Washington, DC, USA, 1966; ISBN 978-084-122-239-7.
129. Glasser, W.G.; Sarkanen, S. *Lignin. Properties and Materials*, 1st ed.; ACS Symposium Series 397; American Chemical Society: Washington, DC, USA, 1989; ISBN 978-084-121-248-0.
130. Lewis, N.G.; Sarkanen, S. *Lignin and Lignan Biosynthesis*; ACS Symposium Series 697; American Chemical Society: Washington, DC, USA, 1998; ISBN 084-123-566-X.
131. Katahira, R.; Elder, T.J.; Beckham, G.T. Chapter 1 A brief introduction to lignin structure. In *Lignin Valorization. Emerging Approaches*, 1st ed.; Beckham, G.T., Ed.; The Royal Society of Chemistry: Croydon, London, UK, 2018; pp. 1–20, ISBN 978-178-801-035-1.
132. Laurichesse, S.; Avérous, L. Chemical modification of lignins: Towards biobased polymers. *Prog. Polym. Sci.* **2014**, *39*, 1266–1290. [\[CrossRef\]](#)
133. Figueiredo, P.; Lintinen, K.; Hirvonen, J.T.; Kostianen, M.A.; Santos, H.A. Properties and chemical modifications of lignin: Towards lignin-based nanomaterials for biomedical applications. *Prog. Mater. Sci.* **2018**, *93*, 233–269. [\[CrossRef\]](#)
134. Xu, Y.; Yuan, L.; Wang, Z.; Wilbon, P.A.; Wang, C.; Chu, F.; Tang, C. Lignin and soy oil-derived polymeric biocomposites by “grafting from” RAFT polymerization. *Green Chem.* **2016**, *18*, 4974–4981. [\[CrossRef\]](#)
135. Yu, Y.; Fu, S.; Song, P.; Lou, X.; Jin, Y.; Lu, F.; Wu, Q.; Ye, J. Functionalized lignin by grafting phosphorus-nitrogen improves the thermal stability and flame retardancy of polypropylene. *Polym. Degrad. Stabil.* **2012**, *97*, 541–546. [\[CrossRef\]](#)
136. Prieur, B.; Meub, M.; Wittermann, M.; Klein, R.; Bellayer, S.; Fontaine, G.; Bourbigot, S. Phosphorylation of lignin: Characterization and investigation of the thermal decomposition. *RSC Adv.* **2017**, *7*, 16866–16877. [\[CrossRef\]](#)
137. Prieur, B.; Meub, M.; Wittermann, M.; Klein, R.; Bellayer, S.; Fontaine, G.; Bourbigot, S. Phosphorylation of lignin to flame retard acrylonitrile butadiene styrene (ABS). *Polym. Degrad. Stabil.* **2016**, *127*, 32–43. [\[CrossRef\]](#)
138. Liu, H.; Chung, H. Lignin-Based Polymers via Graft Copolymerization. *J. Polym. Sci. A Polym. Chem.* **2017**, *55*, 3515–3528. [\[CrossRef\]](#)
139. Gupta, C.; Washburn, N.R. Polymer-grafted lignin surfactants prepared via Reversible Addition–Fragmentation Chain-Transfer polymerization. *Langmuir* **2014**, *30*, 9303–9312. [\[CrossRef\]](#)
140. Ganewatta, M.S.; Lokupitiya, H.N.; Tang, C. Lignin biopolymers in the age of controlled polymerization. *Polymers* **2019**, *11*, 1176. [\[CrossRef\]](#)
141. Kim, Y.S.; Kadla, J.F. Preparation of a thermoresponsive lignin-based biomaterial through atom transfer radical polymerization. *Biomacromolecules* **2010**, *11*, 981–988. [\[CrossRef\]](#) [\[PubMed\]](#)
142. Wang, J.; Yao, J.; Korich, K.; Li, S.; Ma, S.; Ploehn, H.J.; Iovine, P.M.; Wang, C.; Chu, F.; Tang, C. Combining renewable gum rosin and lignin: Towards hydrophobic polymer composites by controlled polymerization. *J. Polym. Sci. A Polym. Chem.* **2011**, *49*, 3728–3738. [\[CrossRef\]](#)
143. Diao, B.; Zhang, Z.; Zhu, J.; Li, J. Biomass-based thermogelling copolymers consisting of lignin and grafted poly (N-isopropylacrylamide), poly (ethylene glycol), and poly (propylene glycol). *RSC Adv.* **2014**, *4*, 42996–43003. [\[CrossRef\]](#)
144. Yu, J.; Wang, J.; Wang, C.; Liu, Y.; Xu, Y.; Tang, C.; Chu, F. UV-Absorbent Lignin-Based Multi-Arm Star Thermoplastic Elastomers. *Macromol. Rapid Commun.* **2015**, *36*, 398–404. [\[CrossRef\]](#)
145. Gao, G.; Dallmeyer, J.I.; Kadla, J.F. Synthesis of lignin nanofibers with ionic-responsive shells: Water-expandable lignin-based nanofibrous mats. *Biomacromolecules* **2012**, *13*, 3602–3610. [\[CrossRef\]](#) [\[PubMed\]](#)
146. Hilburg, S.L.; Elder, A.N.; Chung, H.; Ferebee, R.L.; Bockstaller, M.R.; Washburn, N.R. A universal route towards thermoplastic lignin composites with improved mechanical properties. *Polymer* **2014**, *55*, 995–1003. [\[CrossRef\]](#)
147. Shah, T.; Gupta, C.; Ferebee, R.L.; Bockstaller, M.R.; Washburn, N.R. Extraordinary toughening and strengthening effect in polymer nanocomposites using lignin-based fillers synthesized by ATRP. *Polymer* **2015**, *72*, 406–412. [\[CrossRef\]](#)
148. Kai, D.; Low, Z.W.; Liow, S.S.; Abdul Karim, A.; Ye, H.; Jin, G.; Li, K.; Loh, X.J. Development of lignin supramolecular hydrogels with mechanically responsive and self-healing properties. *ACS Sustain. Chem. Eng.* **2015**, *3*, 2160–2169. [\[CrossRef\]](#)

149. Li, H.; Pang, Z.; Gao, P.; Wang, L. Fe (III)-catalyzed grafting copolymerization of lignin with styrene and methyl methacrylate through AGET ATRP using triphenyl phosphine as a ligand. *RSC Adv.* **2015**, *5*, 54387–54394. [\[CrossRef\]](#)
150. Liu, X.; Yin, H.; Zhang, Z.; Diao, B.; Li, G. Functionalization of lignin through ATRP grafting of poly(2-dimethylaminoethyl methacrylate) for gene delivery. *Colloids Surf. B Biointerfaces* **2015**, *125*, 230–237. [\[CrossRef\]](#) [\[PubMed\]](#)
151. Silmore, K.S.; Gupta, C.; Washburn, N.R. Tunable Pickering emulsions with polymer-grafted lignin nanoparticles (PGLNs). *J. Colloid Interface Sci.* **2016**, *466*, 91–100. [\[CrossRef\]](#) [\[PubMed\]](#)
152. Gupta, C.; Nadelman, E.; Washburn, N.R.; Kurtis, K.E. Lignopolymer Superplasticizers for Low-CO₂ Cements. *ACS Sustain. Chem. Eng.* **2017**, *5*, 4041–4049. [\[CrossRef\]](#)
153. Gupta, C.; Sverdløve, M.J.; Washburn, N.R. Molecular architecture requirements for polymer-grafted lignin superplasticizers. *Soft Matter* **2015**, *11*, 2691–2699. [\[CrossRef\]](#)
154. Liu, Z.; Lu, X.; Xie, J.; Feng, B.; Han, Q. Synthesis of a novel tunable lignin-based star copolymer and its flocculation performance in the treatment of kaolin suspension. *Sep. Purif. Technol.* **2019**, *210*, 355–363. [\[CrossRef\]](#)
155. Nemoto, T.; Konishi, G.-I.; Tojo, Y.; An, Y.C.; Funaoka, M. Functionalization of lignin: Synthesis of lignophenol-graft-poly(2-ethyl-2-oxazoline) and its application to polymer blends with commodity polymer. *J. Appl. Polym. Sci.* **2012**, *123*, 2636–2642. [\[CrossRef\]](#)
156. Mahata, D.; Jana, M.; Jana, A.; Mukherjee, A.; Mondal, N.; Saha, T.; Sen, S.; Nando, G.B.; Mukhopadhyay, C.K.; Chakraborty, R.; et al. Lignin-graft-polyoxazoline conjugated triazole a novel anti-infective ointment to control persistent inflammation. *Sci. Rep.* **2017**, *7*, 46412. [\[CrossRef\]](#) [\[PubMed\]](#)
157. Chung, Y.L.; Olsson, J.V.; Li, R.J.; Frank, C.W.; Waymouth, R.M.; Billington, S.L.; Sattely, E.S. A renewable lignin-lactide copolymer and application in biobased composite. *ACS Sustain. Chem. Eng.* **2013**, *1*, 1231–1238. [\[CrossRef\]](#)
158. Liu, X.; Zong, E.; Jiang, J.; Fu, S.; Wang, J.; Xu, B.; Li, W.; Lin, X.; Xu, Y.; Wang, C.; et al. Preparation and characterization of Lignin-graft-poly(ϵ -caprolactone) copolymers based on lignocellulosic butanol residue. *Int. J. Biol. Macromol.* **2015**, *81*, 521–529. [\[CrossRef\]](#)
159. Sun, Y.; Yang, L.; Lu, X.; He, C. Biodegradable and renewable poly(lactide)-lignin composites: Synthesis, interface and toughening mechanism. *J. Mater. Chem. A* **2015**, *3*, 3699–3709. [\[CrossRef\]](#)
160. Kai, D.; Zhang, K.; Liow, S.S.; Loh, X.J. New dual functional phb-grafted lignin copolymer: Synthesis, mechanical properties, and biocompatibility studies. *ACS Appl. Bio Mater.* **2018**, *2*, 127–134. [\[CrossRef\]](#)
161. Pérez-Camargo, R.A.; Saenz, G.; Laurichesse, S.; Casas, M.T.; Puiggali, J.; Avérous, L.; Müller, A.J. Nucleation crystallization, and thermal fractionation of poly(ϵ -caprolactone)-grafted-lignin: Effect of grafted chains length and lignin content. *J. Polym. Sci. Part B Polym. Phys.* **2015**, *53*, 1736–1750. [\[CrossRef\]](#)
162. Laurichesse, S.; Avérous, L. Synthesis, thermal properties, rheological and mechanical behaviors of lignins-grafted-poly(ϵ -caprolactone). *Polymer* **2013**, *54*, 3882–3890. [\[CrossRef\]](#)
163. Schmidt, B.V.K.J.; Molinari, V.; Esposito, D.; Tauer, K.; Antonietti, M. Lignin-based polymeric surfactants for emulsion polymerization. *Polymer* **2017**, *112*, 418–426. [\[CrossRef\]](#)
164. Tapdiqov, S.Z. A drug-loaded gel based on graft radical co-polymerization of n-vinylpyrrolidone and 4-vinylpyridine with chitosan. *Cell. Chem. Technol.* **2020**, *54*, 429–438. [\[CrossRef\]](#)
165. Cheaburu-Yilmaz, C.N. On the development of chitosan-graft-poly(n-isopropylacrylamide) by raft polymerization technique. *Cell. Chem. Technol.* **2020**, *54*, 1–10. [\[CrossRef\]](#)
166. Kadokawa, J.-I. Preparation and Grafting Functionalization of Self-Assembled Chitin Nanofiber Film. *Coatings* **2016**, *6*, 27. [\[CrossRef\]](#)
167. Mahmoud, G.A.; Sayed, A.; Thabit, M.; Safwat, G. Chitosan biopolymer based nanocomposite hydrogels for removal of methylene blue dye. *SN Appl. Sci.* **2020**, *2*, 968. [\[CrossRef\]](#)
168. Xu, Y.; Liu, B.; Zou, L.; Sun, C.; Li, W. Preparation and characterization of PLLA/chitosan-graft-poly(ϵ -caprolactone) (CS-g-PCL) composite fibrous mats: The microstructure, performance and proliferation assessment. *Int. J. Biol. Macromol.* **2020**, *162*, 320–332. [\[CrossRef\]](#) [\[PubMed\]](#)
169. Kadokawa, J.-I. Fabrication of nanostructured and microstructured chitin materials through gelation with suitable dispersion media. *RSC Adv.* **2015**, *5*, 12736–12746. [\[CrossRef\]](#)
170. Stefan, J.; Lorkowska-Zawicka, B.; Kaminski, K.; Szczubialka, K.; Nowakowska, M.; Korbut, R. The current view on biological potency of cationically modified chitosan. *J. Physiol. Pharmacol.* **2014**, *65*, 341–347. [\[PubMed\]](#)
171. Jiang, T.; Deng, M.; James, R.; Nair, L.S.; Laurencin, C.T. Micro- and nanofabrication of chitosan structures for regenerative engineering. *Acta Biomater.* **2014**, *10*, 1632–1645. [\[CrossRef\]](#)
172. Lai, G.-J.; Shalumon, K.T.; Chen, S.-H.; Chen, J.P. Composite chitosan/silk fibroin nanofibers for modulation of osteogenic differentiation and proliferation of human mesenchymal stem cells. *Carbohydr. Polym.* **2014**, *111*, 288–297. [\[CrossRef\]](#)
173. Jayakumar, R.; Menon, D.; Manzoor, K.; Nair, S.V.; Tamura, H. Biomedical applications of chitin and chitosan based nanomaterials—A short review. *Carbohydr. Polym.* **2010**, *82*, 227–232. [\[CrossRef\]](#)
174. Deng, Z.; Wang, T.; Chen, X.; Liu, Y. Applications of chitosan based biomaterials: A focus on dependent antimicrobial properties. *Mar. Life Sci. Technol.* **2020**, *2*, 398–413. [\[CrossRef\]](#)
175. Wen, J.; Li, Y.; Wang, L.; Chen, X.; Cao, Q.; He, N. Carbon Dioxide Smart Materials Based on Chitosan. *Prog. Chem.* **2020**, *32*, 417–422. (In Chinese)

176. Sashiwa, H.; Aiba, S.-I. Chemically modified chitin and chitosan as biomaterials. *Prog. Polym. Sci.* **2004**, *29*, 887–908. [\[CrossRef\]](#)
177. Crini, G.; Badot, P.-M. Application of chitosan, a natural aminopolysaccharide, for dye removal from aqueous solutions by adsorption processes using batch studies: A review of recent literature. *Prog. Polym. Sci.* **2008**, *33*, 399–447. [\[CrossRef\]](#)
178. Mittal, H.; Ray, S.S.; Kaith, B.S.; Bhatia, J.K.; Sharma, S.J.; Alhassan, S.M. Recent progress in the structural modification of chitosan for applications in diversified biomedical fields. *Eur. Polym. J.* **2018**, *109*, 402–434. [\[CrossRef\]](#)
179. Iyer, B.V.S.; Yashin, V.V.; Hamer, M.J.; Kowalewski, T.; Matyjaszewski, K.; Balazsa, A.C. Ductility, toughness and strain recovery in self-healing dualcross-linked nanoparticle networks studied by computer simulations. *Prog. Polym. Sci.* **2015**, *40*, 121–137. [\[CrossRef\]](#)
180. Derry, M.J.; Fielding, L.A.; Armes, S.P. Polymerization-induced self-assembly of block copolymer nanoparticles via RAFT non-aqueous dispersion polymerization. *Prog. Polym. Sci.* **2016**, *52*, 1–18. [\[CrossRef\]](#)
181. Bednarek, M. Branched aliphatic polyesters by ring-opening (co)polymerization. *Prog. Polym. Sci.* **2016**, *58*, 27–58. [\[CrossRef\]](#)
182. Yildirim, I.; Weber, C.; Schubert, U.S. Old meets new: Combination of PLA and RDRP to obtain sophisticated macromolecular architectures. *Prog. Polym. Sci.* **2018**, *76*, 111–150. [\[CrossRef\]](#)
183. Wang, W.; Lu, W.; Goodwin, A.; Wang, H.; Yin, P.; Kang, N.-G.; Hong, K.; Mays, J.W. Recent advances in thermoplastic elastomers from living polymerizations: Macromolecular architectures and supramolecular chemistry. *Prog. Polym. Sci.* **2019**, *95*, 1–31. [\[CrossRef\]](#)
184. Mocny, P.; Klok, H.-A. Complex polymer topologies and polymer–nanoparticle hybrid films prepared via surface-initiated controlled radical polymerization. *Prog. Polym. Sci.* **2020**, *100*, 101185. [\[CrossRef\]](#)
185. Vivaldo-Lima, E.; Jaramillo-Soto, G.; Penlidis, A. Nitroxide-mediated polymerization (NMP). In *Encyclopedia of Polymer Science and Technology*, 1st ed.; John Wiley & Sons: New York, NY, USA, 2016; pp. 1–48. ISBN 978-047-144-026-0.
186. Olivier, A.; Meyer, F.; Raquez, J.-M.; Damman, P.; Dubois, P. Surface-initiated controlled polymerization as a convenient method for designing functional polymer brushes: From self-assembled monolayers to patterned surfaces. *Prog. Polym. Sci.* **2012**, *37*, 157–181. [\[CrossRef\]](#)
187. Radzevicius, P.; Krivorotova, T.; Makuska, R. Synthesis by one-pot RAFT polymerization and properties of amphiphilic pentablock copolymers with repeating blocks of poly(2-hydroxyethyl methacrylate) and poly(butyl methacrylate). *Eur. Polym. J.* **2017**, *87*, 69–83. [\[CrossRef\]](#)
188. Chmielarz, P.; Fantin, M.; Park, S.; Isse, A.A.; Gennaro, A.; Magenau, A.J.; Sobkowiak, A.; Matyjaszewski, K. Electrochemically mediated atom transfer radical polymerization (eATRP). *Prog. Polym. Sci.* **2017**, *69*, 47–78. [\[CrossRef\]](#)
189. Maharana, T.; Pattanaik, S.; Routaray, A.; Nath, N.; Sutar, A.K. Synthesis and characterization of poly(lactic acid) based graft copolymers. *React. Funct. Polym.* **2015**, *93*, 47–67. [\[CrossRef\]](#)
190. Mehta, A.; Pandey, J.P.; Sen, G. Synthesis of Diallyl dimethyl ammonium chloride grafted polyvinyl pyrrolidone (PVP-g-DADMAC) and its applications. *Mater. Sci. Eng. B Solid State Mater. Adv. Technol.* **2021**, *263*, 114750. [\[CrossRef\]](#)
191. El-Sayed, N.; Awad, H.; El-Sayed, G.M.; Nagieb, Z.A.; Kamel, S. Synthesis and characterization of biocompatible hydrogel based on hydroxyethyl cellulose-g-poly(hydroxyethyl methacrylate). *Polym. Bull.* **2020**, *77*, 6333–6347. [\[CrossRef\]](#)
192. Mahdavi, H.; Mazinani, N.; Heidari, A.A. Poly(vinylidene fluoride) (PVDF)/PVDF-g-polyvinylpyrrolidone (PVP)/TiO₂ mixed matrix nanofiltration membranes: Preparation and characterization. *Polym. Int.* **2020**, *69*, 1187–1195. [\[CrossRef\]](#)
193. Oliveira, T.S.; Brazil, T.R.; Guerrini, L.M.; Rezende, M.C.; Oliveira, M.P. Synthesis and characterization of poly (acrylonitrile-g-lignin) by semi-batch solution polymerization and evaluation of their potential application as carbon materials. *J. Polym. Res.* **2020**, *27*, 340. [\[CrossRef\]](#)
194. Zhang, M.; Yang, P.; Lan, G.; Liu, Y.; Cai, Q.; Xi, J. High crosslinked sodium carboxyl methylstarch-g-poly (acrylic acid-co-acrylamide) resin for heavy metal adsorption: Its characteristics and mechanisms. *Environ. Sci. Pollut. Res.* **2020**, *27*, 38617–38630. [\[CrossRef\]](#)
195. Wang, L.; Zhang, X.; Xu, J.; Wang, Q.; Fan, X. Synthesis of partly debranched starch-g-poly(2-acryloyloxyethyl trimethyl ammonium chloride) catalyzed by horseradish peroxidase and the effect on adhesion to polyester/cotton yarn. *Process Biochem.* **2020**, *97*, 176–182. [\[CrossRef\]](#)
196. Xu, R.-M.; Yang, T.T.; Vidovic, E.; Jia, R.-N.; Zhang, J.-M.; Mi, Q.-Y.; Zhang, J. Cellulose Acetate Thermoplastics with High Modulus, Dimensional Stability and Anti-migration Properties by Using CA-g-PLA as Macromolecular Plasticizer. *Chin. J. Polym. Sci.* **2020**, *38*, 1141–1148. [\[CrossRef\]](#)
197. Wu, Q.; Tiraferri, A.; Li, T.; Xie, W.; Chang, H.; Bai, Y.; Liu, B. Superwetable PVDF/PVDF-g-PEGMA Ultrafiltration Membranes. *ACS Omega* **2020**, *5*, 23450–23459. [\[CrossRef\]](#) [\[PubMed\]](#)
198. Peighambardoust, S.J.; Aghamohammadi-Bavil, O.; Foroutan, R.; Arsalani, N. Removal of malachite green using carboxymethyl cellulose-g-polyacrylamide/montmorillonite nanocomposite hydrogel. *Int. J. Biol. Macromol.* **2020**, *159*, 1122–1131. [\[CrossRef\]](#)
199. Gürsel, U.; Taran, S.; Gökçen, M.; Ari, Y.; Alli, A. Ultraviolet illumination responsivity of the Au/n-Si diodes with and without poly (linolenic acid)-g-poly (caprolactone)-g-poly (t-butyl acrylate) interfacial layer. *Surf. Rev. Lett.* **2020**, *27*, 1950207. [\[CrossRef\]](#)
200. Song, P.; Guo, R.; Ma, W.; Wang, L.; Ma, F.; Wang, R. Synthesis of CO₂-based polycarbonate-g-polystyrene copolymers via NMRP. *Chem. Commun.* **2020**, *56*, 9493–9496. [\[CrossRef\]](#) [\[PubMed\]](#)
201. Klimovica, K.; Pan, S.; Lin, T.-W.; Peng, X.; Ellison, C.J.; LaPointe, A.M.; Bates, F.S.; Coates, G.W. Compatibilization of iPP/HDPE Blends with PE-g-iPP Graft Copolymers. *ACS Macro. Lett.* **2020**, *9*, 1161–1166. [\[CrossRef\]](#)

202. Li, W.; Yu, Z.; Wu, Y.; Liu, Q. Preparation, characterization of feather protein-g-poly(sodium allyl sulfonate) and its application as a low-temperature adhesive to cotton and viscose fibers for warp sizing. *Eur. Polym. J.* **2020**, *136*, 109945. [\[CrossRef\]](#)
203. Czarnecka, E.; Nowaczyk, J. Semi-Natural superabsorbents based on Starch-g-poly(acrylic acid): Modification, synthesis and application. *Polymers* **2020**, *12*, 1794. [\[CrossRef\]](#)
204. Bhosale, R.R.; Gangadharappa, H.V.; Osmani, R.A.M.; Gowda, D.V. Design and development of polymethylmethacrylate-grafted gellan gum (PMMA-g-GG)-based pH-sensitive novel drug delivery system for antidiabetic therapy. *Drug Deliv. and Transl. Res.* **2020**, *10*, 1002–1018. [\[CrossRef\]](#) [\[PubMed\]](#)
205. Patel, R.; Patel, M.; Sung, J.-S.; Kim, J.H. Preparation and characterization of bioinert amphiphilic P(VDF-co-CTFE)-g-POEM graft copolymer. *Polym. Plast. Technol. Mater.* **2020**, *59*, 1077–1087. [\[CrossRef\]](#)
206. Li, W.; Wu, Y.; Wu, J.; Ni, Q. Preparation, characterization of poly(acrylic acid)-g-feather protein-g-poly(methyl acrylate) and application in improving adhesion of protein to PLA fibers for sizing. *React. Funct. Polym.* **2020**, *152*, 104607. [\[CrossRef\]](#)
207. Deng, J.-R.; Zhao, C.-L.; Wu, Y.-X. Antibacterial and pH-responsive Quaternized Hydroxypropyl Cellulose-g-Poly(THF-co-epichlorohydrin) Graft Copolymer: Synthesis, Characterization and Properties. *Chin. J. Polym. Sci.* **2020**, *38*, 704–714. [\[CrossRef\]](#)
208. Cuggino, J.C.; Ambrosioni, F.E.; Picchio, M.L.; Nicola, M.; Jiménez Kairuz, A.F.; Gatti, G.; Minari, R.J.; Calderon, M.; Alvarez Igarzabal, C.I.; Gugliotta, L.M. Thermally self-assembled biodegradable poly(casein-g-N-isopropylacrylamide) unimers and their application in drug delivery for cancer therapy. *Int. J. Biol. Macromol.* **2020**, *154*, 446–455. [\[CrossRef\]](#) [\[PubMed\]](#)
209. Kenawy, E.R.; Seggiani, M.; Cinelli, P.; Elnaby, H.M.H.; Azaam, M.M. Swelling capacity of sugarcane bagasse-g-poly(acrylamide)/attapulgit superabsorbent composites and their application as slow release fertilizer. *Eur. Polym. J.* **2020**, *133*, 109769. [\[CrossRef\]](#)
210. Jiang, P.; Ji, H.; Li, G.; Chen, S.; Lv, L. Structure formation in pH-sensitive micro porous membrane from well-defined ethyl cellulose-g-PDEAEMA via non-solvent-induced phase separation process. *J. Macromol. Sci. Pure Appl. Chem.* **2020**, *57*, 461–471. [\[CrossRef\]](#)
211. Huang, Q.; Xu, Z.; Cai, C.; Lin, J. Micelles with a Loose Core Self-Assembled from Coil-g-Rod Graft Copolymers Displaying High Drug Loading Capacity. *Macromol. Chem. Phys.* **2020**, *221*, 2000121. [\[CrossRef\]](#)
212. Wang, Z.; Wu, L.; Zhou, D.; Ji, P.; Zhou, X.; Zhang, Y.; He, P. Synthesis and Water Absorbing Properties of KGM-g-P(AA-AM-(DMAEA-EB)) via Grafting Polymerization Method. *Polym. Sci. Ser. B* **2020**, *62*, 238–244. [\[CrossRef\]](#)
213. Erdoğan, M.K.; Akdemir, Ö.; Hamitbeyli, A.; Karakışla, M. Preparation of hydrophilic woven fabrics: Surface modification of poly(ethylene terephthalate) by grafting of poly(vinyl alcohol) and poly(vinyl alcohol)-g-(N-vinyl-2-pyrrolidone). *J. Appl. Polym. Sci.* **2020**, *137*, 48584. [\[CrossRef\]](#)
214. Worzakowska, M. The preparation, physicochemical and thermal properties of the high moisture, solvent and chemical resistant starch-g-poly(geranyl methacrylate) copolymers. *J. Thermal. Anal. Calorim.* **2020**, *140*, 189–198. [\[CrossRef\]](#)
215. Delorme, V.; Lichon, L.; Mahindad, H.; Hunger, S.; Laroui, N.; Daurat, M.; Godefroy, A.; Coudane, J.; Gary-Bobo, M.; Van Den Berghe, H. Reverse poly(ϵ -caprolactone)-g-dextran graft copolymers. Nano-carriers for intracellular uptake of anticancer drugs. *Carbohydr. Polym.* **2020**, *232*, 115764. [\[CrossRef\]](#) [\[PubMed\]](#)
216. Kang, D.A.; Kim, K.; Karade, S.S.; Kim, H.; Kim, J.H. High-performance solid-state bendable supercapacitors based on PEGBEM-g-PAEMA graft copolymer electrolyte. *Chem. Eng. J.* **2020**, *384*, 123308. [\[CrossRef\]](#)
217. Tian, B.; Cai, Y.; Zhang, X.; Fan, H.; Li, B.-G. Design of Well-Defined Polyethylene-g-poly-methyltrifluorosiloxane Graft Copolymers via Direct Copolymerization of Ethylene with Polyfluorosiloxane Macromonomers. *Ind. Eng. Chem. Res.* **2020**, *59*, 4557–4567. [\[CrossRef\]](#)
218. Öztürk, T.; Meyvacı, E.; Arslan, T. Synthesis and characterization of poly(vinyl chloride-g- ϵ -caprolactone) brush type graft copolymers by ring-opening polymerization and “click” chemistry. *J. Macromol. Sci. Pure Appl. Chem.* **2020**, *57*, 171–180. [\[CrossRef\]](#)
219. Zha, X.; Sadi, M.S.; Yang, Y.; Luo, T.; Huang, N. Adhesion of cornstarch-g-poly (2-hydroxyethyl acrylate) to cotton fibers in sizing. *J. Adhes. Sci. Technol.* **2020**, *34*, 461–479. [\[CrossRef\]](#)
220. Nicolas, C.; Zhang, W.; Choppé, E.; Fontaine, L.; Montembault, V. Polynorbornene-g-poly(ethylene oxide) Through the Combination of ROMP and Nitroxide Radical Coupling Reactions. *J. Polym. Sci.* **2020**, *58*, 645–653. [\[CrossRef\]](#)
221. İlhan, E.; Karahaliloglu, Z.; Kilicay, E.; Hazer, B.; Denkbaz, E.B. Potent bioactive bone cements impregnated with polystyrene-g-soybean oil-AgNPs for advanced bone tissue applications. *Mater. Technol.* **2020**, *35*, 179–194. [\[CrossRef\]](#)
222. Chen, Y.; Li, Q.; Li, Y.; Zhang, Q.; Huang, J.; Wu, Q.; Wang, S. Fabrication of cellulose nanocrystal-g-poly(acrylic acid-co-acrylamide) aerogels for efficient Pb(II) removal. *Polymers* **2020**, *12*, 333. [\[CrossRef\]](#)
223. Mo, X.-Z.; Wei, F.-X.; Tan, D.-F.; Pang, J.-Y.; Lan, C.-B. The compatibilization of PLA-g-TPU graft copolymer on polylactide/thermoplastic polyurethane blends. *J. Polym. Res.* **2020**, *27*, 33. [\[CrossRef\]](#)
224. Guleria, A.; Kumari, G.; Lima, E.C. Cellulose-g-poly-(acrylamide-co-acrylic acid) polymeric bioadsorbent for the removal of toxic inorganic pollutants from wastewaters. *Carbohydr. Polym.* **2020**, *228*, 115396. [\[CrossRef\]](#) [\[PubMed\]](#)
225. He, M.; Li, T.; Hu, M.; Chen, C.; Liu, B.; Crittenden, J.; Chu, L.-Y.; Ng, H.Y. Performance improvement for thin-film composite nanofiltration membranes prepared on PSf/PSf-g-PEG blended substrates. *Sep. Purif. Technol.* **2020**, *230*, 115855. [\[CrossRef\]](#)
226. Savaş, B.; Öztürk, T. Synthesis and characterization of poly(vinyl chloride-g-methyl methacrylate) graft copolymer by redox polymerization and Cu catalyzed azide-alkyne cycloaddition reaction. *J. Macromol. Sci. Pure Appl. Chem.* **2020**, *1–7*. [\[CrossRef\]](#)

227. Ahuja, D.; Rainu, A.S.; Singh, M.; Kaushik, A. Encapsulation of NPK fertilizer for slow release using sodium carboxymethyl cellulose-g-poly (AA-C0-AM-C0-AMPS)/ Montmorillonite clay-based nanocomposite hydrogels for sustainable agricultural applications. *Trends Carbohydr. Res.* **2020**, *12*, 15–23.
228. Lu, Y.; Wu, F.; Duan, W.; Zhou, X.; Kong, W. Engineering a “PEG-g-PEI/DNA nanoparticle-in- PLGA microsphere” hybrid controlled release system to enhance immunogenicity of DNA vaccine. *Mater. Sci. Eng. C* **2020**, *106*, 110394. [CrossRef]
229. Grebenik, E.A.; Surin, A.M.; Bardakova, K.N.; Dermina, T.S.; Minaev, N.V.; Veryasova, N.N.; Artyukhova, M.A.; Krasilnikova, I.A.; Bakaeva, Z.V.; Sorokina, E.G.; et al. Chitosan-g-oligo(L,L-lactide) copolymer hydrogel for nervous tissue regeneration in glutamate excitotoxicity: In vitro feasibility evaluation. *Biomed. Mater.* **2020**, *15*, 015011. [CrossRef] [PubMed]
230. Barth, H.G.; Jackson, C.; Boyes, B.E. Size Exclusion Chromatography. *Anal. Chem.* **1994**, *66*, 595–620. [CrossRef] [PubMed]
231. Hamielec, A.; Gloor, P.; Zhu, S. Kinetics of, free radical modification of polyolefins in extruders—Chain scission, crosslinking and grafting. *Can. J. Chem. Eng.* **1991**, *69*, 611–618. [CrossRef]
232. Chaimberg, M.; Cohen, Y. Kinetic Modeling of Free-Radical Graft Polymerization. *AIChE J.* **1994**, *40*, 294–311. [CrossRef]
233. Guillot, J.; Leroux, D. Modelling of size-exclusion chromatograms from molecular weight distribution calculations. Application to the grafting of polymers onto functionalized silica. *Macromol. Chem. Phys.* **1994**, *195*, 1463–1470. [CrossRef]
234. Hojabr, S.; Baker, W.; Russell, K.; McLellan, P.; Huneault, M. Melt grafting of glycidyl methacrylate onto polyethylene: An experimental and mathematical modeling study. *Int. Polym. Proc.* **1998**, *13*, 118–128. [CrossRef]
235. Machado, A.; Gaspar-Cunha, A.; Covas, J. Modelling of the grafting of maleic anhydride onto polyethylene in an extruder. *Mater. Sci. Forum* **2004**, *455–456*, 763–766. [CrossRef]
236. Giudici, R. Mathematical modeling of the crafting of maleic anhydride onto polypropylene. *Macromol. Symp.* **2007**, *259*, 354–364. [CrossRef]
237. Diaconescu, R.; Grigoriu, A.-M.; Luca, C. Neural network modeling of monochlorotriazinyl- β -cyclodextrin grafting on cellulosic supports. *Cell. Chem. Technol.* **2007**, *41*, 385–390.
238. Luca, C.; Grigoriu, A.-M.; Diaconescu, R.; Secula, M. Modeling and simulation of monochlorotriazinyl- β -cyclodextrin paper grafting by artificial neural network. *Rev. Chim.* **2011**, *62*, 1033–1038.
239. Grigoriu, A.; Racu, C.; Diaconescu, R.; Grigoriu, A.-M. Modeling of the simultaneous process of wet spinning-grafting of bast fibers using artificial neural networks. *Textile Res. J.* **2012**, *82*, 324–335. [CrossRef]
240. Tong, G.-S.; Liu, T.; Hu, G.-H.; Hoppe, S.; Zhao, L.; Yuan, W.-K. Modelling of the kinetics of the supercritical CO₂ assisted grafting of maleic anhydride onto isotactic polypropylene in the solid state. *Chem. Eng. Sci.* **2007**, *62*, 5290–5294. [CrossRef]
241. Wang, J.; Ran, Y.; Ding, L.; Wang, D. Advances in supercritical CO₂ assisted grafting of polypropylene in solid state. *Chem. React. Eng. Technol.* **2008**, *24*, 173–177.
242. Casis, N.; Estenoz, D.; Vega, J.; Meira, G. Bulk prepolymerization of styrene in the presence of polybutadiene: Determination of grafting efficiency by size exclusion chromatography combined with a new extended model. *J. Appl. Polym. Sci.* **2009**, *111*, 1508–1522. [CrossRef]
243. Badel, T.; Beyou, E.; Bounor-Legaré, V.; Chaumont, P.; Flat, J.; Michel, A. Free radical graft copolymerization of methyl methacrylate onto polyolefin backbone: Kinetics modeling through model compounds approach. *Macromol. Chem. Phys.* **2009**, *210*, 1087–1095. [CrossRef]
244. Gianoglio Pantano, I.; Asteasuain, M.; Sarmoria, C.; Brandolin, A. Graft copolymers for blend compatibilization. Mathematical modeling of the grafting process. In Proceedings of the 2010 AIChE Annual Meeting Conference Proceedings, Salt Lake City, UT, USA, 7–12 November 2010; pp. 1–14.
245. Gianoglio Pantano, I.; Asteasuain, M.; Sarmoria, C.; Brandolin, A. Graft Copolymers for Blend Compatibilization: Mathematical Modeling of the Grafting Process. *Macromol. React. Eng.* **2012**, *6*, 406–418. [CrossRef]
246. Gianoglio Pantano, I.A.; Brandolin, A.; Sarmoria, C. Mathematical modeling of the graft reaction between polystyrene and polyethylene. *Polym. Degrad. Stabil.* **2011**, *96*, 416–425. [CrossRef]
247. Aguiar, L.; Pessôa-Filho, P.; Giudici, R. Mathematical modeling of the grafting of maleic anhydride onto poly(propylene): Model considering a heterogeneous medium. *Macromol. Theory Simul.* **2011**, *20*, 837–849. [CrossRef]
248. Damodaran, V.; Fee, C.; Papat, K. Modeling of PEG grafting and prediction of interfacial force profile using x-ray photoelectron spectroscopy. *Surf. Interface Anal.* **2012**, *44*, 144–149. [CrossRef]
249. Zhou, D.; Gao, X.; Wang, W.-J.; Zhu, S. Termination of surface radicals and kinetic modeling of ATRP grafting from flat surfaces by addition of deactivator. *Macromolecules* **2012**, *45*, 1198–1208. [CrossRef]
250. Nasef, M.; Shamsaei, E.; Ghassemi, P.; Aly, A.; Yahaya, A. Modeling, prediction, and multifactorial optimization of radiation-induced grafting of 4-vinylpyridine onto poly(vinylidene fluoride) films using statistical simulator. *J. Appl. Polym. Sci.* **2013**, *127*, 1659–1666. [CrossRef]
251. Nasef, M.M.; Ali, A.; Saidi, H.; Ahmad, A. Modeling and optimization aspects of radiation induced grafting of 4-vinylpyridine onto partially fluorinated films. *Radiat. Phys. Chem.* **2014**, *94*, 123–128. [CrossRef]
252. Wu, L.L.; Bu, Z.; Gong, C.; Li, B.-G.; Hungenberg, K.-D. Graft Copolymerization of Styrene and Acrylonitrile in the Presence of Poly(propylene glycol): Modeling and Simulation of Semi-Batch and Continuous Processes. *Macromol. React. Eng.* **2012**, *6*, 384–394. [CrossRef]
253. Xie, X.-L.; Tong, Z.-F.; Huang, Z.-Q.; Zhang, Y.-Q. Kinetics model of graft co-polymerization of acrylamide onto mechanically-activated starch in inverse emulsion. *J. Chem. Eng. Chin. Univ.* **2014**, *28*, 567–573.

254. Liu, X.; Nomura, M. Kinetic modeling and simulation of emulsion grafting copolymerization of styrene and acrylonitrile in the presence of polybutadiene seed latex particles. *Ind. Eng. Chem. Res.* **2014**, *53*, 17580–17588. [\[CrossRef\]](#)
255. Zhang, M.; Jia, Y. Kinetic study on free radical grafting of polyethylene with acrylic acid by reactive extrusion. *J. Appl. Polym. Sci.* **2014**, *131*, 40990. [\[CrossRef\]](#)
256. Sirirat, T.; Vatanatham, T.; Hansupalak, N.; Rempel, G.; Arayaprane, W. Kinetics and modeling of methyl methacrylate graft copolymerization in the presence of natural rubber latex. *Korean J. Chem. Eng.* **2015**, *32*, 980–992. [\[CrossRef\]](#)
257. Oliveira, D.; Dias, R.; Costa, M. Modeling RAFT Gelation and Grafting of Polymer Brushes for the Production of Molecularly Imprinted Functional Particles. *Macromol. Symp.* **2016**, *370*, 52–65. [\[CrossRef\]](#)
258. Saeb, M.; Rezaee, B.; Shadman, A.; Formela, K.; Ahmadi, Z.; Hemmati, F.; Kermaniyan, T.; Mohammadi, Y. Controlled grafting of vinylic monomers on polyolefins: A robust mathematical modeling approach. *Des. Monomers Polym.* **2017**, *20*, 250–268. [\[CrossRef\]](#)
259. Hernández-Ortiz, J.; Van Steenberge, P.; Reyniers, M.-F.; Marin, G.; D'hooge, D.; Duchateau, J.; Remerie, K.; Toloza, C.; Vaz, A.; Schreurs, F. Modeling the reaction event history and microstructure of individual macrospecies in postpolymerization modification. *AIChE J.* **2017**, *63*, 4944–4961. [\[CrossRef\]](#)
260. Hernández-Ortiz, J.; Van Steenberge, P.; Duchateau, J.; Toloza, C.; Schreurs, F.; Reyniers, M.-F.; Marin, G.; D'hooge, D. Sensitivity Analysis of Single-Phase Isothermal Free Radical-Induced Grafting of Polyethylene. *Macromol. Theory Simul.* **2018**, *27*, 1800036. [\[CrossRef\]](#)
261. Hernández-Ortiz, J.; Van Steenberge, P.; Duchateau, J.; Toloza, C.; Schreurs, F.; Reyniers, M.-F.; Marin, G.; D'hooge, D. The Relevance of Multi-Injection and Temperature Profiles to Design Multi-Phase Reactive Processing of Polyolefins. *Macromol. Theory Simul.* **2019**, *28*, 1900035. [\[CrossRef\]](#)
262. Penlidis, A.; MacGregor, J.F.; Hamielec, A.E. Dynamic modeling of emulsion polymerization reactors. *AIChE J.* **1985**, *31*, 881–889. [\[CrossRef\]](#)
263. Iedema, P.D.; Grcev, S.; Hoefsloot, H.C.J. Molecular weight distribution modeling of radical polymerization in a CSTR with long chain branching through transfer to polymer and terminal double bond. *Macromolecules* **2003**, *36*, 458–476. [\[CrossRef\]](#)
264. Dias, R.; Costa, M. A new look at kinetic modeling of nonlinear free radical polymerizations with terminal branching and chain transfer to polymer. *Macromolecules* **2003**, *36*, 8853–8863. [\[CrossRef\]](#)
265. Krallis, A.; Kiparissides, C. Mathematical modeling of the bivariate molecular weight-Long chain branching distribution of highly branched polymers: A population balance approach. *Chem. Eng. Sci.* **2007**, *62*, 5304–5311. [\[CrossRef\]](#)
266. Kryven, I.; Iedema, P.D. A novel approach to population balance modeling of reactive polymer modification leading to branching. *Macromol. Theory Simul.* **2013**, *22*, 89–106. [\[CrossRef\]](#)
267. Wang, R.; Luo, Y.; Li, B.-G.; Zhu, S. Modeling of Branching and Gelation in RAFT Copolymerization of Vinyl/Divinyl Systems. *Macromolecules* **2009**, *42*, 85–94. [\[CrossRef\]](#)
268. Yaghini, N.; Iedema, P.D. Molecular weight and branching distribution modeling in radical polymerization with transfer to polymer and scission under gel conditions and allowing for multiradicals. *Macromolecules* **2014**, *47*, 4851–4863. [\[CrossRef\]](#)
269. Penlidis, A.; Vivaldo-Lima, E.; Hernández-Ortiz, J.; Saldívar-Guerra, E. Chapter 12: Polymer Reaction Engineering. In *Handbook of Polymer Synthesis, Characterization, and Processing*, 1st ed.; John Wiley & Sons: New York, NY, USA, 2013; pp. 251–271, ISBN 978-047-063-032-7.
270. Zhu, S.; Hamielec, A. Polymerization kinetic modeling and macromolecular. In *Polymer Science: A Comprehensive Reference*, 1st ed.; Matyjaszewski, K., Möller, M., Eds.; Elsevier B.V.: London, UK, 2012; Chapter 4.32; Volume 4, pp. 779–831, ISBN 978-008-087-862-1.
271. Quintero-Ortega, I.; Vivaldo-Lima, E.; Luna-Bárcenas, G.; Alvarado, J.; Louvier-Hernández, J.; Sanchez, I. Modeling of the Free-Radical Copolymerization Kinetics with Cross Linking of Vinyl/Divinyl Monomers in Supercritical Carbon Dioxide. *Ind. Eng. Chem. Res.* **2005**, *44*, 2823–2844. [\[CrossRef\]](#)
272. Dong, P.; Sun, H.; Quan, D. Synthesis of poly(L-lactide-co-5-amino-5-methyl-1,3-dioxan-2-ones) [P(L-LA-co-TAc)] containing amino groups via organocatalysis and post-polymerization functionalization. *Polymer* **2016**, *97*, 614–622. [\[CrossRef\]](#)